

Fall 11-14-2017

Evaluation of Energy Released from Nuclear Criticality Excursions in Process Solutions

Corey Michael Skinner
University of New Mexico

Follow this and additional works at: https://digitalrepository.unm.edu/ne_etds



Part of the [Nuclear Engineering Commons](#)

Recommended Citation

Skinner, Corey Michael. "Evaluation of Energy Released from Nuclear Criticality Excursions in Process Solutions." (2017).
https://digitalrepository.unm.edu/ne_etds/65

This Thesis is brought to you for free and open access by the Engineering ETDs at UNM Digital Repository. It has been accepted for inclusion in Nuclear Engineering ETDs by an authorized administrator of UNM Digital Repository. For more information, please contact disc@unm.edu.

Corey Michael Skinner

Candidate

Nuclear Engineering

Department

This thesis is approved, and it is acceptable in quality and form for publication:

Approved by the Thesis Committee:

Dr. Robert D. Busch , Chairperson

Dr. Cassiano R.E. de Oliveira

Dr. David L.Y. Louie

Evaluation of Energy Released from Nuclear Criticality Excursions in Process Solutions

by

Corey Michael Skinner

B.S., Nuclear Engineering, University of New Mexico, 2016

THESIS

Submitted in Partial Fulfillment of the
Requirements for the Degree of

**Master of Science
Nuclear Engineering**

The University of New Mexico
Albuquerque, New Mexico

December, 2017

©2017, Corey Michael Skinner

ACKNOWLEDGEMENTS

I would like to thank my advisor, Dr. Robert D. Busch, for his support, patience, and mentorship. I would also like to thank Dr. Cassiano R.E. de Oliveira for his knowledge and assistance with physical modeling and simulation techniques, as well as Dr. David L.Y. Louie of Sandia National Laboratories for his understanding of the problem domain and applications. Additionally, I want to thank Dr. Louis F. Restrepo of Atkins Global NS for his foundational work and his guidance. Finally, I would like to express appreciation to Dr. Alan Levin and Patrick Frias of DOE-HSS (AU-30) for overseeing this research. This work is supported by the DOE Health, Safety and Security Nuclear Safety Research and Development Program under WAS Project No. 2016HS201601210.

Evaluation of Energy Released from Nuclear Criticality Excursions in Process Solutions

by

Corey Michael Skinner

B.S. Nuclear Engineering, University of New Mexico, 2016

M.S. Nuclear Engineering, University of New Mexico, 2017

ABSTRACT

Typically, the staff of a nonreactor nuclear facility or a processing facility involving nuclear material are not expected to have a strong technical background in nuclear criticality physics, as that is not the purpose of these sites, yet handle material with the potential to undergo a criticality excursion. Such excursions have occurred 22 times in the past, 21 of which involved an aqueous solution material. Therefore, it would be useful to have a general model capable of providing a quick estimation of the consequences of a criticality excursion in a processing plant. To this end, correlations developed utilizing experimental data from previous tests were analyzed, from which it was determined that two bounding empirical correlations are applicable to such a system with a relatively high degree of accuracy. Additionally, a computational model was adapted using Monte Carlo nuclear physics and a time- and volume-element discretization scheme. This model was used to predict the evolution and estimate the consequences of first-pulse excursions from both a SILENE experimental excursion and the historical Wood River Junction accident.

The model was able to predict the power peak and total energy from the SILENE experiment when a pressure gradient damping factor was applied. Further work is needed to adequately account for the reactivity feedback from volume changes and balance the pressure effects with the density effects.

Contents

List of Figures	ix
List of Tables	xii
Chapter 1 – Introduction	1
1.1 Nuclear Criticality Excursions	1
1.2 Definition of Criticality	3
1.3 Characteristics of a Solution Criticality Excursion	4
1.4 Open and Closed Systems	8
1.5 General Bounds and Estimation	9
Chapter 2 – Summary of Literature Review	11
2.1 Criticality Accidents and Studies	11
2.2 Fission Yield Estimations	14
2.3 Excursion Modeling	21
2.4 Conclusions of Literature Review	24
Chapter 3 – Estimation of Fission Yield	25
3.1 Empirical Models	25
3.1.1 Olsen’s Model	29
3.1.2 Tuck’s Model	33
3.1.3 Barbry’s Model	40
3.1.4 Nomura’s Model	43

3.2	Summary of Empirical Models	49
Chapter 4 – Computational Model.....		53
4.1	Calculation Details	54
4.2	Computational Constants and Settings.....	72
Chapter 5 – Computational Results		75
4.3	SILENE S4-346.....	75
4.4	Wood River Junction.....	85
4.5	Limiting Acceleration	94
Chapter 6 – Concluding Remarks		101
Appendices: Computational Model Source Code.....		105
Appendix A – Driver Script File: transientmodel.py		107
Appendix B – File Operations Library: tm_fileops.py		111
Appendix C – Volume and Material Discretization: tm_material.py		114
Appendix D – Calculational Parameters: tm_constants.py.....		118
Nomenclature and Acronyms		120
References.....		122

List of Figures

Figure 1-1: Typical Solution System Criticality Excursion.....	7
Figure 2-1: Specific Fission Yields in Experiments at CRAC and SILENE (Barbry, 1987)	19
Figure 3-1: Olsen’s Model – Chronological (With Outlier Data).....	31
Figure 3-2: Olsen’s Model – Chronological	32
Figure 3-3: Olsen’s Model – Yield-Ordered (With Outlier Data)	32
Figure 3-4: Olsen’s Model – Yield-Ordered.....	33
Figure 3-5: Tuck’s General Solution Model – Chronological (With Outlier Data)	36
Figure 3-6: Tuck’s General Solution Model – Chronological	36
Figure 3-7: Tuck’s General Solution Model – Yield-Ordered (With Outlier Data)	37
Figure 3-8: Tuck’s General Solution Model – Yield-Ordered.....	37
Figure 3-9: Tuck’s Uranium Model – Chronological (With Outlier Data)	38
Figure 3-10: Tuck’s Uranium Model – Chronological	38
Figure 3-11: Tuck’s Uranium Model – Yield-Ordered (With Outlier Data)	39
Figure 3-12: Tuck’s Uranium Model – Yield-Ordered.....	39
Figure 3-13: Barbry’s Model – Chronological (With Outlier Data).....	41
Figure 3-14: Barbry’s Model – Chronological	42
Figure 3-15: Barbry’s Model – Yield-Ordered (With Outlier Data)	42
Figure 3-16: Barbry’s Model – Yield-Ordered.....	43
Figure 3-17: Nomura’s Non-Boiling Model – Chronological (With Outlier Data).....	45
Figure 3-18: Nomura’s Non-Boiling Model – Chronological	46
Figure 3-19: Nomura’s Non-Boiling Model – Yield-Ordered (With Outlier Data)	46

Figure 3-20: Nomura’s Non-Boiling Model – Yield-Ordered.....	47
Figure 3-21: Nomura’s Boiling Model – Chronological (With Outlier Data).....	47
Figure 3-22: Nomura’s Boiling Model – Chronological	48
Figure 3-23: Nomura’s Boiling Model – Yield-Ordered (With Outlier Data)	48
Figure 3-24: Nomura’s Boiling Model – Yield-Ordered.....	49
Figure 3-25: Bounded Fission Yield Ratio – Chronological (With Outlier Data).....	50
Figure 3-26: Bounded Fission Yield Ratio – Chronological	50
Figure 3-27: Bounded Fission Yield Ratio – Yield-Ordered (With Outlier Data)	51
Figure 3-28: Bounded Fission Yield Ratio – Yield-Ordered.....	52
Figure 4-1: Computational Model Flowchart	55
Figure 4-2: Cylindrical Discretization	56
Figure 4-3: Annular Discretization	57
Figure 4-4: Radial Discretization.....	57
Figure 5-1: Experimental Results of SILENE Excursion S4-346 (Barbry et al., 2009)...	76
Figure 5-2: SILENE S4-346 Base Power Profile	79
Figure 5-3: SILENE S4-346 Base Energy Profile	80
Figure 5-4: SILENE S4-346 Base Neutron Multiplication Factor Profile	80
Figure 5-5: SILENE S4-346 Axial Profile at 0 ms, Solution Height = 45.5 cm	82
Figure 5-6: SILENE S4-346 Base Axial Profile at 4.3 ms, Solution Height = 56.07 cm.	82
Figure 5-7: SILENE S4-346 Damped Power Profile.....	83
Figure 5-8: SILENE S4-346 Damped Energy Profile	83
Figure 5-9: SILENE S4-346 Damped Neutron Multiplication Factor Profile.....	84

Figure 5-10: SILENE S4-346 Damped Axial Profile at 7.7 ms, Solution Height = 52.5 cm	85
Figure 5-11: Wood River Junction Base Power Profile.....	88
Figure 5-12: Wood River Junction Base Energy Profile	89
Figure 5-13: Wood River Junction Base Multiplication Factor Profile.....	89
Figure 5-14: Wood River Junction Axial Profile at 0 ms, Solution Height = 23.5 cm.....	90
Figure 5-15: Wood River Junction Base Axial Profile at 1.0 ms, Solution Height = 28.7 cm.....	90
Figure 5-16: Wood River Junction Damped Power Profile.....	91
Figure 5-17: Wood River Junction Damped Energy Profile	92
Figure 5-18: Wood River Junction Damped Multiplication Factor Profile.....	92
Figure 5-19: Wood River Junction Damped Axial Profile at 3.5 ms, Solution Height = 28.6 cm.....	93
Figure 5-20: SILENE S4-346 Limited Power Profile.....	95
Figure 5-21: SILENE S4-346 Limited Energy Profile	95
Figure 5-22: SILENE S4-346 Limited Multiplication Factor Profile.....	96
Figure 5-23: SILENE S4-346 Limited Axial Profile at 12.2 ms, Solution Height = 51.9 cm.....	97
Figure 5-24: Wood River Junction Limited Power Profile.....	98
Figure 5-25: Wood River Junction Limited Energy Profile	98
Figure 5-26: Wood River Junction Limited Multiplication Factor Profile.....	99
Figure 5-27: Wood River Junction Limited Axial Profile at 9.4 ms, Solution Height = 28.3 cm.....	100

List of Tables

Table 2-1: Criticality Accident Fission Yields (T. P. McLaughlin, 1991)	13
Table 3-1: Accidents Analyzed via Empirical Models	26
Table 3-2: Physical Parameters for Empirical Models	28
Table 3-3: Results of Olsen’s Model	31
Table 3-6: Results of Tuck’s Model	34
Table 3-7: Results of Barbry’s Model	40
Table 3-8: Results of Nomura’s Model	44
Table 4-1: Constants of Computational Model.....	73
Table 5-1: Summary of Properties for SILENE Excursion S4-346.....	76
Table 5-2: Initial SILENE Material Definitions	77
Table 5-3: Initial Wood River Junction Material Definitions.....	87

Chapter 1 – Introduction

1.1 Nuclear Criticality Excursions

Substantial amounts of nuclear material are involved in the operations of nuclear facilities that process fissionable materials, which include spent fuel processing, high enrichment fuel processing, as well as other nonreactor applications. This nuclear fuel can take the form of aqueous acid solutions containing fissile materials, which have an inherent danger of achieving nuclear criticality under certain conditions. Such fissile materials are primarily considered to be those containing plutonium or uranium-235 at various levels of concentration and enrichment.

Accidental criticality excursions have occurred in solutions processing situations previously, and all known historical examples of these events have been characterized in a report from Los Alamos National Laboratory (T. McLaughlin et al., 2000). These events have had consequences ranging from an interruption of work due to evacuation procedures, to the direct contribution to the fatality of workers either working directly with or nearby the accidental excursion.

The potential severity of these events has led to the development of safety guidelines and site assessments, and strict regulations involving the use and handling of fissile materials. There is a wealth of experimental data available for criticality excursions in solution systems, including data gathered from the historical accidents. Additionally, several experimental facilities have previously operated, such as the CRAC and SILENE solution reactor experiments at Valduc in France (Barbry, Fouillaud, Grivot, & Reverdy, 2009), as

well as the KEWB experiments at Santa Susana Field Laboratory in California during the 1950's.

While the analysis of a nuclear excursion evolution of a solution criticality event is useful and should be performed in the hopes of developing some easier rule-of-thumb style estimations, a somewhat recent report by McLaughlin includes the statement that “For operations with significant quantities of fissile materials in solution form, there are significant reported experimental data, and more being generated. Practically all site- and process-specific criticality accident characterizations and evaluations should be able to be performed by the direct use of these data. The absence of computer codes and software models of physical processes such as bubble generation does not appear to be an impediment to the implementation of well-founded emergency plans and procedures. On the contrary, it is always preferable to solve issues with directly applicable experimental data, and such data appear to be largely available for solution criticality accidents” (T. P. McLaughlin, 2003).

Indeed, there are many guidelines and regulations in place to prevent the occurrence of an accidental criticality excursion. All sites should be specifically evaluated for conditions pertaining to that site, and a safety analysis report constructed. However, the existence of a more general model for quick and rapid estimations of the consequences of a nuclear criticality excursion resulting from solution materials would be useful in emergency planning. It's with such an application in mind that the work documented within this thesis was completed.

Previous models have been developed in an attempt to predict the consequences of a criticality event in a solution system. This thesis attempts to document those models and analyze the effectiveness and implications of them when compared to both historical and experimental data. Simple empirical models for the estimation of fission yields as well as a more complicated computational model for the evolution of an accident are analyzed, and the applicability of these models is determined. More modern approaches are explored in terms of computational power achievable and information available on the physical properties and parameters involved.

1.2 Definition of Criticality

A system of fissile material may undergo an excursion when both geometric and material conditions allow for a state of criticality, where the number of neutrons removed from the system are equivalent to the number of neutrons generated in the system. This implies that the fission rate and the number of neutrons present in the system at any given time remain steady and unchanging.

Three general states of criticality are typically discussed, those being subcritical, critical, and supercritical. A subcritical system is one in which the neutron generation intrinsic to the system does not exceed the neutron losses, and so the net effect is one of decreasing neutron population and therefore decreasing energy generation. A critical system is the balance of neutron gains within the system equating the neutron losses, which preserves the power of the system and results in a steady-state energy generation. Finally, a supercritical system is defined as the production of neutrons out-competing the loss of neutrons, with the net effect of increasing neutron population and energy generation.

A supercritical system is further separated into delayed and prompt supercriticality. When a nucleus undergoes a fission event, neutrons that are immediately released are termed prompt neutrons, and those that are emitted as part of a decay process from the generated fission fragment are termed delayed neutrons. Delayed neutrons are generated between milliseconds to minutes after the generating fission event, and a delayed supercritical system is used as a control mechanism for standard nuclear reactor operations, because this is a transitional state at which the system can be responded to and reasonably controlled while changing the net energy production. The more extreme case of supercriticality is one in which the system is considered supercritical in response to only prompt neutrons generated by the fission process, known as prompt supercriticality. A prompt supercritical system is a generally uncontrolled excursion that rapidly increases in energy and neutron population, and changes made at this scale are very quickly propagated into system at a rate that is difficult or impossible to react to.

When referring to the state of criticality of a system, a common term used is the effective neutron multiplication factor, also known as k_{eff} . This factor is the resulting eigenvalue from reactor kinetics models, but can be thought of on a high-level approximation as the ratio of neutrons in one instant to the ratio of neutrons in the next. Thus, with a k_{eff} equal to unity, the system is deemed critical. If k_{eff} is less than one, the system is subcritical, and if k_{eff} is greater than one, it is supercritical.

1.3 Characteristics of a Solution Criticality Excursion

Criticality excursions in a solution system have different properties from those in a solid metal or reactor system. While neutronics parameters are initially calculated similarly

under a point reactor kinetics model, the material properties and evolution of the excursion are quite different (T. McLaughlin et al., 2000).

A criticality excursion in a solution system imparts energy directly into the solution material, typically an aqueous acid medium containing some fraction of enriched uranium or plutonium material for a fuel processing or nonreactor facility. The energy deposited into the solution by the fission events of a nuclear criticality can have several different effects on the evolution of the excursion.

Criticality events can result in an increase in temperature of the solution material, which may eventually lead to boiling or chemical dissociation of the materials present within the system. Solution boiling may be a terminating effect of criticality, as material is removed from the system in a gaseous or vapor state, as well as the overall density of the solution system changing to accommodate voids produced by the nucleation process of boiling. The density change from boiling will impact the material properties of the critical solution, causing a negative reactivity coefficient. The rising action of boiling bubbles may also be a terminating effect, pushing the fissile material upwards or away, or causing a mixing action of the involved materials, which may induce negative reactivity feedback and terminate the excursion.

Additionally, ionizing radiation produced by the criticality event may cause the production of radiolytic gas within the solution system (Spiegler, Bumpus, & Norman, 1962), specifically involving the radiolysis of hydrogen and oxygen for aqueous solutions. During a slow transient, radiolytic gases are continually removed in the form of gas bubbles, which nucleate at physical sites such as container walls or cooling coils.

During a fast transient such as that caused by prompt supercriticality, however, this gas cannot diffuse to a nucleation site at a fast enough rate to allow for surface nucleation to be an effective formation mechanism. The alternative is that radiolytic effects due to ionizing energy deposition will eventually overcome the chemical recombination effects, and radiolytic gas will nucleate away from surfaces within the solution at a high enough concentration (Forehand, 1981). Similar to boiling, this gas nucleation has the properties of decreasing reactivity both through overall density reduction, mixing action of solution components, or through physical motion or removal of fissile material.

For extremely rapid reactivity insertions caused by a large amount of material motion or a dramatic geometry change, energy deposition through criticality builds up very rapidly. This can cause a disproportionately large amount of pressure to accumulate within the solution container, causing a pressure-gradient driven expulsion of solution material (T. McLaughlin et al., 2000). This type of event is typically terminated through a combination of density changes and geometry changes caused by splashing and ejection.

In the event that fissile material is not removed from a solution system by the first pulse, a “sloshing” effect can develop that results in repeated criticality events, or multiple pulses of an excursion. As the solution is continually pushed upwards from fission energy deposition having a criticality-termination effect, gravity returns it to a critical geometry and induces a re-criticality. This type of oscillating event normalizes to a plateau of energy deposition, where the rapid transient is overcome and the solution system undergoes a general energy production phase, which typically leads to boiling (Barbry, 1994).

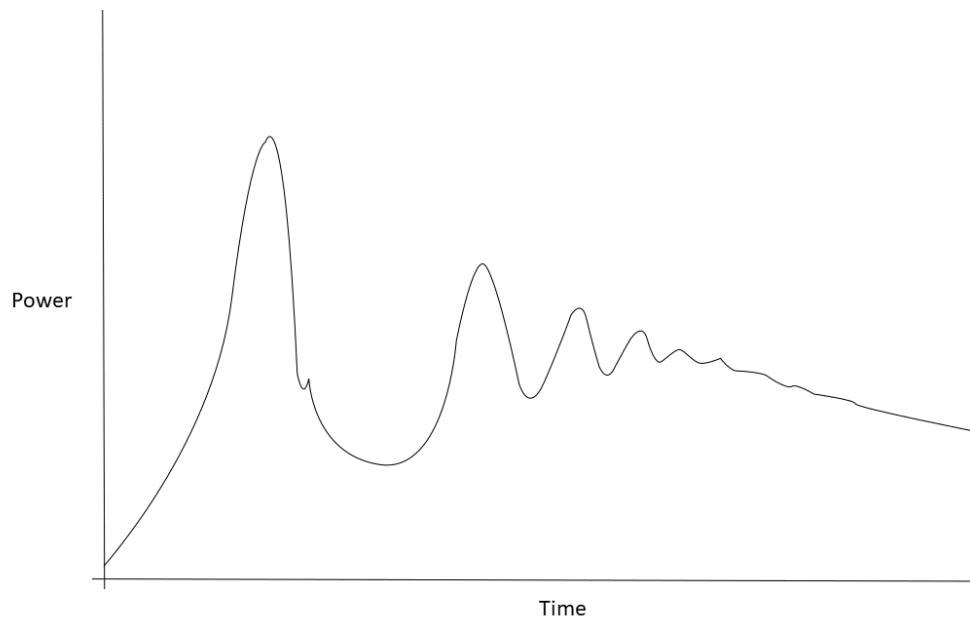


Figure 1-1: Typical Solution System Criticality Excursion

As shown in Figure 1-1, which is a generic trend produced from SILENE data results (Barbry, 1994) (T. McLaughlin et al., 2000), a very generic solution criticality event consists of a first initial spike of power, then by a period of rapid oscillations leading to a power plateau region of relatively constant energy production.

The fissile material seen in processing facilities also takes the form of a powder, which can result in criticality when subjected to a reactivity increase through mixing with water. A criticality event of these initiating conditions has personnel safety implications in situations such as fire-fighting either a powder fire or a facility fire using a water distribution sprinkler system, conventional methods for which will result in a critical “sludge” or mud-like material. Such an excursion has not yet occurred in a processing facility; however, the general consequence estimation should not be drastically affected by a change of initiating events in a scenario like this.

1.4 Open and Closed Systems

A criticality event in a solution-based system can be characterized overall by whether the structure containing the fissile media is considered an open or a closed system. An open system provides an easy avenue for the expulsion or removal of the fissile material from the geometry, either by ejection from the container into the atmosphere or into a separate container configuration of the processing system, such as a feed pipe. A closed system allows no such avenue for material removal, and so the solution system is typically terminated by material changes rather than by geometry changes (DOE, 1994), such as dilution, mixing, evaporation, or human intervention.

An open system tends to be showcased by a single-pulse excursion, and is typically rapidly terminating. The single burst induces a large pressure gradient on the solution material, pushing it away from the system. Historical examples of this effect can be found in the criticality accidents that occurred on July 24, 1964 at the United Nuclear Fuels Recovery Plant in Wood River Junction, Rhode Island; as well as that which occurred on December 10, 1968 at the Mayak Production Association near Chelyabinsk, Russia (T. McLaughlin et al., 2000). An open system or system with connected piping generally has a single-pulse criticality with total fissions not numbering much higher than 1×10^{15} fissions per liter of fissile solution in the container (Barbry, 1987).

A closed system promotes multiple criticality pulses and a longer-lasting nuclear excursion. A historical example of a criticality event being terminated by solution boiling can be seen in the accident that occurred at the Idaho Chemical Processing Plant on October 16, 1959, which terminated after 15 to 20 minutes of boiling following multiple excursions (T. McLaughlin et al., 2000). A closed system tends to have an upper bound

of approximately 1.6×10^{16} fissions generated per liter based on results from solution criticality experiments (Barbry, 1987).

Additionally, extreme examples of criticality excursions in solution materials taking place over an extended period of many hours can be seen in the accidents that occurred at Hanford Works on April 7, 1962; the Novosibirsk Chemical Concentration Plant on May 15, 1997; and the JCO Fuel Fabrication Plant in Tokai-Mura, Japan on September 30, 1999 (T. McLaughlin et al., 2000). These accidents are governed by extenuating environmental circumstances external to the intrinsic solution evolution properties. For example, the JCO Fuel Fabrication Plant accident involved a uranyl nitrate solution that was enclosed in a precipitation vessel and subjected to heat removal via a cooling jacket, which allowed for an extended duration of criticality and a lengthy excursion evolution over the course of 19 hours and 40 minutes.

1.5 General Bounds and Estimation

Solution criticality excursions are bounded by an upper energy release developed by an integrated fission yield of 4×10^{19} total fissions in the case of the excursion that occurred at the Idaho Chemical Processing Plant in October 16, 1959; and by a lower energy release developed by an integrated fission yield of 1×10^{15} total fissions in the case of the accident at Windscale Works in England on August 24, 1970. For a single pulse excursion, the lowest pulse yield from a historical accident in a solution system is 1×10^{16} total fissions, which occurred at the Hanford site on April 7, 1962 as well as at Y-12 in Oak Ridge on June 16, 1958. The highest single pulse yield from a solution accident was approximately 2×10^{17} fissions from the accident at the Mayak Production Association on January 2, 1958 (T. McLaughlin et al., 2000).

Within the bounds of known data, the existence of a general model for estimating the consequences of a criticality excursion in a solution material would be useful for the safety analysis of such a system, and having the ability to quickly estimate the consequences of a criticality excursion could lead to more informed design choices and procedure plans. This thesis is an attempt at both a collection of known analysis techniques for a solution criticality system, as well as an analysis of those techniques. To that end, a literature review consisting of readily-available relevant information was conducted. From this literature review, empirical models developed from experimental data were selected and analyzed for fitness to parameters from historical accidents. Additionally, a computational model was developed and tested against known parameters for these excursions.

Chapter 2 – Summary of Literature Review

To provide a more complete picture of the physics and state of solutions criticality modeling available to the general researcher or personnel safety worker at the time of this writing, a literature review was conducted, the results of which are included within this section. The literature review primarily concerns the energy deposition of criticality excursions, the methods and models used for calculation, and the historical records and precedence for criticality excursions in both accident scenarios and experiments conducted. Many reports and documents were sourced, the most relevant of which are listed here.

2.1 Criticality Accidents and Studies

A Review of Criticality Accidents 2000 Revision (T. McLaughlin et al., 2000)

This 2000 report from Los Alamos National Laboratory is both a technical introduction to the science of a criticality excursion and the evolution thereof, as well as a review of the historical accidents that have occurred. Much of the data for the known accidents was obtained from this document, and it was treated as the primary source of information in the event of conflicting information such as accident fission yield, due to both its thorough documentation and its relative modernity in reporting the information to date.

Specifically, accident geometries, fission yields, and durations were obtained from this document, as well as the implications and damage produced by the accidents. The first segment of this report covers processing accidents and solution excursions in detail, while the remaining sections discuss reactor accidents and critical assembly excursions that have occurred at various facilities in the past.

It should be noted that this document is considered to be the most current version of a chain of documents pertaining to the chronicling of criticality accidents as of the time of this writing, beginning with “A Review of Criticality Accidents” by William Stratton (Stratton, 1967), which was later revised by David Smith (D. Smith & Stratton, 1989). The current version includes additional information not known at the time of Smith’s revision pertaining to one Japanese accident and 19 Russian accidents.

Process Criticality Accident Likelihoods, Consequences, and Emergency Planning

(T. P. McLaughlin, 1991)

McLaughlin describes criticality accidents in several configurations and material types, as well as uses the evolution of CRAC experiment 19 as an example of the typical evolution expected from a criticality excursion in a solution system. No guiding models or analysis techniques for a solution excursion are discussed, but an argument is made for a case-specific analysis for an incidental criticality event rather than adopting simplistic values such as those tabulated within the document. However, tabulated values for the expected fission yields of various systems are included for reference, and are reported here in Table 2-1.

Table 2-1: Criticality Accident Fission Yields (T. P. McLaughlin, 1991)

System Description	Burst Yield (fissions)	Total Yield (fissions)
Solutions under 100 gallons	1×10^{17}	3×10^{18}
Solutions over 100 gallons	1×10^{18}	3×10^{19}
Liquid/Powder	3×10^{20}	3×10^{20}
Liquid/Metal Pieces	3×10^{18}	1×10^{19}
Solid Uranium	3×10^{19}	3×10^{19}
Solid Plutonium	1×10^{18}	1×10^{18}
Large Storage Arrays (< Prompt Critical)	–	1×10^{19}
Large Storage Array (> Prompt Critical)	3×10^{22}	3×10^{22}

SILENE Reactor Results of Selected Typical Experiment (Barbry, 1994)

This document specifically pertains to the evaluation of data from experiments conducted at the SILENE facilities. Much of the technical data for the SILENE reactors, including material composition, geometry, and expected yields are contained within this document.

This document is primarily a summary and data report for the SILENE reactor experiments, with an emphasis on developing commonalities between the conducted experiments to develop a “typical” excursion from the solution reactor.

Review of the CRAC and SILENE Criticality Accident Studies (Barbry et al., 2009)

Barbry’s 2009 report revisits much of the information learned during the CRAC and SILENE experimental studies conducted in France. This report showcases the evolution of a solution excursion under experimental conditions, and reports on the neutronic parameters such as reactivity insertion and period of evolution, as well as the thermal-hydraulic parameters such as pressure increase and duration of evolution.

Process Criticality Accident Likelihoods, Magnitudes, and Emergency Planning – A

Focus on Solution Accidents (T. P. McLaughlin, 2003)

This conference paper presents an argument for the redesign of emergency planning for criticality accidents based on the then-recent publication of previously unreported criticality accidents, primarily those occurring in Russia. The same model as previously covered in Barbry's work (Barbry, 1987) is presented, further details of which can be found in the Empirical Models section of this document.

2.2 Fission Yield Estimations

Nuclear Criticality Safety – Estimation of the Number of Fissions of a Postulated Criticality Accident (ISO, 2011)

This document contains a tabulated summary of criticality accidents that have occurred, which has been verified against the data present in the 2000 report of historical criticality accidents (T. McLaughlin et al., 2000). Also contained within are details on the primary features of experimental solution facilities, experimental metal facilities, and experimental heterogeneous facilities. These are very basic overviews of these facilities, and details on individual experiments performed are not given.

Many simplified formulae are also listed, including those seen in previously reviewed documents and those contained in the Empirical Models section of this document.

Between listed boundaries on fission yields for experimental facilities and the given simplified correlations, this document has a wealth of information for fission yield determination, both in terms of the simple duration and volume based empirical models, and more complicated models involving further parameters of the accident characteristics and geometries.

Simplified Methods of Estimating the Results of Accidental Solution Excursions

(Tuck, 1974)

Tuck makes use of the data from six solution criticality accidents that have occurred and from the KEWB and CRAC experiments to posit models for the characterization of solution accidents, one of which pertains to the number of fissions in any five-second interval for a uranium-specific solution, and one of which pertains to the total number of fissions for both uranium and plutonium solutions. These models are shown in the Empirical Models section of this report.

Tuck validates these models against a simplified code system named EXCUR developed at Rocky Flats, which is used to compute the variation of power during the first spike of a solution excursion based on calculated shutdown coefficients, as well as using data from both the CRAC and KEWB experiments to model the evolution of an excursion.

Empirical Method for Estimating the Total Number of Fissions from Accidental Criticality in Uranium and Plutonium Systems (Olsen, Hooper, Uotinen, & Brown, 1974)

Olsen posits several models for estimation of the accident fission yield within this document. The first model presented is based on data from the CRAC experiments in France, and contains an estimate for the total fission yield in the plateau region of a criticality excursion evolution, and in the burst region. The total yield of the overall excursion can be calculated by the summation of those two values. This model is explored further in the Empirical Models section of this report.

Olsen also notes that the models contained within this document may be applied to a plutonium system, but the predicted fission yield values will be conservatively high due to the presence of Pu-240, which undergoes spontaneous fission. The same conservatism should be expected for a slightly enriched uranium solution system, due to the higher concentration of U-238.

United States Nuclear Regulatory Commission Regulatory Guides 3.33, 3.34, and 3.35 (USNRC, 1977), (USNRC, 1979a), (USNRC, 1979b)

Several US NRC Regulatory Guides were also sourced for the purposes of establishing a reasonable estimation on how to evaluate solution criticality within a nonreactor facility. It must be noted that at the time of this writing, these reports have been officially withdrawn beginning in December of 1997, with the intention of being superseded by Regulatory Guide 3.71. However, Regulatory Guide 3.71, as of Revision 2 to that document, contains no further mention of the foundational hypothetical accident scenario as described in these regulatory guides. As of the time of Revision 2 to Regulatory Guide 3.71, the accident scenarios are now based on information described in Appendix C of ANSI/ANS standard number 8.23 (ANS, 2007).

The hypothetical accident described within these documents and used as an establishing parameter for a regulatory position is based on the following stipulations:

- Ventilated cell with shielding equivalent to 5 feet of concrete of 142 pounds per cubic foot density
- Initial burst of 1×10^{18} fissions in 0.5 seconds, followed by 47 bursts of 1.9×10^{17} fissions at ten-minute intervals for eight hours

- Termination by evaporation of 100 liters of a solution containing 400 grams per liter of uranium at less than 5% enrichment
- Concentrations of fission products and transuranics in the solution corresponding to irradiated fuel assuming 100% dilution, plus those produced within the incident
- Noble gases are assumed to be removed prior to the incident

Based on comparisons with the known parameters and evolution characteristics for historical and experimental excursions, this hypothetical system is believed to be unsuitable for analysis, and non-representative of a typical solution excursion system. The incredible hypothetical accident in combination with the supersession of these reports should be taken into account for any analysis purposes.

Airborne Release Fractions/Rates and Respirable Fractions for Nonreactor Nuclear Facilities (DOE, 1994)

The originating document for this project was a proposed revision to Chapter 6 of this DOE handbook. Chapter 6 specifically refers to the existence of respirable fractions and radiological releases pertaining to criticality excursions, consisting of both metallic and solution systems. This document details the evidence of respirable fractions and airborne release of material from these accidents, and contains simplified data on the estimation of fission yields from given accidents.

Model to Estimate the Maximum Fission Yield in Accidental Solution Excursions
(Barbry, 1987)

This document was produced by Francis Barbry from the CEA de Valduc (Valduc Center for Nuclear Studies) in France, following his work with the CRAC and SILENE experiments. Barbry promotes the utility of a simple model for estimation of the effective fission yield of a criticality excursion in a solution system, and based on CRAC and SILENE data, posits a relationship dependent on the volume of the solution and on the duration of the excursion. This relationship is presented in more detail within the Empirical Models section of this report.

Within this document, Barbry also posits the existence of a boiling threshold that occurs at approximately 1×10^{16} fissions per liter. Once this value is reached within an excursion evolution, boiling of the solution begins, which leads to a decrease in the overall density and can contribute to criticality termination. The figure developed by Barbry provides the accident evolution model and the boiling threshold is included in this

document as Figure 2-1 for reference purposes.

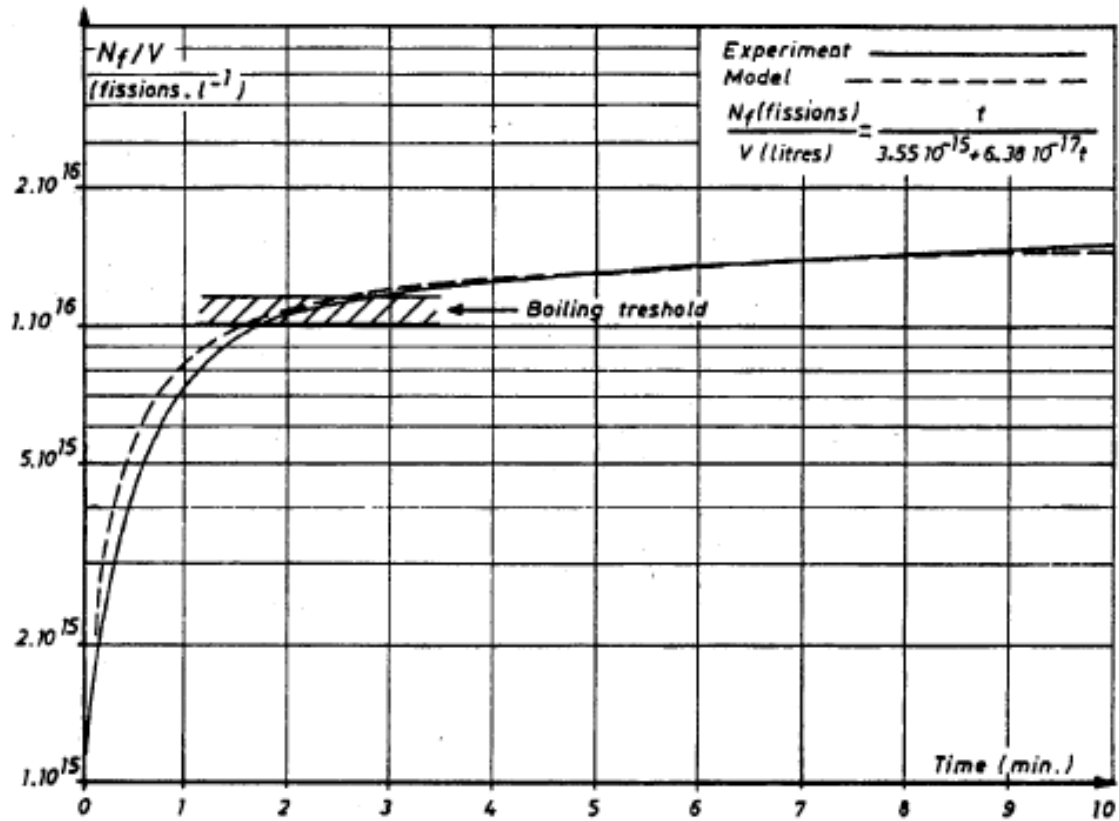


Figure 2-1: Specific Fission Yields in Experiments at CRAC and SILENE (Barbry, 1987)

Simplified Evaluation Models for Total Fission Number in a Criticality Accident

(Nomura & Okuno, 1995)

Nomura and Okuno develop a thermal property analysis of CRAC experiments and ten processing accidents to showcase a reliance on solution boiling for the overall fission yield expected from a criticality excursion in a solution system. A model for both a boiling and for a non-boiling solution are developed that are dependent only on solution volume, which are detailed in the Empirical Models section of this report.

Additionally, models for the characterization of a fuel-rod water system accident are developed using similar liquid boiling properties, which are validated against experimental data from SPERT, a low-enriched pressurized water reactor.

Applicability of Simplified Methods to Evaluate Consequences of Criticality

Accident Using Past Accident Data (Nakajima, 2003)

Nakajima develops a tabulated listing of criticality accidents that have occurred in nuclear fuel processing plants known at the time of writing. This includes 13 accidents from Russia, seven from the USA, one from the UK, and one from Japan. Using these data, Nakajima provides a comparison between simplified fission yield correlations established by Tuck, Olsen, Barbry, and Nomura.

Nakajima concludes that Nomura's formula and Barbry's formula with infinitive duration agreed fairly well with known data for solution accidents as a function of solution volume. Olsen's formula and Barbry's formula as a function of duration reproduce the upper envelope with the exception of the Idaho Chemical Processing Plant accident in October of 1959 and the Tokai-Mura accident in September of 1999. The conclusion is made that because the Tokai-Mura accident underwent a solution cooling process that produced a large amount of power for a long time, a new formula would be required that takes this into account.

2.3 Excursion Modeling

A Review of the SILENE Criticality Excursions Experiments (Barbry, 1993)

This report is a fairly detailed, though non-exhaustive account of the data seen in the SILENE experiments. The first table in the report contains first peak and total fission values for select experiments, as well as other information such as duration, volume, doubling time, pressure change, total potential reactivity addition, and temperature change.

Using the maximum energies measured during the CRAC and SILENE excursions for up to a seven dollar reactivity insertion, an empirical equation in terms of the specific total number of fissions and the excursion duration is given, which is the same model developed by Barbry as detailed in the Empirical Models section of this report.

Barbry reports that the volume of radiolytic gas formed during the course of a solution excursion is proportional to the number of fissions, reaching $\sim 1.1 \times 10^{-13}$ cubic centimeters per fission (i.e., 110 liters of gas for 10^{18} fissions). The threshold for the formation of radiolysis bubbles is estimated at 1.5×10^{15} fissions per liter of fissile solution. The solution is assumed to be brought to a boiling point at a released energy level of about 0.33 Megajoules per liter, or $\sim 1.1 \times 10^{16}$ fissions per liter. The level of the boiling pseudo-plateau described in the paper is marked as dependent on the amount of excess reactivity present in the system.

Production of Void and Pressure by Fission Track Nucleation of Radiolytic Gas Bubbles During Power Bursts in a Solution Reactor (Spiegler et al., 1962)

This report contains a lot of information on the development of radiolytic gas generation models, primarily based on data from the KEWB experiments. Reactivity coefficients and feedback models for void production in solution criticality systems are discussed within this document, and several values for gas production coefficients are provided for both spherical cores and cylindrical cores in the form of volume of gas produced per unit of energy deposited into the system.

The fluid dynamics of the gas bubbles in the solution system are discussed, as well as assumptions involving the uniform radius of radiolytic gas bubbles and that the bubbles are in equilibrium with both the dissolved gas concentration and the solution properties. Many of these assumptions were accounted for in the Computational Model section of this document.

Nuclear Excursions in Aqueous Solutions of Fissile Materials (Hetrick & Smith, 1987)

This conference paper is a short summary of work performed by David Hetrick and Adrienne Smith, a more complete picture of which can be found within Smith's published master's thesis (A. Smith, 1989). This model is based on a simple axial discretization of a cylindrical solution reactor, where the volume is governed by equations of state derived from quasi-steady state thermodynamics related to the isobaric and isothermal compressibility factors.

Hetrick and Smith rely on the usage of neutronics models to calculate changing reactivity with a changing cylindrical height and diameter, and so the system is propagated via a displacement scheme, which alters the overall feedback of the system. Additional

information is provided for the radiolytic gas models, the majority of the details of which can be found in the Computational Model section of this document.

Estimating Maximum Pulse Yields for Solution Criticality Accidents (Hetrick & McLaughlin, 1993)

Hetrick and McLaughlin present a reactivity calculation based on the Nordheim-Fuchs model of point reactor kinetics and the inhour equation of neutron population to determine the evolution of a solution-based criticality accident. Being a short document from conference proceedings, little is given in the form of calculational details, but the principles of the Nordheim-Fuchs model were used for the Computational Model section of this document.

The Code CRITEX to Simulate Transient Criticality in Fissile Solutions (Bickley, Mather, & Shaw, 1987)

An overview of the calculational capability of the CRITEX code is provided within this conference paper. CRITEX as described takes a known power profile as input and relies on numerical integration of reactivity feedback due to radiolytic gas generation and the Doppler effect of nuclear cross-section evolution with temperature. CRITEX is also described as allowing for the mixing of gas and averaging of temperature, as well as for the water vapor production via boiling of the solution.

Simulation of Criticality Accident Transients in Uranyl Nitrate Solution with COMSOL Multiphysics (Hurt, Pevey, & Angelo, 2012)

This conference paper by Hurt, Pevey, and Angelo describes a coupled solver using COMSOL multiphysics models along with MCNP to allow for the adjustment of reactivity due to temperature feedback and radiolytic gas generation effects. The computational model is analyzed against experimental results for a 50 cent reactivity insertion in the SILENE core.

2.4 Conclusions of Literature Review

While many empirical models have been developed based on experimental values, the state of a Monte Carlo applicable computational modeling system useable by a safety worker or the general public could not be directly ascertained. For the most part, such code systems are developed as part of a contract with either specific applications in mind, or as a general research experiment for the purposes of emulating a known power profile to be used as an input parameter for those simulations. A code system that is able to dynamically evolve an excursion based solely on material properties that can be determined from the solution in use at a generic processing facility is not readily available.

Chapter 3 – Estimation of Fission Yield

Several avenues of analysis for the evolution and expected yield of solution criticalities were evaluated in the process of this work. Empirical models that have been proposed as the results of previous work performed on experimental data were applied to known accident scenarios, and two accurate models can be assumed to be bounding: the model provided by Barbry being a generally accurate conservative estimate of the fission yield and the uranium model provided by Tuck being a generally accurate under-estimation of the fission yield.

3.1 Empirical Models

Several examples of simplified models for criticality fission yield determination can be found in the ISO Standard 16117 (ISO, 2011). Only the models involving simple, easily determined quantities such as volume, mass, and duration were considered useful for analysis purposes, as it's less likely that a processing facility or other host facility of a fissile solution media will know quantities such as reactivity insertion rate at the time of a criticality excursion. Most of the models described within the ISO Standard 16117 were discarded for reasons of complexity when describing a typical solution processing accident.

The models discussed were fit to the historical accident data, and compared for accuracy. The accidents used in this analysis (T. McLaughlin et al., 2000) are shown in Table 3-1.

Table 3-1: Accidents Analyzed via Empirical Models

Location	Date	Chronological Number	Fissile Media	Approximate Total Fission Yield
Mayak Production Association	3/15/1953	1	Pu	2.0×10^{17}
Mayak Production Association	4/21/1957	2	U(90)	1.0×10^{17}
Mayak Production Association	1/2/1958	3	U(90)	2.0×10^{17}
Oak Ridge Y-12 Plant	6/16/1958	4	U(93)	1.3×10^{18}
Los Alamos Scientific Laboratory	12/30/1958	5	Pu	1.5×10^{17}
Idaho Chemical Processing Plant	12/30/1958	6	U(91)	4.0×10^{19}
Mayak Production Association	12/5/1960	7	Pu	2.5×10^{17}
Idaho Chemical Processing Plant	1/25/1961	8	U(90)	6.0×10^{17}
Siberian Chemical Combine, Tomsk	7/14/1961	9	U(22.6)	1.2×10^{15}
Hanford Works	4/7/1962	10	Pu	8.0×10^{17}
Mayak Production Association	9/7/1962	11	Pu	2.0×10^{17}
Siberian Chemical Combine, Tomsk	1/30/1963	12	U(90)	7.9×10^{17}
Siberian Chemical Combine, Tomsk	12/2/1963	13	U(90)	1.6×10^{16}
Wood River Junction, Rhode Island	7/24/1964	14	U(93)	1.3×10^{17}
Electrosta Machine Building Plant	11/3/1965	15	U(6.5)	1.0×10^{16}
Mayak Production Association	12/16/1965	16	U(90)	5.5×10^{17}
Mayak Production Association	12/10/1968	17	Pu	1.3×10^{17}
Windscale Works	8/24/1970	18	Pu	1.0×10^{15}
Idaho Chemical Processing Plant	10/17/1978	19	U(82)	2.7×10^{18}
Siberian Chemical Combine, Tomsk	12/13/1978	20	Pu metal	3.0×10^{15}
Novosibirsk Chemical Concentration Plant	5/15/1997	21	U(70)	5.5×10^{15}
JCO Fuel Fabrication Plant	9/30/1999	22	U(18.8)	2.5×10^{18}

Within this document, these accidents will be referred to by their chronological number. It is also important to note that accident Number 21, occurring at the Novosibirsk Chemical Concentration Plant on May 15, 1997, has an unknown volume and fissile composition. The implication is that while accident Number 21 is a historic accident involving solutions processing of a fissile material, it is not able to be correctly modeled using any of the empirical methods following due to a lack of relevant information. It is assumed that any current or future processing facility will have knowledge of the solution volume and relevant instrumentation for determination of the excursion duration. Also of import is that accident Number 20, occurring at the Siberian Chemical Combine in Tomsk on December 13, 1978 is a plutonium metal ingot accident and does not involve a solution system. Accident 20 is the only accident involving a metal system, and as such is not included in the analysis process for these models, as other metal system accidents that have historically occurred are either critical assemblies for experimentation or moderated reactor systems.

The empirical formulae analyzed are primarily based upon physical parameters of the accidents, specifically the volume of the fissile solution in liters and duration of the excursion in seconds if known. These parameters are detailed in Table 3-2, along with the fissile density for characterization purposes (T. McLaughlin et al., 2000). For those accidents where the excursion duration is limited to less than one minute, a value of 10 seconds is substituted for the models that rely upon excursion duration, as this provides a reasonable estimation of the fission yields as well as being a reasonable estimation time for the evolution of a burst excursion (T. McLaughlin et al., 2000). Also included in Table 3-2 is the ranking of the accident by a fission yield number in increasing order,

with the accidents having the largest fission yield being higher numbered than those with a lower fission yield.

Table 3-2: Physical Parameters for Empirical Models

Accident Number	Solution Volume (L)	Fissile Density (g/L)	Duration (s)	Yield Number	Approximate Total Fission Yield
1	31	26.1	< 1 min	13	2.0×10^{17}
2	30	102	600	7	1.0×10^{17}
3	58.4	376.7	< 1 min	12	2.0×10^{17}
4	56	37.5	1200	19	1.3×10^{18}
5	160	18.4	< 1 min	10	1.5×10^{17}
6	800	38.6	1200	22	4.0×10^{19}
7	19	44.7	6600	14	2.5×10^{17}
8	40	180	180	16	6.0×10^{17}
9	42.9	39.2	< 1 min	2	1.2×10^{15}
10	45	28.7	135000	18	8.0×10^{17}
11	80	15.8	6000	11	2.0×10^{17}
12	35.5	63.9	37200	17	7.9×10^{17}
13	64.8	29.8	57600	6	1.6×10^{16}
14	41	50.5	5400	9	1.3×10^{17}
15	100	36.5	< 1 min	5	1.0×10^{16}
16	28.6	69.2	25200	15	5.5×10^{17}
17	28.8	52.1	900	8	1.3×10^{17}
18	40	51.8	10	1	1.0×10^{15}
19	345.5	19.3	7200	21	2.7×10^{18}
20	0.54	18700	< 1 min	3	3.0×10^{15}
21	unknown	unknown	97500	4	5.5×10^{15}
22	45	69.3	70800	20	2.5×10^{18}

It is also important to note that accidents 9, 13, 15, and 18 are considered general outliers for all tested models, due to a relatively small number of fissions in comparison to values for other accidents. The characterization of these accidents as outliers is considered to lend conservatism to the models discussed, and relative model accuracy will be analyzed without taking into account the reported fission yields of these accidents. For the tables of results shown for each model, these outlier accidents will be highlighted. Because these

accidents have a low yield of fissions, neglecting them from analysis is considered a conservative approach to maintaining relative accuracy for each model.

For each model analyzed, a visualization of the data both with and without the outlier accidents specific to that model is presented. These visualizations are presented on a semi-logarithmic plot area where the y-axis is a ratio of the calculated fission yield to the expected fission yield. For ease of use in reading these figures, a line is drawn through the point of perfect accuracy, or through the points where the y-axis aligns to $y = 1 \times 10^0 = 1.0$, showing that all points with values above this line are overpredicted by the model in question, and all points with values below this line are underpredicted by the model. This allows for a rough visualization of the conservatism for each model analyzed.

The models analyzed are presented in chronological order, where the results can be seen from Olsen's Model (1974), Tuck's Model (1974), Barbry's Model (1987), and Nomura's Model (1995) in the following sections.

3.1.1 Olsen's Model

Olsen, Hooper, Uotinen, and Brown developed a model of measuring both the burst and plateau fission yield for an excursion involving a uranium or plutonium solution (Olsen et al., 1974). The burst fissions are represented by N_B and the plateau fissions are represented as N_P in Equations 3.1 and 3.2. As is the case with other models analyzed, V is the volume of the solution in liters and t is the duration of the excursion in seconds. For this model, the duration of the burst yield is considered to be negligible, whereas the full duration of the accident is used for the plateau

definition.

$$N_B = 2.95 \times 10^{15} \cdot V^{0.82} \quad (3.1)$$

$$N_P = 3.2 \times 10^{18} \cdot (1 - t^{-0.15}) \quad (3.2)$$

The total fission yield N_f of the excursion is then represented by the sum of the burst and plateau yields, as shown in Equation 3.3.

$$N_f = N_B + N_P \quad (3.3)$$

The approximate results of this model are shown in Table 3-4. Because the burst fission yield is not known for all historical accidents, the percent difference is calculated with respect to the total yield of the accident for comparison purposes.

The average percent yield of the total fission yield as estimated by Olsen's model is 599 %. This shows a trend of over prediction with a high degree of conservatism with exception to very large yields like that posed by Number 6, but is not considered to be a particularly accurate estimation.

For comparison, graphical representations of the results of Olsen's model are included as Figures 3-1 and 3-2, as a ratio of the calculated fission yield to the reported fission yield with respect to the chronological ordering of the accidents. Figures 3-3 and 3-4 contain the data with the accidents ordered by the reported fission yield.

Table 3-3: Results of Olsen's Model

Accident Number	Burst Percent Difference	Plateau Percent Difference	Total Percent Difference
1	-75	634	658
2	-52	1874	1922
3	-58	634	675
4	-93	61	67
5	26	878	1005
6	-98	-94	-92
7	-86	837	851
8	-89	188	198
9	5261	122273	127634
10	-91	232	240
11	-46	1066	1119
12	-93	221	228
13	463	16036	16600
14	-52	1683	1731
15	1187	14584	15872
16	-91	354	362
17	-64	1474	1509
18	5974	93357	99431
19	-87	-12	-1
22	-97	4	6

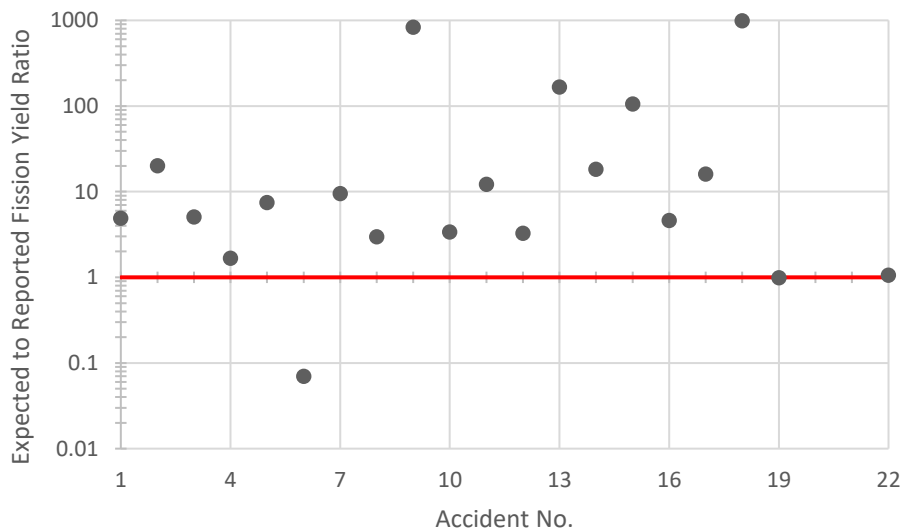


Figure 3-1: Olsen's Model – Chronological (With Outlier Data)

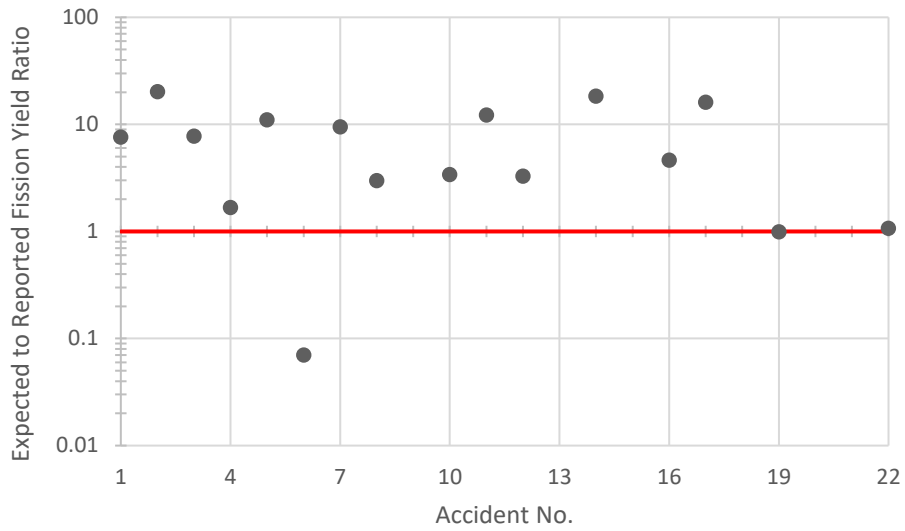


Figure 3-2: Olsen’s Model – Chronological

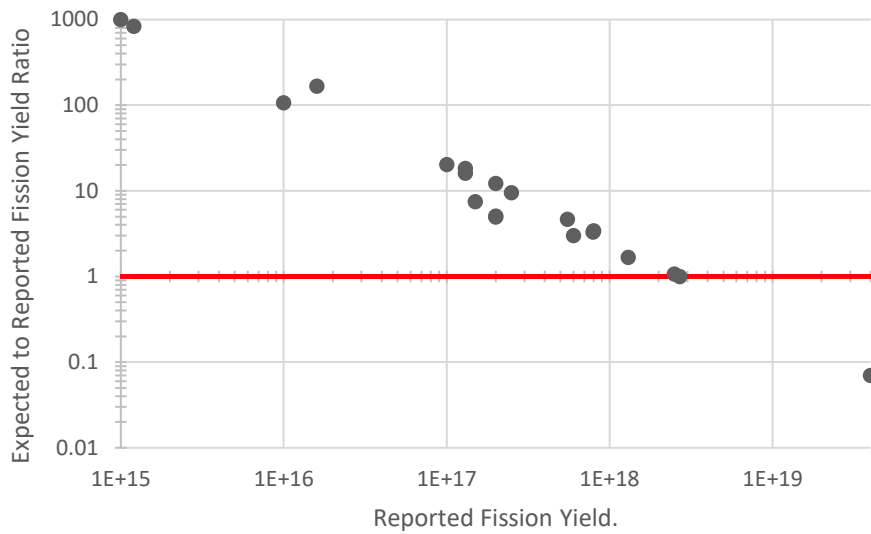


Figure 3-3: Olsen’s Model – Yield-Ordered (With Outlier Data)

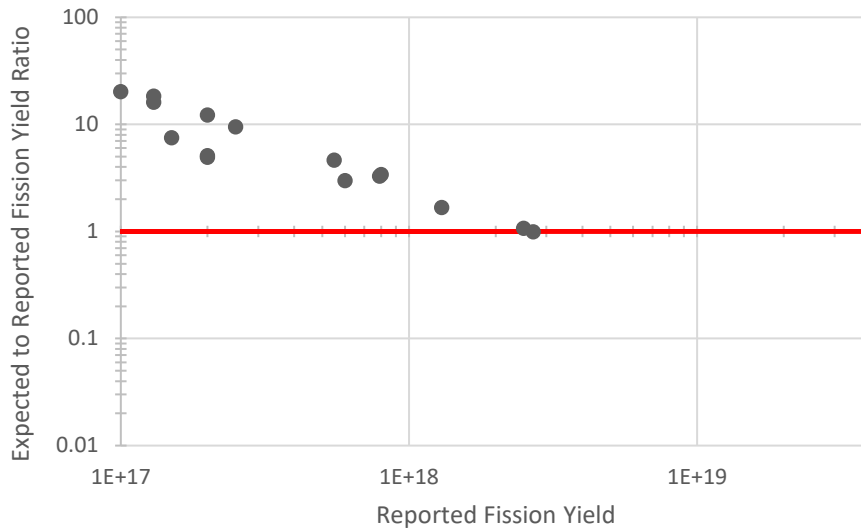


Figure 3-4: Olsen’s Model – Yield-Ordered

3.1.2 Tuck’s Model

Tuck develops correlations that are largely based on the KEWB and CRAC experiments for analyzing solution system excursions (Dunenfeld & Stitt, 1963). Tuck posits several formulae (Tuck, 1974), the simplest being that shown in Equation 3.4, which was what was used for estimation purpose in the previous version of the DOE Handbook (DOE, 1994). As with other models analyzed, N_f represents the integrated fission yield and V represents the solution volume in liters.

$$N_f = 10^{17} \cdot V \tag{3.4}$$

Correlations specific to both uranium and plutonium solution systems are also posed, however the plutonium solution system is considered relatively complex, being reliant on the solution volumetric feed rate, and so was not considered for analysis purposes of a simple model. The uranium correlation shown in Equation 3.5 was analyzed against all accident systems.

$$N_f = 2.4 \times 10^{15} \cdot V \quad (3.5)$$

The results of the Tuck correlations are showcased in Table 3-6, where the percent difference measures the difference between the calculated fission yield and the reported fission yield as compared to the reported fission yield.

Table 3-6: Results of Tuck's Model

Accident Number	General Solution Model Percent Difference	Uranium Solution Model Percent Difference
1	1450	-62
2	2900	-28
3	2820	-29
4	330	-89
5	10566	156
6	100	-95
7	660	-81
8	566	-84
9	357400	8480
10	462	-86
11	3900	-4
12	349	-89
13	40400	872
14	3053	-24
15	99900	2300
16	420	-87
17	2115	-46
18	399900	9500
19	1068	-71
22	80	-95

The general solution model shows a large amount of over-prediction, having an average percent error of 1927 % neglecting the outlier accidents. The model that Tuck poses for uranium systems shows a general trend of under-prediction, with an average percent difference of -51 %, indicating also a high degree of accuracy. Tuck's uranium model is therefore considered to be both accurate and an under-prediction.

For both of these models, accident Number 5 is shown as a general over-estimate.

Because these models are dependent on the volume of the system, and accident Number 5 is an organic plutonium solution occurring at the Los Alamos Scientific Laboratory on December 30, 1958 with an exceptionally large fissile volume, this is considered somewhat atypical for an accident scenario modeled in these parameters. The general criticality excursion in a solution would be considered to occur without the use of a multi-layered solution and induced via stirring. For such conditions, an alternative bounding model should be considered.

Visualization of the general solution model can be seen in Figure 3-5 with the outlier data and in Figure 3-6 without the outlier data in chronological order, and in Figure 3-7 and Figure 3-8 by reported fission yield with and without outlier data, respectively. A visualization of Tuck's model for uranium solutions fit to general accidents can be seen in Figure 3-9 with the outlier data and in Figure 3-10 without the outlier data in chronological order, and in Figure 3-11 and Figure 3-12 with and without the outlier data by fission yield number.

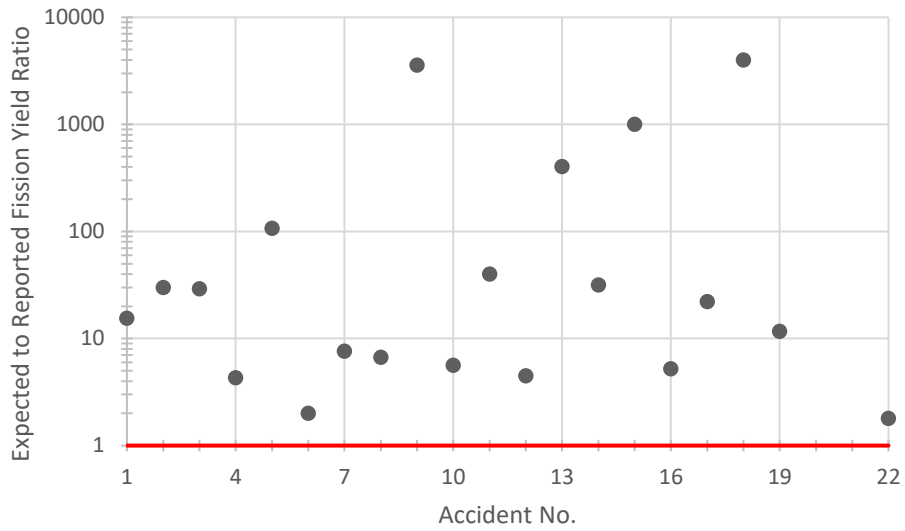


Figure 3-5: Tuck's General Solution Model – Chronological (With Outlier Data)

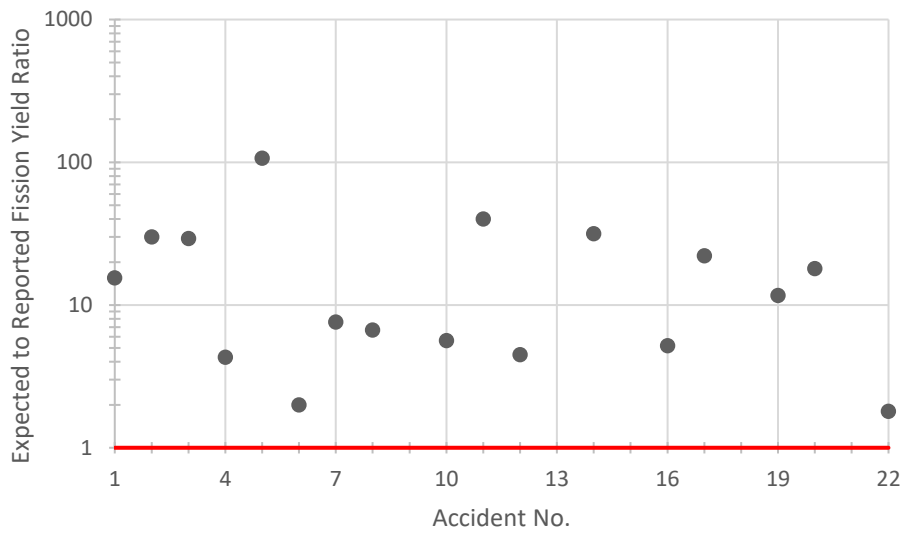


Figure 3-6: Tuck's General Solution Model – Chronological

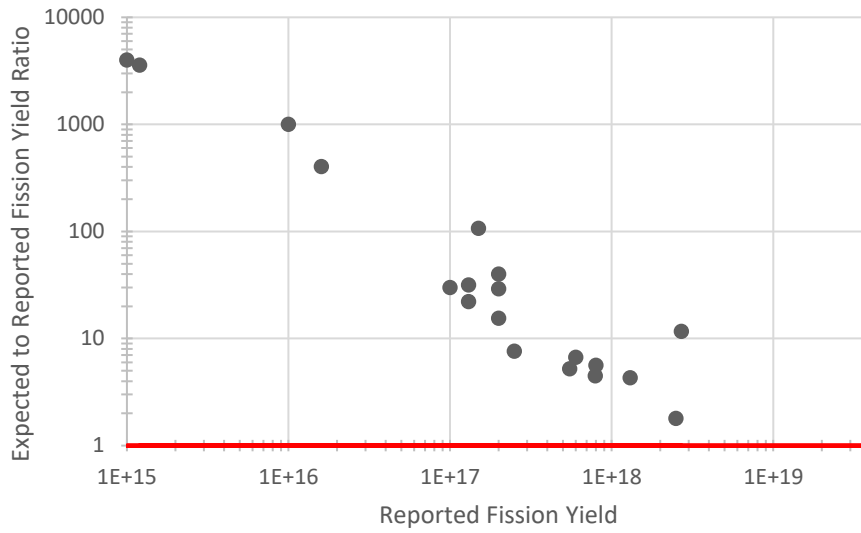


Figure 3-7: Tuck’s General Solution Model – Yield-Ordered (With Outlier Data)

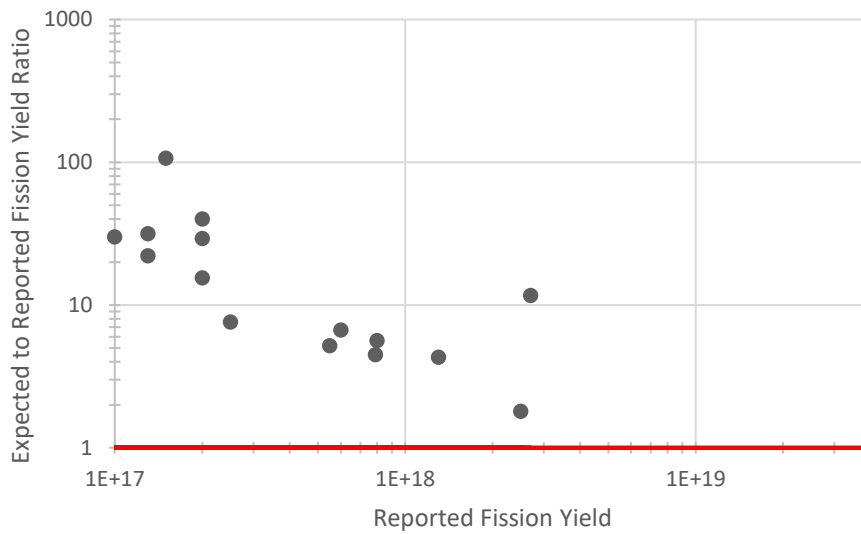


Figure 3-8: Tuck’s General Solution Model – Yield-Ordered

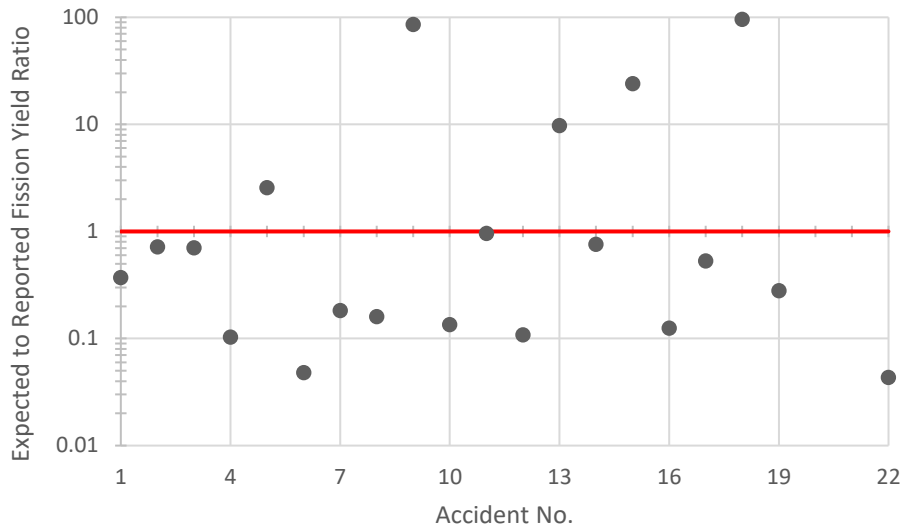


Figure 3-9: Tuck's Uranium Model – Chronological (With Outlier Data)

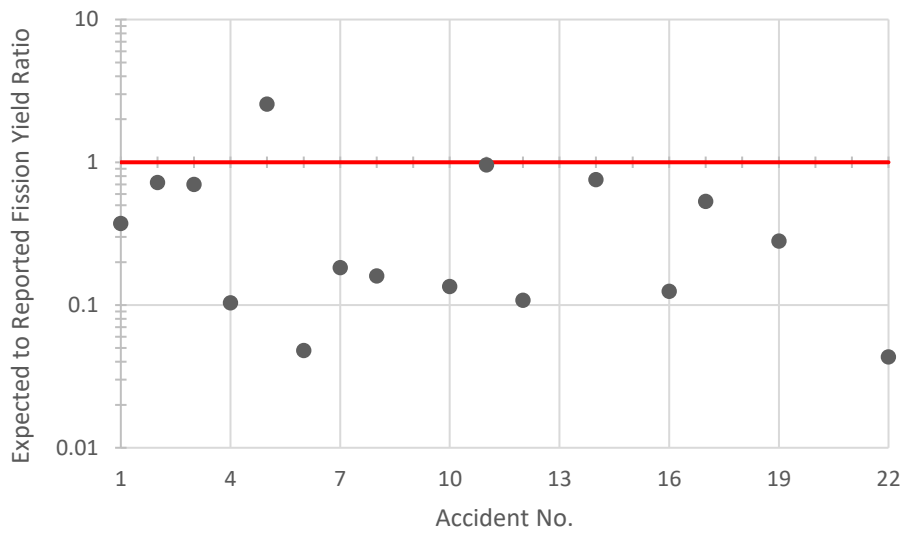


Figure 3-10: Tuck's Uranium Model – Chronological

3.1.3 Barbry’s Model

One of the four simple models analyzed was that presented in “Model to Estimate the Maximum Fission Yield in Accidental Solution Excursions” by Francis Barbry (Barbry, 1987). Based on the CRAC and SILENE experiments, Barbry provides the empirical model shown in Equation 3.6, where N_f is the total fission yield, t is the duration of the excursion in seconds, and V is the volume of the solution in liters.

$$N_f(t) = \frac{t}{3.55 \times 10^{-15} + 6.38 \times 10^{-17} \cdot t} \cdot V \quad (3.6)$$

This equation for the total fission yield provides the results showcased in Table 3-7.

Table 3-7: Results of Barbry’s Model

Accident Number	Percent Difference
1	26
2	330
3	137
4	-35
5	767
6	-70
7	18
8	-20
9	28972
10	-11
11	521
12	-29
13	6241
14	389
15	8032
16	-18
17	227
18	9451
19	81
22	-71

Neglecting the small-yield outlier accidents 9, 13, 15, and 18, the average percent difference of this formula is 85 %, showing a general trend of overestimation of reported yields, with the underestimation values being relatively small. This formula is therefore believed to be the closest approximation of both conservatism and accuracy.

The graphical representation of Barbry’s formula applied to the chronological accidents can be seen in Figures 3-13 and 3-14. These data are plotted on a semi-logarithmic scale where the y-axis is the ratio of calculated fission yield to reported fission yield, such that any values above $y = 1 \times 10^0 = 1.0$, are overpredicted, and any values below 1.0 are underpredicted. The data both with and without the outliers is shown. Barbry’s formula ordered by the reported fission yield value is shown in Figure 3-15 and 3-16, with and without the outliers, respectively.

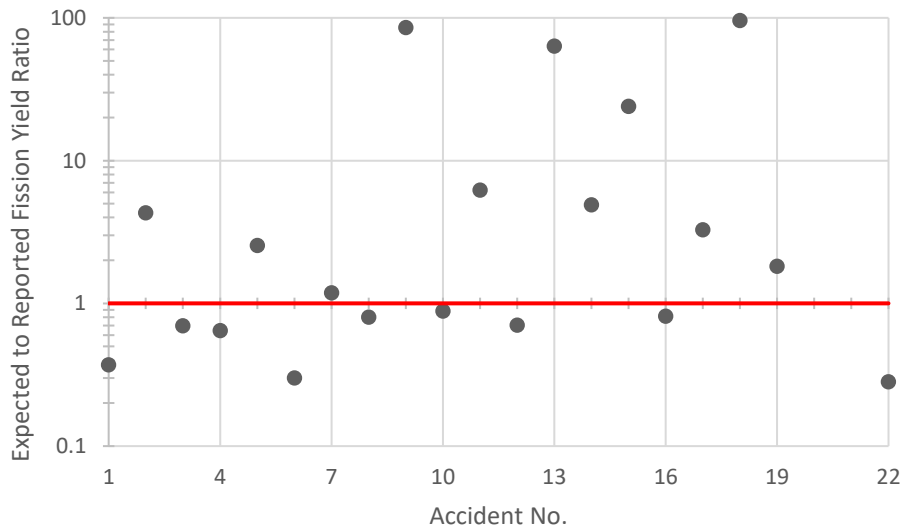


Figure 3-13: Barbry’s Model – Chronological (With Outlier Data)

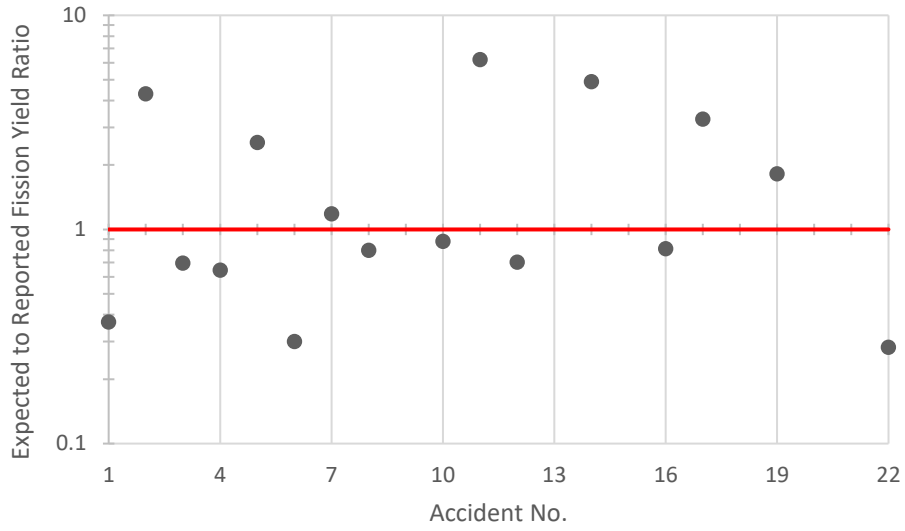


Figure 3-14: Barbry’s Model – Chronological

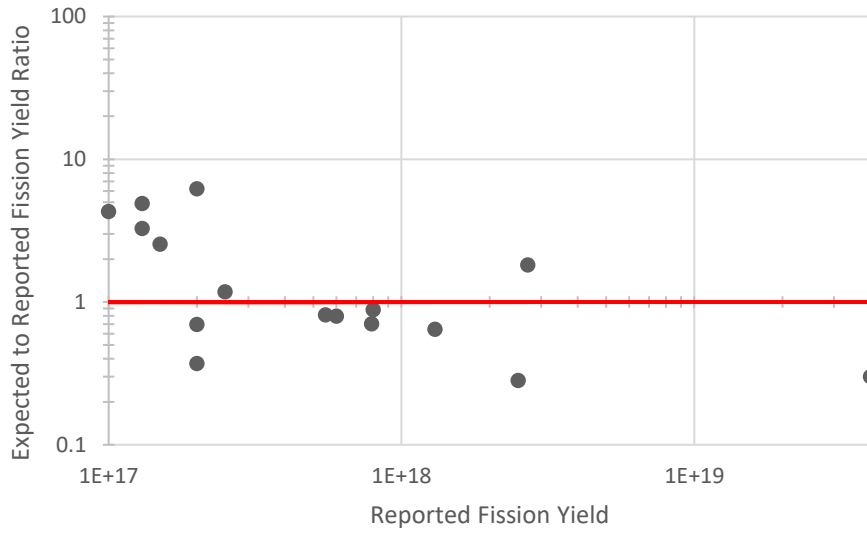


Figure 3-15: Barbry’s Model – Yield-Ordered (With Outlier Data)

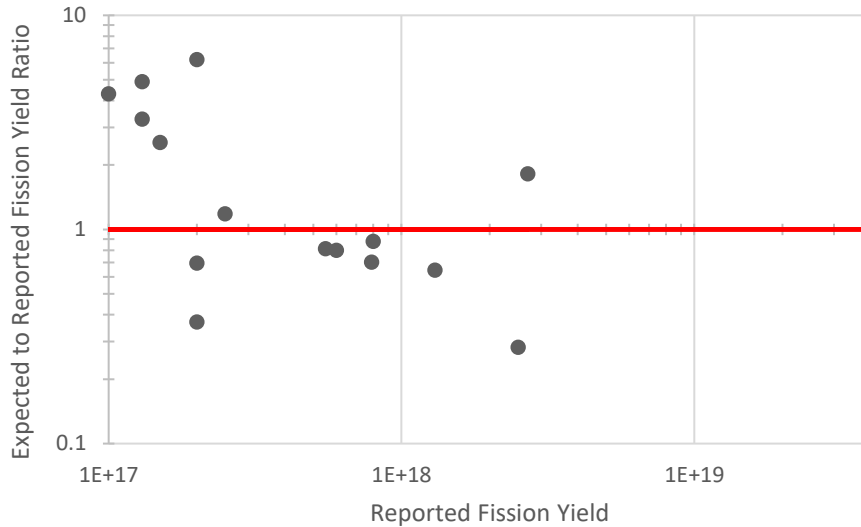


Figure 3-16: Barbry’s Model – Yield-Ordered

3.1.4 Nomura’s Model

Nomura and Okuno pose two potential models for the estimation of the total fission yield from a solution criticality accident (Nomura & Okuno, 1995). Their models are differentiated based on excursions that result in boiling versus excursions that do not result in boiling. The estimation for the fission yield N_f in a solution without boiling is given by Equation 3.7, and the fission yield N_f in a solution with boiling is given by Equation 3.8, where in both cases V represents the solution volume in liters.

$$N_f = 2.6 \times 10^{16} \cdot V \quad (3.7)$$

$$N_f = 6 \times 10^{16} \cdot V \quad (3.8)$$

These correlations give rise to the data presented in Table 3-8, where the accidents known to involve a period of boiling are also denoted. Both the non-boiling model and the boiling model were compared with the reported fission yield for all accidents, however, in the interest of establishing an overall fitness of model.

The average percent difference for the non-boiling model neglecting the outlier accidents 9, 13, 15, and 18 is 427 %. The boiling model without the outlier accidents provides an average percent difference of 1116%. It should be noted that the non-boiling model predicts closer results for the accidents that are known to involve or potentially involve boiling, with the exception of accident number 6, which occurred at the Idaho Chemical Processing Plant on October 16, 1959. This accident is the only accident that would fall under the assumptions made by Nomura in the development of his model, involving enough boiling of the solution material to cause a material loss. For simple estimation purposes using Nomura’s methods, it is probably most effective to use the non-boiling approximation unless boiling is explicitly noted to have occurred.

Table 3-8: Results of Nomura’s Model

Accident Number	Involved Boiling	Non-Boiling Model Percent Difference	Boiling Model Percent Difference
1	Maybe	303	830
2	Maybe	680	1700
3	Maybe	659	1652
4	Yes	12	158
5	No	2673	6300
6	Yes	-48	20
7	No	97	356
8	No	73	300
9	No	92850	214400
10	No	46	237
11	No	940	2300
12	No	16	169
13	No	10430	24200
14	No	720	1792
15	No	25900	59900
16	Maybe	35	212
17	No	476	1229
18	No	103900	239900
19	No	203	601
22	No	-53	8

For visualization purposes, plots of the ratio of calculated fission yield to reported fission yield for the non-boiling model with and without the outlier accidents are included in Figures 3-17 and 3-18 in chronological order and in Figures 3-19 and 3-20 in order of ranking by reported fission yield; and for the boiling model in Figures 3-21 and 3-22 in chronological order and in Figures 3-23 and 3-24 in order of ranking by the reported fission yield. As with other models analyzed, the data points above a value of 1.0 are overestimated by the model, and the data points below a value of 1.0 are underestimated.

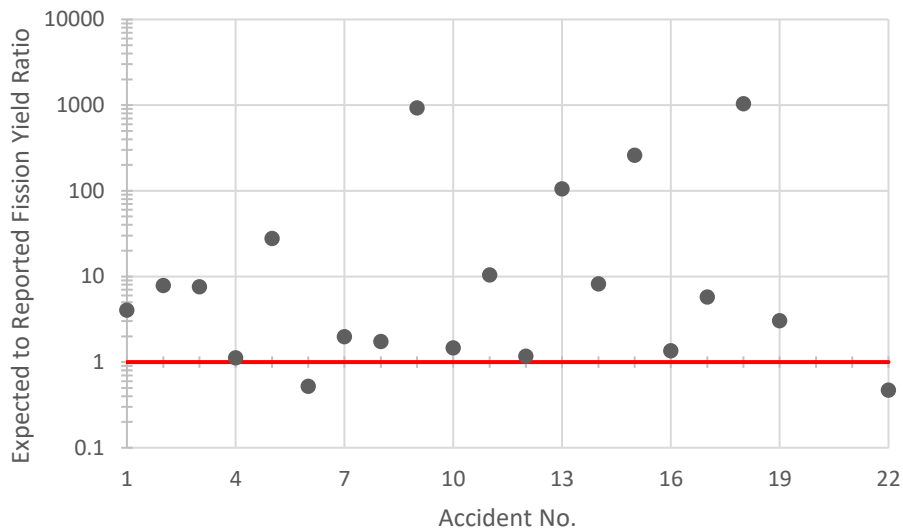


Figure 3-17: Nomura’s Non-Boiling Model – Chronological (With Outlier Data)

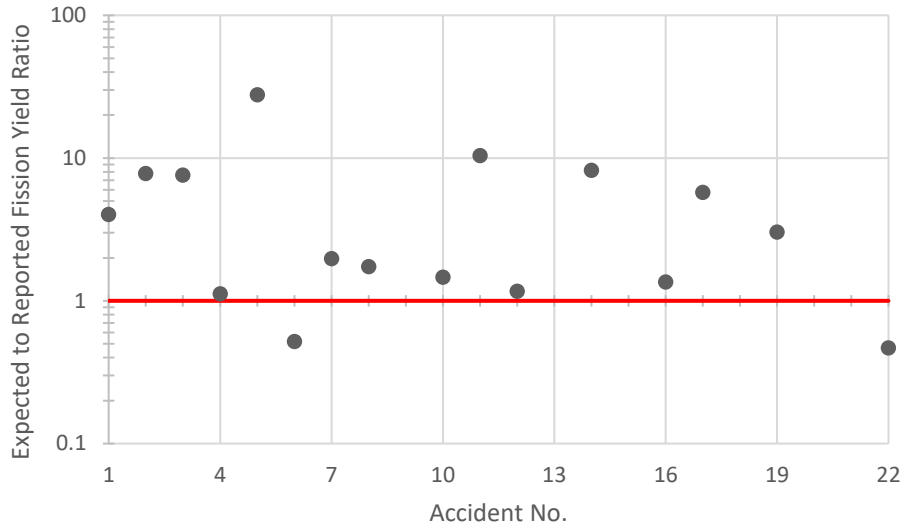


Figure 3-18: Nomura’s Non-Boiling Model – Chronological

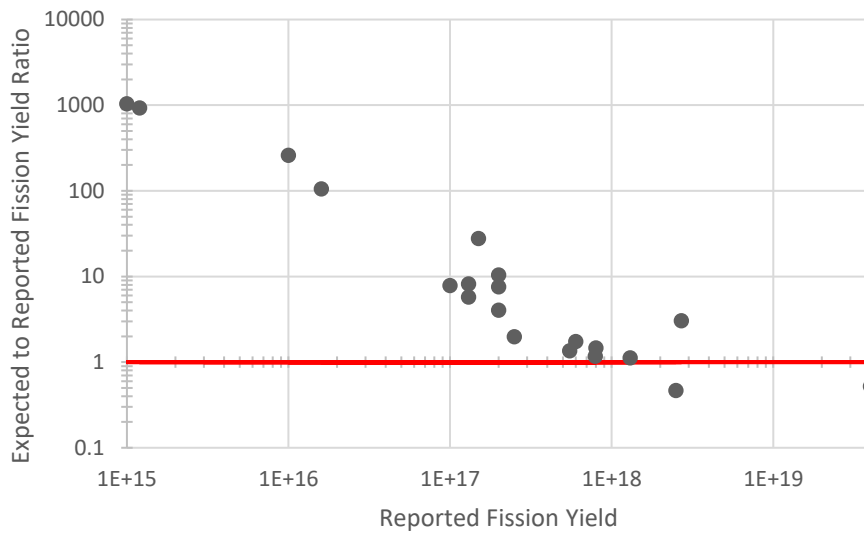


Figure 3-19: Nomura’s Non-Boiling Model – Yield-Ordered (With Outlier Data)

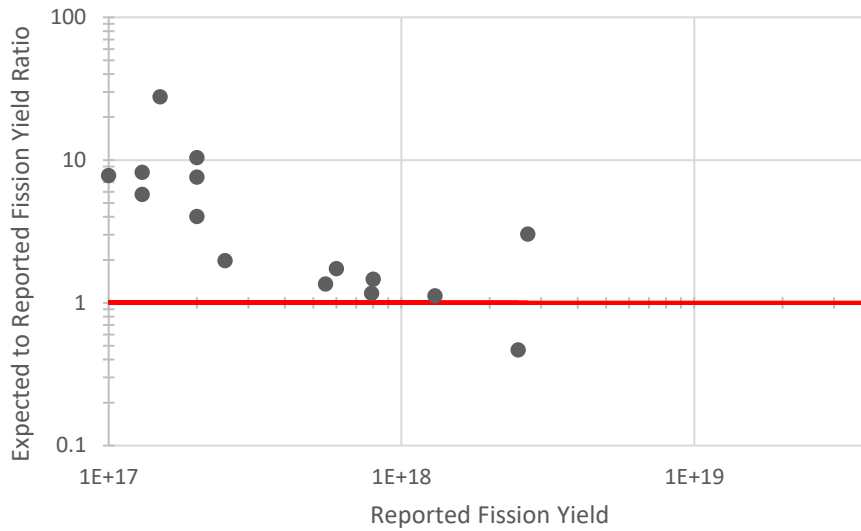


Figure 3-20: Nomura’s Non-Boiling Model – Yield-Ordered

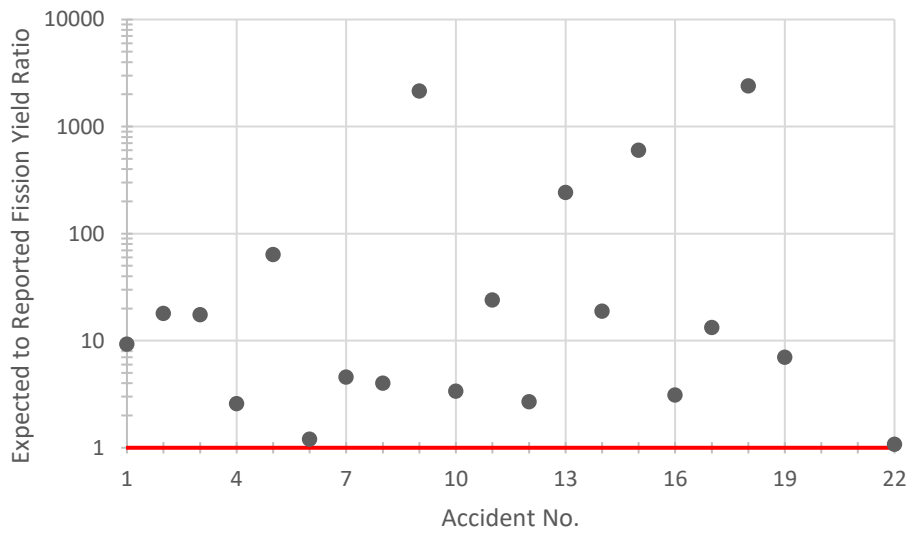


Figure 3-21: Nomura’s Boiling Model – Chronological (With Outlier Data)

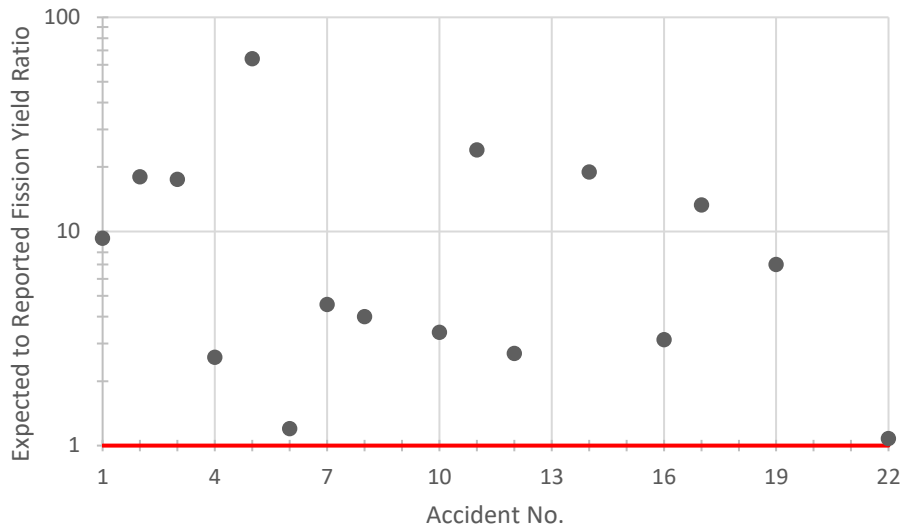


Figure 3-22: Nomura’s Boiling Model – Chronological

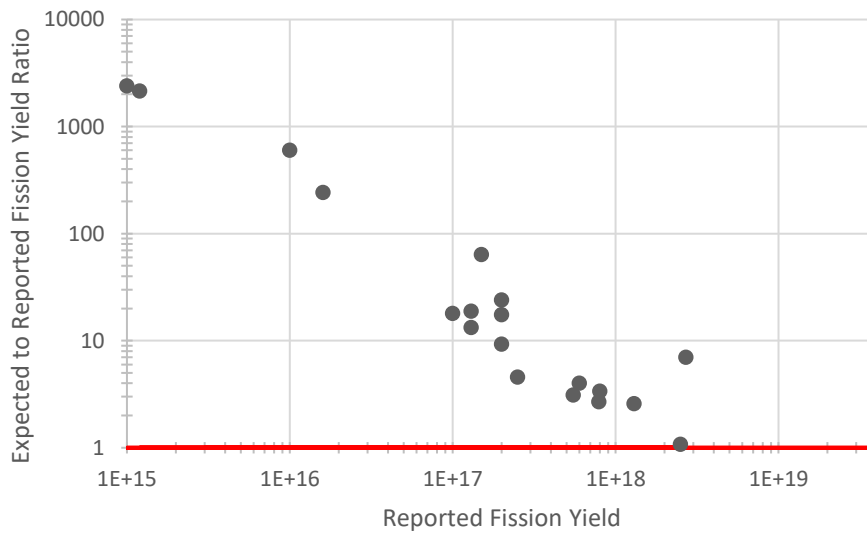


Figure 3-23: Nomura’s Boiling Model – Yield-Ordered (With Outlier Data)

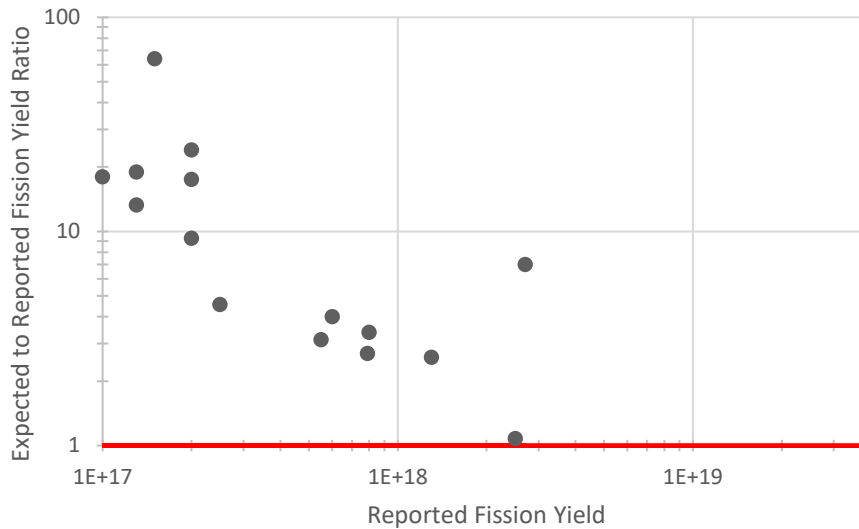


Figure 3-24: Nomura’s Boiling Model – Yield-Ordered

3.2 Summary of Empirical Models

The two models that have the closest accuracy are Barbry’s model and Tuck’s model for uranium solutions. Barbry’s model has a tendency to overestimate the fission yields when outliers are neglected, while Tuck’s uranium model has a tendency to underestimate the fission yields when outliers are neglected. Because Barbry’s model is dependent on the duration of the excursion involved, it is important to note that for those excursions with a reported duration of less than one minute, typically the single-burst excursions, a value of 10 seconds was substituted for the duration term.

Combined, these two models can reasonably be assumed to be bounding estimates for a typical accident scenario. While not a perfect estimate, the general trend as shown in Figure 3-25 is that Barbry’s model and Tuck’s model bound the reported yields while maintaining general accuracy. Neglecting the established outlier data of accidents 9, 13, 15, and 18 as shown in Figure 3-26, the bounded value is typically not more than one order of magnitude away from the reported yield of the accident. On both Figure 3-27

and Figure 3-28, the line representing unity is defined, showing where the true value of the reported yield would occur, and providing an indication of the relative accuracy of both bounding models.

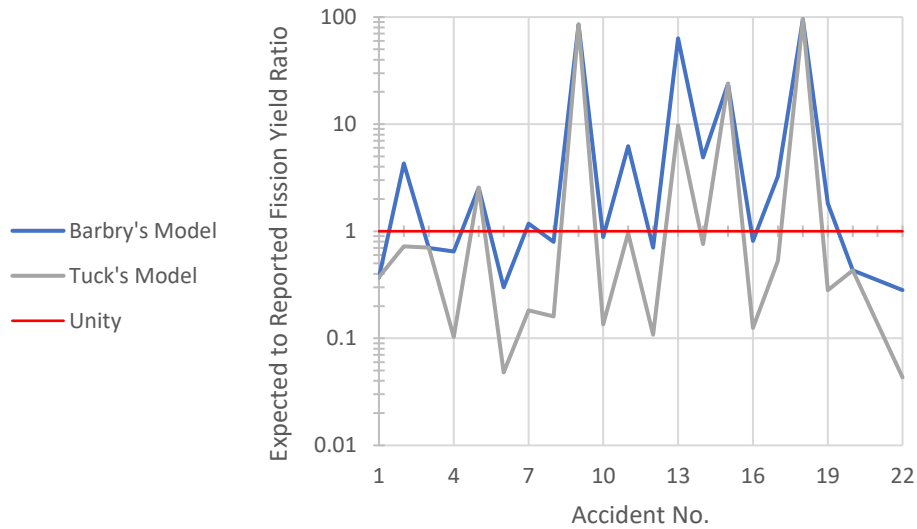


Figure 3-25: Bounded Fission Yield Ratio – Chronological (With Outlier Data)

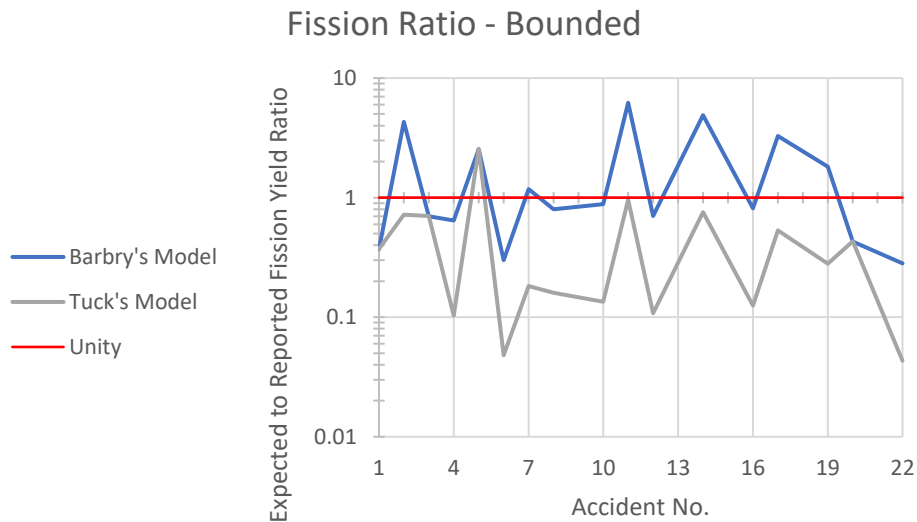


Figure 3-26: Bounded Fission Yield Ratio – Chronological

When the accidents are ordered by reported fission yield, a trend of general over-prediction to general under-prediction is made apparent, as shown in Figures 3-27 and 3-28. While still within an order of magnitude of accuracy, the implication is that for excursions with a larger predicted fission yield, the bounding correlations should be assumed to be less conservative than for excursions or accidents with smaller predicted fission yields. The scale change that occurs on each subsequent set of figures should be noted, as the outlier accidents being neglected does increase the overall accuracy of the models involved.

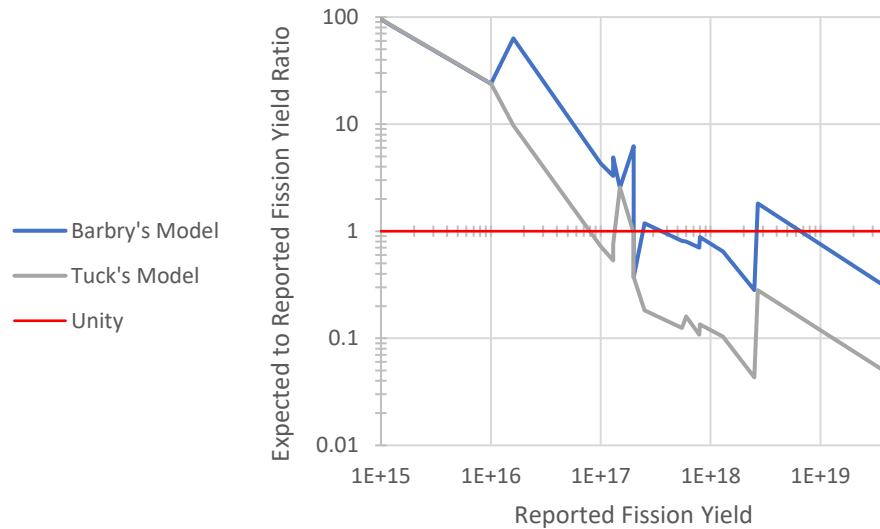


Figure 3-27: Bounded Fission Yield Ratio – Yield-Ordered (With Outlier Data)

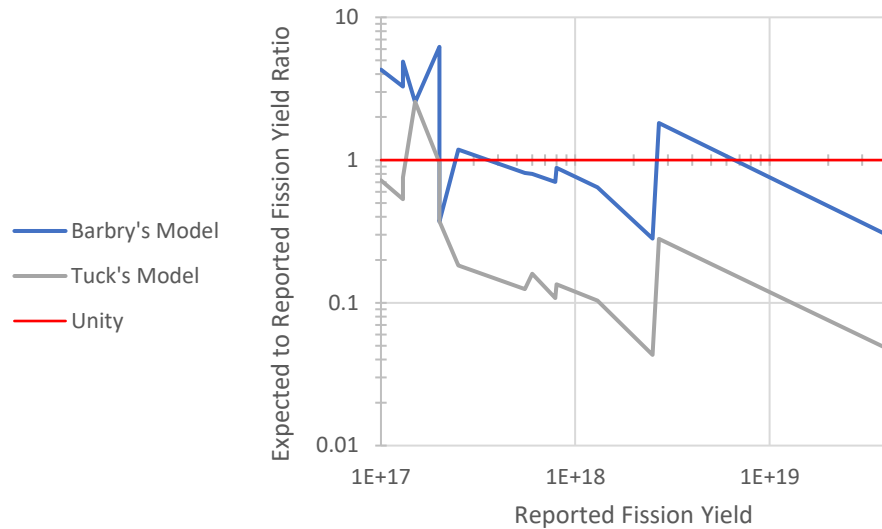


Figure 3-28: Bounded Fission Yield Ratio – Yield-Ordered

This is considered to be a reasonable bounding approximation for a typical solution accident at a processing facility, as these correlations are not dependent on any data other than solution volume and the excursion duration, which should be parameters easily determined for most situations. If a conservative estimate is required, Barbry’s model should serve as a reasonable approximation without sacrificing accuracy. Note that the volumes analyzed ranged from 19 liters to 800 liters and the durations from 10 seconds to 37.5 hours. For more accurate assessments specific to a facility or for a situation where uncommon features or elements may impact a criticality excursion that occurs, a full criticality safety evaluation should be performed for the site in question.

Chapter 4 – Computational Model

A computational model was developed to simulate the evolution of the initial spike in a criticality excursion in a solution system. This model utilizes both a time and volumetric discretization approach, and makes use of Python 3.6.3 and the SERPENT 1.1.7 Monte Carlo particle transport code with a specific focus on volumetric expansion as a termination effect. This computational model uses various correlations and empirical equations of state to evolve the solution system between neutronics calculations performed by SERPENT, resulting in a series of input files and output files written that can be used for analysis purposes.

The evolution of a criticality excursion is typically considered to have a large initial burst of fissions, followed by some series of re-criticality excursions and a plateau region. This is largely dependent on whether the solution is an open or closed system.

An open solution system will have a large initial fission spike that shifts the material and results in an overall negative reactivity insertion due to the density decrease. Following that, the solution is either splashed out as a termination effect or falls back into the container for a re-criticality event, eventually stabilizing in density for the plateau region and leading to boiling and radiolytic gas generation.

A closed solution system is considered to have an extended criticality punctuated by reactivity changes caused by ripples or waves in the solution due to splashing effects. This configuration is likely to result in boiling unless an avenue is provided for solution ejection to termination (i.e., into a pipe system or drain).

Both an open system and a closed system will have a large burst excursion or fission spike in the initial moments of the reaction, where a large number of fissions occur over a small period of time. An attempt was made at modeling this event using the SERPENT Monte Carlo program (Leppänen, Pusa, Viitanen, Valtavirta, & Kaltiasenaho, 2015), as well as the Python programming language, version 3.6.3.

An object-oriented approach was taken in Python, where the volumetric regions of a cylindrical solution material were discretized into both radial and axial components, and the neutronics parameters of the event are obtained from SERPENT. Using SERPENT flux tallies for each discretized volume, a neutron flux profile is obtained and used for subsequent thermal calculations.

4.1 Calculation Details

A large amount of work was performed by Adrienne Bobbette Smith in her 1989 thesis for the University of Arizona, “Nuclear Excursions in Aqueous Solutions of Fissile Materials” (A. Smith, 1989). Smith’s work formed the basis of the modeling technique used herein, and was expanded upon and modified for this work. Smith’s model was constructed for use with the DARE P Continuous System Simulation Language developed at the University of Arizona, a compiler for which is at present difficult to find, so the analysis that follows is an attempt at modernization of both the model and a means to execute the model on what is considered a modern and relatively open computational platform as of the time of this writing. If it is desired to faithfully reproduce the work found in Smith’s original thesis, the DARE P language was found to be related to various other analog system simulation languages that have fallen out of general use (Korn, 1989).

For the constructed simulation, four core Python modules were constructed, with the titles “*transientmodel.py*”, “*tm_constants.py*”, “*tm_material.py*”, and “*tm_fileops.py*”. The driver script file that contains the main function is *transientmodel.py*, and so this is what would be executed while running the program. The global calculational parameters are contained within *tm_constants.py*, and so this file is effectively the settings for the program that get imported into the other modules. The framework for volumetric discretizations is contained within *tm_material.py*, and so all evolution of each individual system occurs within this file. The file *tm_fileops.py* contains the interface with SERPENT by means of input and output files, as well as the methods for appending to an output file. A general flowchart of the program structure can be seen in Figure 4-1.

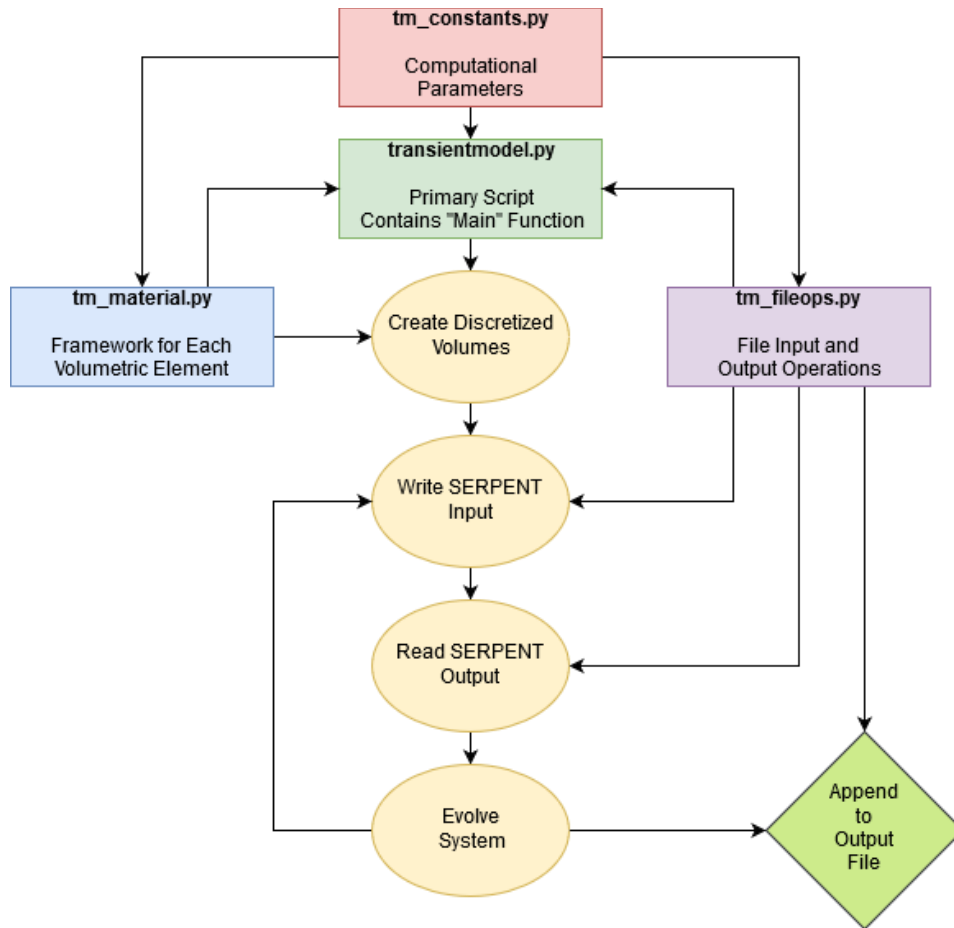


Figure 4-1: Computational Model Flowchart

The simulation is initialized with known material parameters and geometry for a given system. The geometry is simplified into a right-angle cylindrical or annular profile using a radius and height for input, while the material parameters are reliant on the ZAID for each isotope in the solution and the associated number density. These parameters are discretized both radially and axially into a variable number of regions and converted into a SERPENT input file using Python version 3.6.3. An example of this discretization scheme for five axial regions is shown in Figure 4-2 for a cylindrical geometry and Figure 4-3 for an annular geometry. An example of the radial discretization is shown in Figure 4-4 for a cylindrical geometry. An annular geometry would be similarly defined with the centermost cylinder removed.

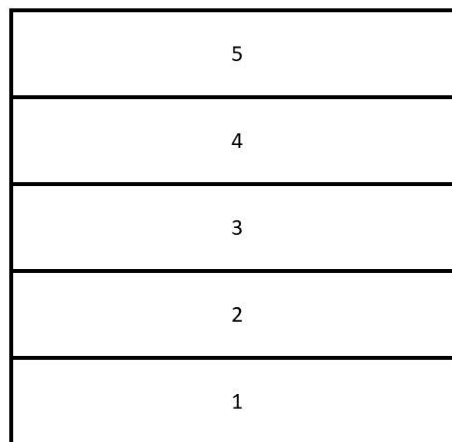


Figure 4-2: Cylindrical Discretization

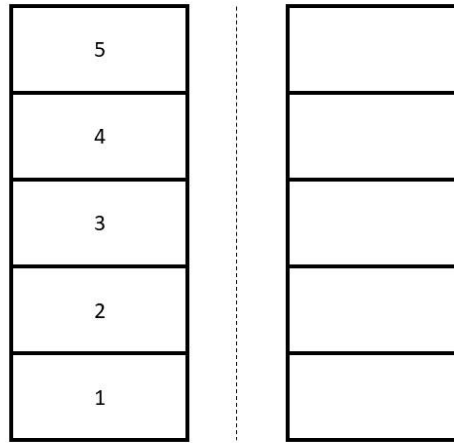


Figure 4-3: Annular Discretization

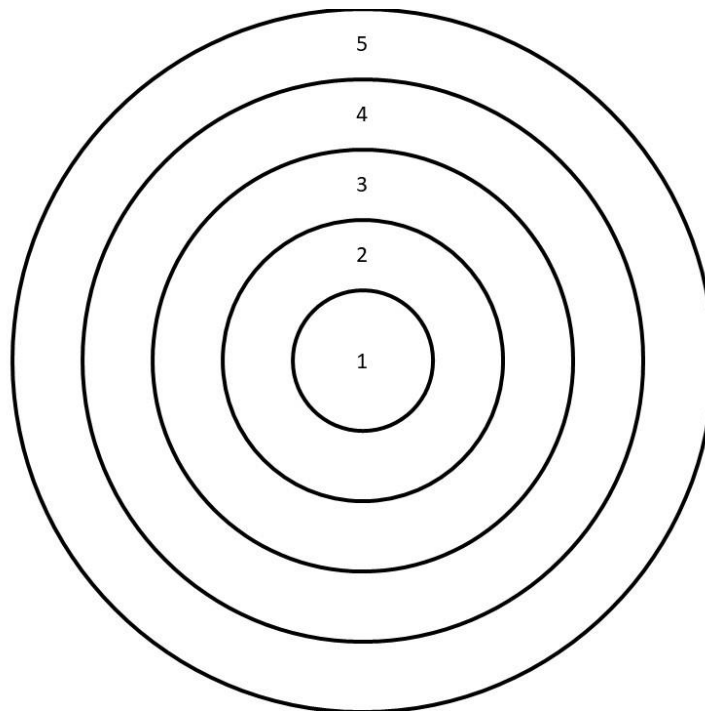


Figure 4-4: Radial Discretization

After developing an initial profile of volumetric discretization based on the framework contained in *tm_material.py*, the main method will then call the SERPENT 1.1.7 program using GNU Bash version 4.3.11 on the Linux Subsystem for Windows environment. Small modifications would need to be made to this portion of the program for an alternative environment or operating system to be used, but such modifications are not out of the question, and should be fairly straightforward to implement.

SERPENT performs Monte Carlo neutronics calculations to search for a multiplication eigenvalue k_{eff} (Leppänen et al., 2015), and prints an output file containing various parameters and calculational results. Of import in these results are the neutron lifetime l , the multiplication value k_{eff} , and the average number of neutrons emitted per fission $\bar{\nu}$. Note that SERPENT calculates both an “implicit” and an “analog” value for k_{eff} and l , where the implicit value is defined for the given universe and the analog value is defined for the whole geometry. Based on the structure of the generic SERPENT input file that was used, the analog value was selected for these parameters.

Volumetric neutron tallies are also given as parameters to the SERPENT program for each material in the input file, and those tallies are read from an output file and used as a representation for the number of fissions and the general flux profile within the system. Detector responses in SERPENT are normalized to a full-geometry detector count, resulting in a fractional fission profile for the system. An initiating integrated system power is chosen for the excursion in units of fissions per second, generally of a high magnitude to facilitate the expansion of the material, such that Monte Carlo calculations do not take up much time in the linear evolution period of a solution excursion.

From the neutron profile obtained from SERPENT, the true number of fissions N_i in each volume segment i is calculated by the use of Equation 4.1, where f_i is the fraction of total fission events that occur in volume segment i , W is the total power production of the system in units of fissions per second, and Δt is the discretized duration in time in units of seconds.

$$N_i = W \cdot f_i \cdot \Delta t \quad (4.1)$$

The assumption is made that on average, 180 MeV of energy is deposited into the solution material per fission event, which allows for an equation of state to be used. Prior to that, however, an acceleration is calculated for the center of mass of each volumetric discretization to allow for a volumetric expansion. The center of mass acceleration is calculated simply by means of a pressure balance, accounting for gravitational effects on the material producing both hydrostatic pressure and a negative acceleration. This calculation is shown in Equation 4.2, where C_i is the height of the center of mass of volume element i in the z -direction of a cylindrical coordinate system, A_i is the cross-sectional area of the base of volume element i , P_i is the gauge pressure at the top of volume element i , and m_i is the mass of the solution contained within volume element i .

$$\frac{d^2 C_i}{dt^2} = \frac{A_i}{m_i} \cdot (P_{i-1} - P_i) - \Lambda \cdot v_{COM_i} - g \quad (4.2)$$

For these calculations, the pressure at the top of the cylindrical material is assumed to be at an atmospheric gauge pressure of zero, and the initial pressures are calculated based on simple gravitational acceleration and solution density throughout the material. An example of this is shown in Equation 4.3, where $P_{(i-1)_0}$ is the initial pressure at the

bottom of element i due to the hydrostatic effects of gravity, $P_{(i)_0}$ is the pressure at the top of volume element i , which is assumed to be zero at the top-most element, g is the gravitational acceleration acting on the fluid, d is the fluid density, which is constant over the initial state of the solution, and h_i is the height of solution present on top of volume element i . The center of mass is assumed to be the geometric center of the volume element i in question, because the density is assumed to be consistent throughout the element. All elements initially start with the same density, while the mass would be determined from the volume of the element. All axial elements of the same radial discretization are considered to have the same mass, as the units are discretized evenly based on length.

$$P_{(i-1)_0} = P_{(i)_0} + d \cdot g \cdot h_i \quad (4.3)$$

The Λ in Equation 4.2 represents a dissipation term, which is a factor that attempts to account for the damping effect of friction and deformation of the walls of the tank (A. Smith, 1989). This value is on the order of 3000-4400 per second. This is applied only for the volume regions in the outermost radial discretizations, where the fluid would be in contact with the boundaries of the tank. This term is multiplied by the current velocity of the center of mass of volume region i , represented as v_{COM_i} , which is initially zero at the start of the excursion. The value for gravitational acceleration constant g in the negative z -direction of a cylindrical coordinate system is assumed to be 9.80665 meters per second squared.

Each value for the center of mass acceleration is then used to expand the solution axially from the bottom upwards. It is assumed that the container the solution is in does not

expand in the radial direction or in the negative z-direction and fixes the solution geometrically. That is, for any open system or closed system with a venting opening, the pressure at the top of the solution is always atmospheric, which allows for an easier vector for expansion in the positive z-direction as the path of least resistance, and splashing and expansion in the radial directions is completely negated by the material of the solution container.

The solution is expanded upwards starting from the lowest base because the base of the container is a fixed point in space, at a z-coordinate of zero in a cylindrical coordinate system. This allows for the acceleration to be accounted for in this region, and the height adjusted accordingly based on the principle that the center of mass in a volume element is the geometric center of that volume element, as each volume element is assumed to have a uniform density within itself during the course of the expansion process. The height of the volume element is then adjusted, and the volume element immediately above is shifted upwards before the center of mass acceleration is applied. This shifting technique prevents the material from being “locked” in space about the initial center of mass and allows for a natural expansion vector, as the surrounding solution pressures are the primary drivers of volumetric expansion.

The principles of an incompressible fluid are applied here to prevent the system from being solely driven by pressure in terms of compression and expansion. If the volume element would be compressed to such a point that the fluid density is below the original starting density of that volume element, then the compression is simply limited to the original volume of the element, and the velocity of the center of mass at that point in time is set to be zero. This prevents a solution from compressing to unphysical quantities due

to a pressure balance equation, and the incompressibility of the aqueous fluid is preserved. For an expanding fluid, the density is adjusted, as it is assumed that the fluid is being intermixed with atmosphere via a splashing or aerosolization effect to fill the voids while preserving mass.

The center of mass is adjusted based on classical kinematics involving acceleration, where $v_{COM_{initial}}$ is the initial center of mass velocity at the current time-step, and $v_{COM_{final}}$ is the final center of mass velocity for that time-step, which can be calculated as in Equation 4.4, where C is the position of the center of mass on the z-axis from the bottom of the solution container at a z-coordinate of zero, and Δt is the discretized time-step of the overall excursion evolution.

$$v_{COM_{final}} = v_{COM_{initial}} + \frac{d^2C}{dt^2} \cdot \Delta t \quad (4.4)$$

This allows for a change in the center of mass position ΔC to be calculated as shown in Equation 4.5, where the new position of the center of mass C can then be calculated simply by adding the value for ΔC .

$$\Delta C = v_{COM_{initial}} \cdot \Delta t + \frac{1}{2} \cdot \frac{d^2C}{dt^2} \cdot \Delta t^2 \quad (4.5)$$

Knowing the center of mass position and the position of the bottom of the volume element accounting for the shift from acceleration of the elements below allows for the position of the height of the element to be calculated, which is then used for the shift of the elements above this volume element. The height H_i of the volume element i is calculated as shown in Equation 4.6, where B_i is the base height of volume element i .

Both the height of the top of the element H and the height of the base of the element B are measured from the base of the total solution system at the z -coordinate of zero. As previously stated, the assumption made here is that each volume element i has a constant density, and so the center of mass of the volume element is always in the geometric center of that volume element.

$$H_i = B_i + 2 \cdot (C_i - B_i) \quad (4.6)$$

After expanding the volume based on current pressures, but before executing neutronic calculations for the next time-step, an equation of state is applied to each volume element. The isobaric expansion coefficient β_0 and the isothermal compressibility κ_0 for the pure liquid is obtained using a Python wrapper for the CoolProp library (Bell, Wronski, Quoilin, & Lemort, 2014) assuming that the intensive thermophysical properties for the aqueous solution material do not diverge drastically from those of water (Barbry, 1994).

The isobaric expansion coefficient and isothermal compressibility for the pure liquid are adjusted to account for the addition of radiological gas produced by the excursion as shown in Equations 4.7 and 4.8 to get an overall isobaric expansion coefficient β and an overall isothermal compressibility κ . The volume element is considered to produce radiological gas if the number of fissions per liter exceeds a threshold value. The value used for this threshold is 1.5×10^{15} fissions per liter, a value obtained from experimental analysis of the SILENE experiments (Barbry, 1993) that does not diverge drastically from previous work performed (Spiegler et al., 1962). So long as the volumetric fission yield does not exceed this value, it is assumed that the radiolytic gas produced is of a low

enough density that chemical recombination effects of the gas exceed the gaseous nucleation effects, preventing vapor bubbles from forming. Pertaining to the radiological gas production within the system, the surface tension of the liquid is represented by σ , and is also obtained from the CoolProp calculational reference library (Bell et al., 2014). The volume fraction of radiologic gas in the system is represented as f_e . The radius of the radiolytic gas bubbles that are nucleated r_b is assumed to be a constant value of 5×10^{-8} meters (Kimpland, 1993), independent of temperature, liquid pressure, surface tension, dissolved gas concentration, and uranium concentration (Spiegler et al., 1962).

$$\kappa = \kappa_0 \cdot (1 - f_e) + \frac{f_e}{P + \frac{4 \cdot \sigma}{3 \cdot r_b}} \quad (4.7)$$

$$\beta = \beta_0 \cdot (1 - f_e) + \frac{f_e}{T} \cdot \frac{\left(P + \frac{2 \cdot \sigma}{r_b}\right)}{\left(P + \frac{4 \cdot \sigma}{3 \cdot r_b}\right)} \quad (4.8)$$

The volume fraction of radiolytic gas in the system is calculated as derived from the ideal gas law involving temperature T , pressure P , and volume V (A. Smith, 1989); as shown in Equation 4.9. This equation is dependent on the assumption that the mass fraction of gas in the system is a function only of the mass of the solution present, and that the solution mass does not appreciably deplete by means of radiolytic gas production. That is, even with a relatively higher-order integrated fission yield of 1×10^{19} total fissions for a solution system, any alteration to the mass content of the overall solution present is almost completely negligible. Therefore, the mass of the solution times the mass fraction of gas to the overall solution results in only the term for the mass of the gas present in the solution, m_{gas} . Note that R_{gas} is the representation for the specific ideal gas constant for

the hydrogen-1 nuclide, which is the only gas being accounted for in an aqueous nitrate system. This is due to the effects of a fast transient excursion, where diffusion of gas from the fuel to nucleation sites is too slow for surface nucleation to be effective, so the hydrogen gas concentration increases until the solution effectively behaves like a gas bubble chamber at a critical concentration of gas production (Spiegler et al., 1962).

$$f_e = \frac{m_{gas} \cdot R_{gas} \cdot T}{V \cdot \left(P + \frac{2 \cdot \sigma}{r_b} \right)} \quad (4.9)$$

The fission gas produced once the reaction reaches the given threshold value of 1.5×10^{15} fissions per liter (Barbry, 1993) is dependent upon a radiolytic yield term for the gas in question, in this case hydrogen. The yield term is a function of energy deposition via fission events, and based on analysis of the KEWB and CRAC experiments (Forehand, 1981) is considered to be approximated as 2.3×10^{-4} kilograms of H_2 gas produced per MegaJoule of energy deposited into the system.

The temperature change ΔT of the volume element is then calculated as shown in Equation 4.10, where the mass-specific constant volume heat capacity c_v of the aqueous solution is again assumed to not diverge drastically from the value for water and therefore is obtained from the CoolProp library (Bell et al., 2014). Because the heat capacity is determined as an intensive property of the fluid, the mass of the solution present m must be accounted for. The amount of energy deposited into the solution contained in the volume element in question by means of fission events within time-step of length Δt is represented as ΔE . The volume difference through pressure-based expansion as previously calculated for this time-step is represented as ΔV .

$$\Delta T = \frac{1}{c_v \cdot m} \cdot \left(\Delta E - \frac{\beta \cdot T}{\kappa} \cdot \Delta V \right) \quad (4.10)$$

Knowing the change in temperature and the change in volume, the compressibility equations can be used to calculate the change in the average pressure of the volume element, as shown in Equation 4.11, which is reliant on the current volume of the element.

$$\Delta P = \frac{\beta}{\kappa} \cdot \Delta T - \frac{1}{\kappa \cdot V} \cdot \Delta V \quad (4.11)$$

It is important to note that these equations have negative terms as a function of the change in volume, ΔV . An account is made for this by performing the calculation without the inclusion of these negative terms to get an overall pressure at each discretized time step, and then expanding the solution volume element based on that pressure. After expansion, the temperature and pressure are then reduced based on the ΔV term in the equation, which prevents any unrealistic pressure accumulation by not taking the effects of volumetric expansion into account. These volumetric terms are a limiting factor on the expansion of the material, and the effect of taking them into account is realized in subsequent time-steps of the calculation.

The pressure change calculated is applied to the volume element as a change to the average pressure of that element. For each element, the pressure is assumed to be linearly defined according to a hydrostatic model as in the initial conditions of the solution, such that only gravitational effects and height affect the pressure as shown in Equation 4.3, where h_i is the distance measured in the negative z-direction on a cylindrical coordinate axis of solution existing on top of the point of measurement i .

Because the average pressure of the volume element is at the center of mass position due to the constant density assumption for each volume element, the pressure at the top of the volume element is linearized with the average pressure to obtain the pressure at the bottom of the volume element. For reference, the pressure calculations are shown in Equation 4.12, from which Equation 4.13 may be determined through simple algebra, where \bar{P}_i represents the average pressure, or the pressure at the point of the center of mass, of volume element i .

$$\bar{P}_i = \frac{(P_i + P_{i-1})}{2} \quad (4.12)$$

$$P_{i-1} = 2 \cdot \bar{P}_i - P_i \quad (4.13)$$

Because the top of the solution system is known to be at a fixed atmospheric pressure, the bottom-most or maximum pressure calculations begin from the top of the solution system discretizations, contrary to the volumetric expansion calculations, which begin from the bottom of the solution system discretizations. A continuity of pressure is maintained by asserting that the top-most pressure value of one element is equivalent to the bottom-most pressure value of the element directly above it.

Once the solution volume elements are expanded and have their intensive thermophysical properties and state values updated, the neutronic calculations are run for the next time-step. At each time-step calculation, an output file for the calculation is appended to with values for the current time elapsed, the number of fissions that occurred during that time-step, the total integrated number of fissions at that point in time, the maximum temperature within the solution, and neutronics parameters including the neutron lifetime,

the effective multiplication factor k_{eff} , and the uncertainty σ_{eff} associated with the effective multiplication factor in the form of $k_{eff} + 2 \cdot \sigma_{eff}$, which provides a conservative 95% confidence interval to the multiplication factor.

Using the neutronic parameters obtained from SERPENT Monte Carlo calculations, the total system power at the next time-step W is then propagated based on a point-reactor kinetics model that relies on the total system power at the previous time-step W_0 as shown in Equation 4.14, where k_{eff} is the effective multiplication factor, Λ_p is the prompt neutron generation time, β_d is the delayed neutron production fraction, and Δt is the time-step duration. This propagation equation is based on the principles of a prompt supercriticality event, where the evolution of the accident happens on a small time-scale. The prompt neutron generation time Λ_p is given by simply dividing the prompt neutron lifetime given by the SERPENT Monte Carlo calculations by the effective multiplication factor. The expression for reactivity ρ is defined in Equation 4.15.

$$W = W_0 \cdot \exp\left(\frac{\rho - \beta_d}{\Lambda_p} \cdot \Delta t\right) \quad (4.14)$$

$$\rho = \frac{k_{eff} - 1}{k_{eff}} \quad (4.15)$$

As detailed, the overall system power in fissions per second is then assigned to a power in each discretized volume element based on the fission fraction profile obtained from the SERPENT tallies, and the calculation then propagates until the multiplication factor falls below a determined number and the solution is assumed to be subcritical. The limit on the multiplication factor k_{eff} for termination used in this thesis is 0.98, which is conservative

given the probabilistic nature of Monte Carlo calculations, but other values may be substituted fairly easily.

The multiplication factor is governed both by material properties and by geometry properties. After each evolution of the solution system, the new volumes are converted into a SERPENT-compatible input file format using the surface and universe-based system of establishing geometry (Leppänen et al., 2015).

The material properties are also adjusted at each time-step analyzed. The density of the system is recalculated for each discretized volume element based on the assumption that there are not enough fissions in each volume element occurring during an excursion to reasonably affect the mass of the system. So, the initial mass of that volume element is divided by the new volume after the expansion stage, which results in a new density. Due to the conservation of mass principles of recalculating a new density upon expansion, the homogenized voids in the solution are considered to be a result of marginal aerosolization due to the splashing effect of expansion. This phenomenon likely has additional considerations to take into account in terms of interactions with the physical properties of the expansion mechanism that are outside the scope of this simple model.

Material properties are also dependent on the temperature of the material, which affects the neutronic cross-sections for absorption and scattering, which can in turn drastically influence the value for the multiplication factor. SERPENT utilizes a temperature-interpolation method for adjusting cross-sections based on temperature, where the libraries for temperature of each nuclide are adjusted every 300 degrees Celsius starting from a value of 300 Kelvin. The cross-section library to use for each material is

determined by rounding the temperature value of each volume element to the nearest applicable SERPENT cross-section library specific to that temperature. The thermal scattering kernel for light water is also updated, as hydrogen to oxygen bonds affect the neutron scattering cross-section in aqueous solutions. This kernel is assigned to each material and is adjusted every 50 degrees Celsius starting from 300 Kelvin. The thermal scattering kernel for light water of each volume element is adjusted by rounding the temperature of that volume element to the closest appropriate value of a SERPENT thermal scattering kernel library to use for that element.

With respect to the initial event, the initial energy deposition of the system due to the excursion fission events prior to the point of the calculational starting power is calculated. This is based on the assumption that the energy build-up of the system during the beginning stages of evolution of the excursion does not appreciably contribute to a pressure gradient driven acceleration prior to the starting power value, to the extent of being negligible with respect to hydrostatic pressure. The overall energy deposition is applied to the temperature value of each volumetric element under the assumption that the prior geometric fission profile during the initial stages of the first-spike excursion evolution does not differ in an appreciable way from the initial geometric fission profile provided by the first Monte Carlo calculation performed by SERPENT.

The initial energy deposition to the system is calculated by integrating the power equation with respect to time. Because a Nordheim-Fuchs model is used for the power evolution, the evolution period τ is calculated as seen in Equation 4.16 based on the initial neutronic parameters determined from the first SERPENT calculation.

$$\tau = \frac{\Lambda_p}{(\rho - \beta_d)} \quad (4.16)$$

Knowing the period, the estimated time of evolution of the excursion T_e in seconds from a point of power of 1 fission per second can be calculated as in Equation 4.17, where the initial power was selected as an appreciably low value, seeing as how the Nordheim-Fuchs model asymptotically approaches zero, and a limit must be set on the excursion evolution time. The value for P_{calc} in this equation is the power at which the evolution calculations begin at a computational time of zero.

$$T_e = \ln\left(\frac{P_{calc}}{1}\right) \cdot \tau \quad (4.17)$$

This allows for the number of fissions N_e that occurred during the excursion prior to the initiation of the calculations to be determined from Equation 4.18, again assuming that the initial power of the event was 1 fission per second.

$$N_e = \exp\left(\frac{T_e}{\tau} - 1\right) \cdot 1 \quad (4.18)$$

Additionally, this model was set to match experimental parameters via the inclusion of an inertial pressure gradient damping factor of 0.1, with Kimpland and Smith stating that the acceleration of the center of mass caused by the Newtonian pressure balance on the system should be reduced by an order of magnitude to account for various inadequacies in the model (Hetrick & Smith, 1987). These inadequacies are considered to be a result of the crude pressure gradient in a single region and of the preselected input power shapes used for Smith's model (A. Smith, 1989). The results of the use of this factor are included in this report, but despite not using a pre-selected power shape for the reaction, the model

was still evolving faster than experimental results. This could be due to the initial complaint about the simplified pressure gradient in a single region, as well as any other material factors caused by turbulence within the solution, atmosphere mixing with the solution to cause an appreciable density decrease, and an insufficient discretization for a potentially unstable model as the thermodynamic evolution equations are applied in an explicit fashion of dependence on previously calculated values, rather than in an implicit numerical fashion. Also note that because the system is assumed to be physically bounded by the container it is in, there are no interactions between elements in the radial discretization regions being taken into account with the exception of a fission power profile, with all expansion assumed to be taking place in the positive z-direction of a cylindrical coordinate system.

4.2 Computational Constants and Settings

The use and settings for the Python calculational tool including many of the equation constants are primarily contained within the file *tm_constants.py*. For general use, the constants of the defined models are listed in Table 4-1 organized by the discretization parameters (parameters that are used for the overall discretization of both the volume and the time-step size), the calculational parameters (parameters used for the equation of state and radiolytic production), and neutronic parameters (parameters used as input settings for the SERPENT calculation pertaining to neutronics data).

All modules of the Python 3.6.3 code written for this project make an attempt to follow the PEP 8 style guide for Python code (van Rossum, Warsaw, & Coghlan, 2001), and should be easy to reference and utilize. The full code listing is included in this thesis in the form of Appendices, along with specific implementation details and general

instructions for modification and use. Any person with a working version of the SERPENT executable should be able to easily modify this code for their own personal use for any given cylindrical system of fissionable material under a variable value for axial, radial, and time discretization size.

Table 4-1: Constants of Computational Model

Parameter	Variable – Code Representation	Value	Units
Discretization Parameters			
Constant time-step size as a magnitude: power of 10^x	TIMESTEP_MAGNITUDE	-4	s
Number of axial discretizations	NUM_AXIAL	5	None
Number of radial discretizations	NUM_RADIAL	3	None
Calculational Parameters			
Initiating power level at which to start the calculations	INIT_POWER	1×10^{18}	$\frac{\text{fissions}}{\text{s}}$
Threshold for production of radiolytic gas	THRESHOLD	1.5×10^{15}	$\frac{\text{fissions}}{\text{l}}$
Radius of radiolytic gas bubbles upon nucleation	RAD_GAS_BUBBLE	5.0×10^{-8}	m
Gravitational acceleration constant	GRAV	9.80665	$\frac{\text{m}}{\text{s}^2}$
Specific ideal gas constant for diatomic hydrogen-1 nuclides	RH2	4.12497×10^6	$\frac{\text{m}^3 \cdot \text{Pa}}{\text{kg} \cdot \text{K}}$
Generation constant for radiolytic hydrogen-1	RADIOLYTIC_G	2.30×10^{-4}	$\frac{\text{kg}}{\text{MJ}}$
Dissipation term – accounts for friction and material resistance during expansion	DISSIPATION	4400	s^{-1}
Value of k_{eff} at which the solution is considered subcritical	SUBCRITICAL_LIMIT	0.98	None

Table 4-1: Constants of Computational Model (Continued)

Neutronics Parameters			
Number of particle histories per Monte Carlo calculation	NUM_PARTICLES	10000	neutrons
Number of Monte Carlo calculations to perform for convergence	NUM_CYCLES	500	cycles
Number of Monte Carlo cycles to drop for Shannon entropy convergence	NUM_DROPS	50	cycles

Additionally, it should be noted that the SERPENT Monte Carlo program includes an option for the analysis of unresolved resonance probability tables for the neutronic-cross sections (Leppänen et al., 2015). Within the code listings included in this report, and for the results generated from these calculations, the unresolved resonance probability peak calculations were not utilized. This was primarily to facilitate the rapid development and testing of the model, and because for a highly enriched homogenous solution the overall effect of an unresolved resonance is largely negligible.

Because the net result of performing these unresolved resonances is a self-shielding effect that has to be carried out during tracking, the transport cycle of the code slows down quite considerably (Leppänen et al., 2015). Subsequent users should make the judgment call on whether to include unresolved resonance probability calculations, as the net self-shielding effect is greater for more complicated geometries, material profiles, and lower fissile enrichments.

Chapter 5 – Computational Results

The computational model was utilized for the simulation of two well-characterized scenarios based on historical and experimental data. Experimental data is in the form of a SILENE excursion, while the historical model is provided by the Wood River Junction, Rhode Island accident, which occurred on July 24, 1964 (Nakache, Shapiro, Soodak, Marotta, & Schamberger, 1964).

4.3 SILENE S4-346

The SILENE reaction selected for analysis was the S4-346 experiment, consisting of an approximate three dollar rapid reactivity insertion, accomplished by means of a neutron-absorbing poison rod situated in the center of the annular core (Barbry et al., 2009). The general configuration of the SILENE reactor is an annular cylinder with an 18.0 centimeter outer radius and a 3.8 centimeter inner radius for containing the solution material inside.

SILENE S4-346 contained 40.2 liters of a 93% enriched uranyl nitrate solution at a concentration of 70.9 grams of uranium per liter of solution. The reactor experienced evolution at a reciprocal period of 428 per second to a peak power of 2.40×10^{19} fissions per second for an integrated yield of 1.50×10^{17} fissions due to an inserted reactivity of 2.96 dollars (Barbry et al., 2009). As shown in Figure 5-1, the S4-346 excursion had a first spike evolution to termination that occurred on a time scale of tens of milliseconds. The approximate properties of the SILENE S4-346 excursion are detailed in Table 5-1.

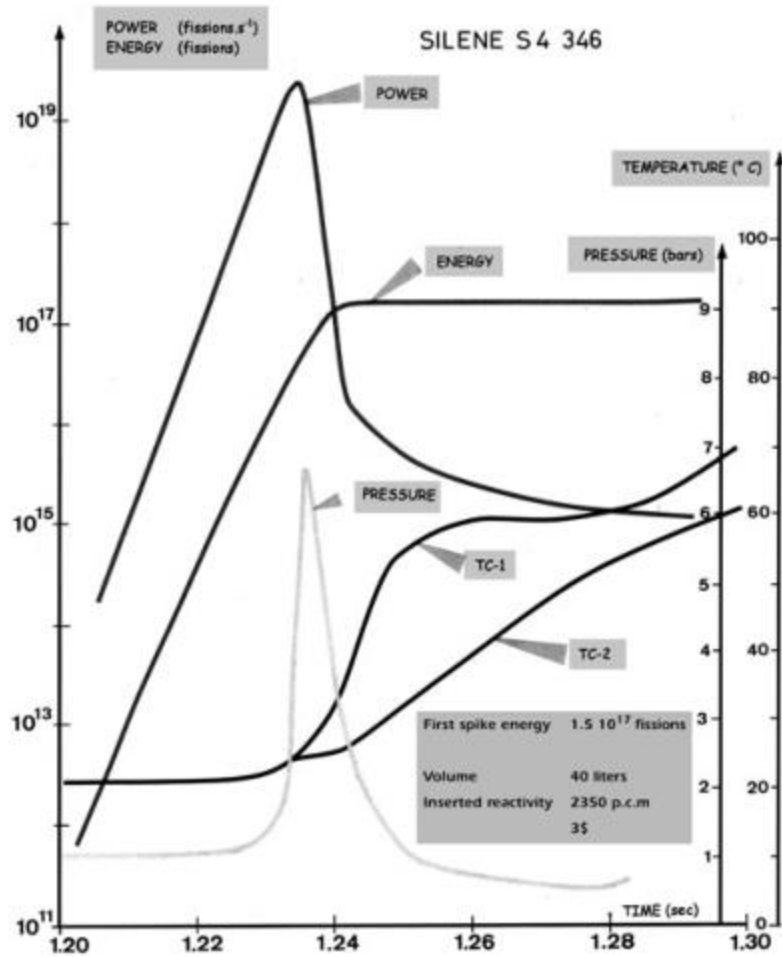


Figure 5-1: Experimental Results of SILENE Excursion S4-346 (Barbry et al., 2009)

Table 5-1: Summary of Properties for SILENE Excursion S4-346

Property	Value
Initial Inverse Period	428 s^{-1}
Peak Power	$2.40 \times 10^{19} \text{ fissions/s}$
Total Energy Deposition	$1.50 \times 10^{17} \text{ fissions}$
Time of Evolution from $\sim 6 \times 10^{16}$ fissions/s to Point of Peak Power	$\sim 0.02 \text{ s}$
Change in Temperature	60 °C, majority after termination
Peak Pressure	7 bar

The neutronics aspect of the calculation performed by SERPENT requires material definitions to perform Monte Carlo analysis on tracked particles. These definitions are given in terms of a volumetric concentration of each isotope, referred to as a number

density. The composition of a typical SILENE composition developed by Barbry was used for these calculations (Barbry, 1994) and can be seen in Table 5-2, where the number density provided to SERPENT is in units of atoms per barn-centimeter. As a note, a barn is defined as 1×10^{-24} square centimeters, meaning number density is in terms of atoms per unit volume. In the words of Barbry’s data report, this “is a mean composition used as reference in the calculations, since it is obvious that the value of these parameters must have varied during the experiments, reprocessing and various adjustments” (Barbry, 1994).

Because the density of the solution material changes in time over the course of the accident evolution, these values are initial definitions only, and are adjusted based on the new calculated density of the solution after each volumetric expansion stage. The typical SILENE material definitions used are based on an initial mass density of the solution of 1.161 grams per cubic centimeter at a total uranium concentration of 70 grams of uranium per liter of solution. The general U-235 enrichment is 92.7%.

Table 5-2: Initial SILENE Material Definitions

Isotope	ZAID	Number Density $\left(\frac{\text{atoms}}{\text{b-cm}}\right)$
Hydrogen	1001	6.258×10^{-2}
Nitrogen	7014	1.569×10^{-3}
Oxygen	8016	3.576×10^{-2}
Uranium-234	92234	1.060×10^{-6}
Uranium-235	92235	1.686×10^{-4}
Uranium-236	92236	4.350×10^{-7}
Uranium-238	92238	1.170×10^{-5}

The reactivity addition used for the experiment was 2.96 dollars, where a dollar value of reactivity ρ is measured as the delta- k reactivity over the delayed neutron fraction β_d , as shown in Equation 5.1. The delayed neutron fraction for this system is approximately 0.008 as calculated by SERPENT and reported by Barbry (Barbry, 1994). This means that the starting value of k_{eff} must be approximately 1.024.

$$\rho_{\$} = \frac{k_{eff} - 1}{k_{eff}} \cdot \frac{1}{\beta_d} \quad (5.1)$$

Differences in the initial reactivity values become apparent when using a SERPENT model to obtain the multiplication factor eigenvalue as compared to what is presented by calculations based on the experimental parameters. This is likely a factor of the neutron-absorbing poison rod still being present within the system, as there's no physical manifestation of an "instantaneous" reactivity insertion, it may only be approximated by removing the poison rod. Additionally, the stainless steel material for the reactor containment structure was not modeled in SERPENT. The structural material would normally contribute some neutron removal factor due to the neutron absorption probability inherent in those materials.

In order to preserve the pressure-based acceleration term, the circular cross-sectional area of the cylindrical reactor was preserved, as expansion was limited to the positive z-direction in a cylindrical coordinate system. The value for k_{eff} contributing to an approximate initial reactivity that matches the experimental parameters was obtained by varying the height of the solution system to compensate for missing material parameters and potential experimental uncertainties. The model of the SILENE excursion is therefore

geometrically represented by an outer radius of 18.0 centimeters, an inner radius of 3.8 centimeters, and a height of 45.5 centimeters. This is considered a reasonable approximation to make, as reactivity drives the excursion evolution, while the discretized calculation of pressure is applied to a fractional profile of the height. The expansion of the system is the terminating factor, so preserving the base cross-sectional area is of greater import to the system integrity than preserving the height of the system. The criticality excursion is considered to be terminated upon reaching a value of 0.98 for the multiplication factor k_{eff} .

The SILENE excursion was initially calculated with the base model, meaning without the pressure gradient damping factor used by Hetrick and Smith to match physical values (Hetrick & Smith, 1987). Such a calculation will be referred to as a “base calculation”, while a run involving the damping factor will be referred to as a “damped calculation”. This provides a power profile for the accident shown in Figure 5-2, and an overall energy production shown in Figure 5-3.

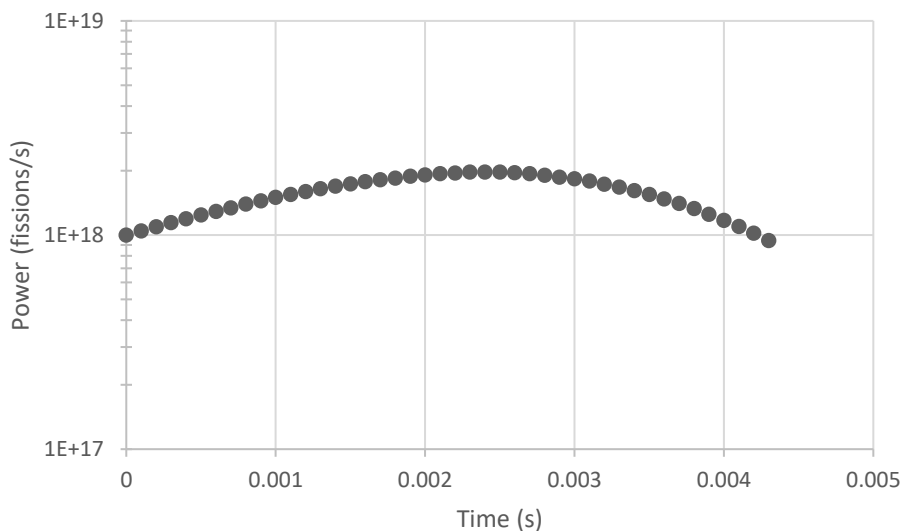


Figure 5-2: SILENE S4-346 Base Power Profile

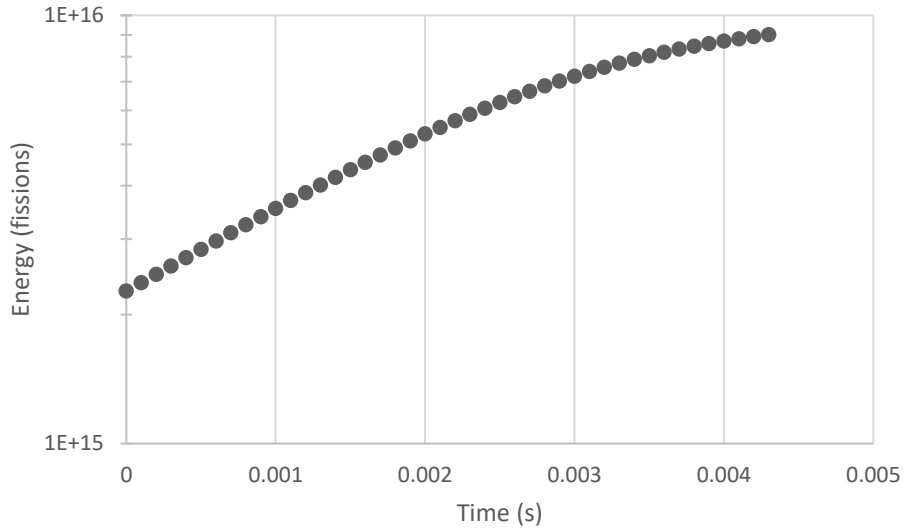


Figure 5-3: SILENE S4-346 Base Energy Profile

The calculated effective neutron multiplication factor over time can be seen in Figure 5-4, where the evolution of the accident to termination by the changing density effects can be seen. Also evident is the statistical uncertainty produced by the nature of Monte Carlo calculations, introducing irregularities to the data curve, but the general trend of termination is clear.

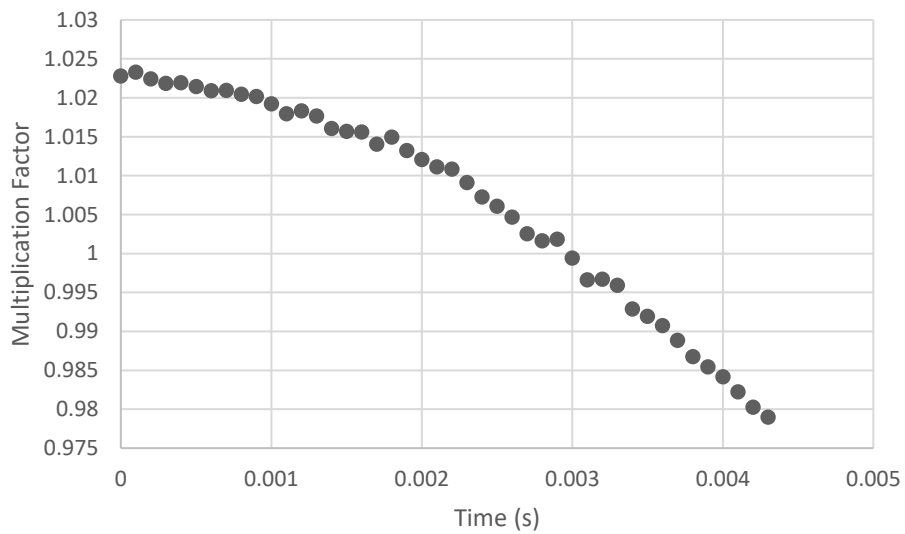


Figure 5-4: SILENE S4-346 Base Neutron Multiplication Factor Profile

As can be seen in comparison to the experimental data, this accident terminates on a much faster time-scale and at a lower power than would be expected, resulting in a lower overall energy yield by approximately an order of magnitude. A reasonable deduction to make would be that a limiting factor makes sense to apply to this system, to closer match those experimental values.

It is possible to produce a pictorial representation of the material and geometric profile within SERPENT. The initial state and the final state of the solution discretization in the form of an axial cross-sectional view are presented in Figures 5-5 and 5-6, to provide a graphical representation of the evolution of the volumetric profile. Note that SERPENT 1.1.7 does not allow for specific colors to be assigned to materials, and so each material is represented by a randomly-selected color with the exception of atmospheric void material, which is black. Additionally, the profile is normalized to a 1000 by 1000 pixel image size, and so axial aspect ratio cannot be preserved. However, the relative geometric locations of each material discretization should be fairly straightforward to determine.

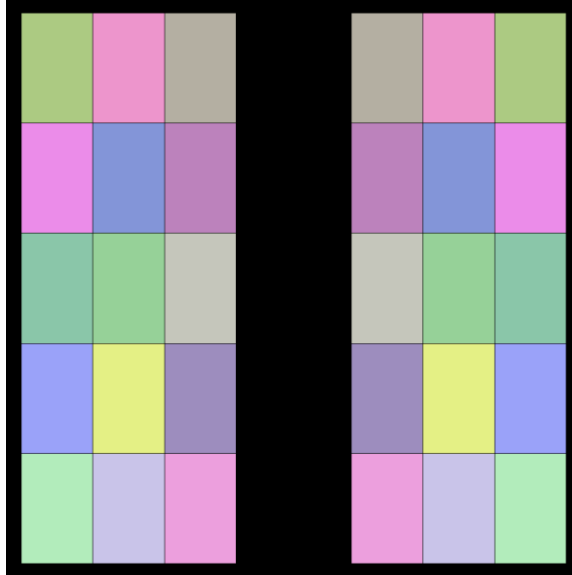


Figure 5-5: SILENE S4-346 Axial Profile at 0 ms, Solution Height = 45.5 cm

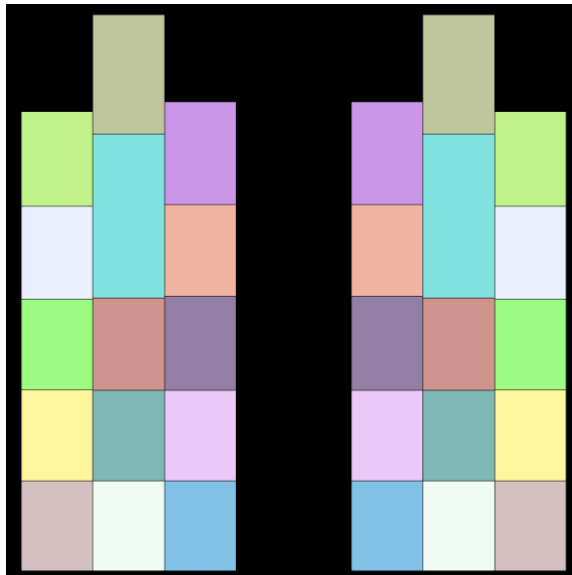


Figure 5-6: SILENE S4-346 Base Axial Profile at 4.3 ms, Solution Height = 56.07 cm

As evidenced in the geometric profile pictures of the axial cross-section of the SILENE reactor, the use of an atmospheric boundary condition at the top of the reactor results in a large expansion of the materials located towards the top. The bottom-most materials remain in their non-aerosolized liquid state.

Introduction of a pressure gradient damping factor of 0.1 multiplied to the calculated acceleration term produces the damped profiles seen in Figures 5-7, 5-8, and 5-9 for the power, energy, and neutron multiplication factor respectively.

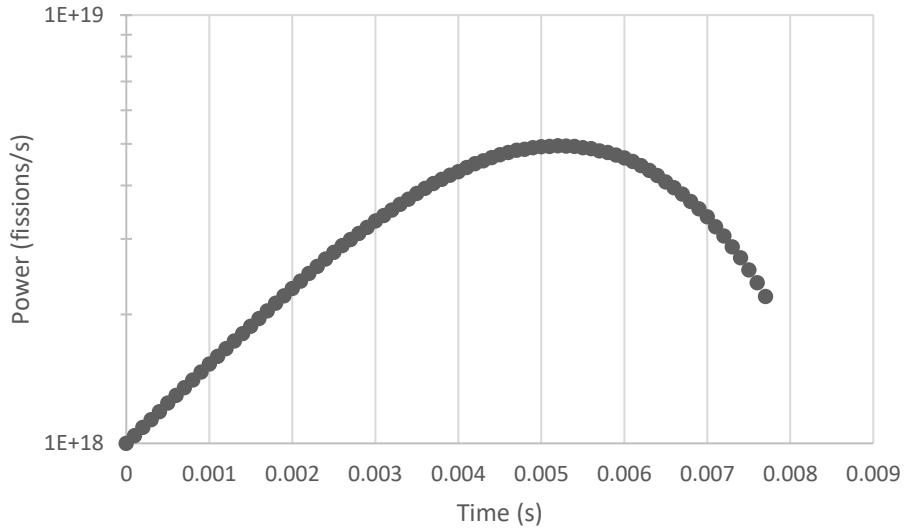


Figure 5-7: SILENE S4-346 Damped Power Profile

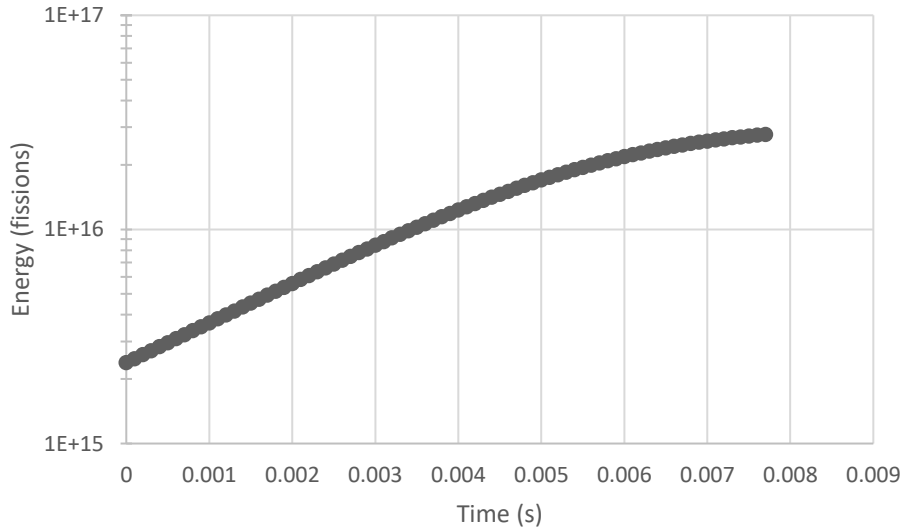


Figure 5-8: SILENE S4-346 Damped Energy Profile

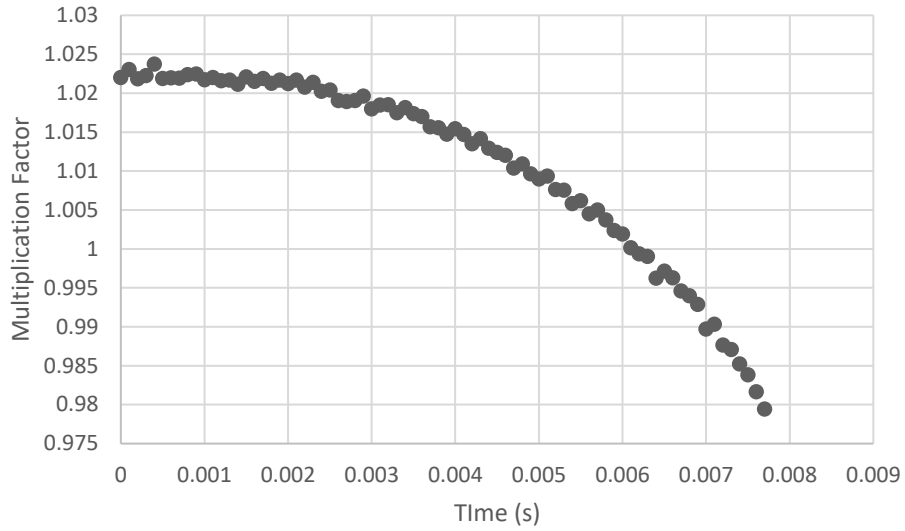


Figure 5-9: SILENE S4-346 Damped Neutron Multiplication Factor Profile

As seen, even with the damping factor used by Hetrick and Smith, this interpretation of the model still results in a much faster termination of criticality than what is seen by experimental results. While the initial geometric profile remains the same as that shown in Figure 5-5, the axial cross-section of the material for the final calculated step of the damped evolution can be seen in Figure 5-10.

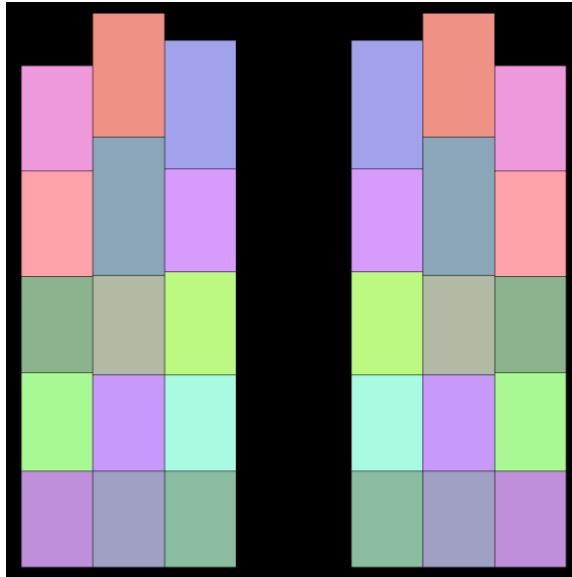


Figure 5-10: SILENE S4-346 Damped Axial Profile at 7.7 ms, Solution Height = 52.5
cm

Within this profile, it can be seen that the central volumetric region did not expand as quickly relative to the undamped profile. Because of the dissipation constant utilized on the material regions adjacent to walls of the solution container, the base profile was able to build up in center of mass velocity at a much quicker rate, and so the solution height reached a larger value before the criticality was terminated. While with the pressure gradient damping factor applied to overall acceleration, the central region for the damped calculations was able to more closely match the dissipated expansion of the boundary regions, and the solution expanded with a much more uniform profile. Again, expansion was primarily seen towards the top of the solution container, where the atmospheric boundary condition is set.

4.4 Wood River Junction

The historical excursion that was seen at Wood River Junction is of a very similar material composition to that seen in the SILENE experiments, being comprised of a 93%

enriched uranyl nitrate solution in a carbonate reagent makeup vessel. This accident has a reported two excursions with two different initiating events (T. McLaughlin et al., 2000), however only the first pulse of this accident will be subject to analysis by the computational model developed.

The exact material composition of the solution involved in the Wood River Junction accident is not known, but it is known that the 93% enriched uranyl nitrate solution involved was contained in a reagent makeup vessel along with an amount of sodium carbonate. The chemical stoichiometry of sodium carbonate is Na_2CO_3 . While carbon has an appreciable scattering cross section for neutrons, it is not believed to have been present in a high enough concentration to adversely affect the energy spectrum of the involved neutrons in a prompt critical pulse scenario, and so both carbon and oxygen are neglected from the overall solution. However, sodium has an appreciable nuclear neutron absorption cross-section, and an analysis was performed to obtain the sodium to uranium ratio present within the system, determined to be a value of 0.358 (Nakache et al., 1964).

Based on the assumption that the overall density of the uranyl nitrate solution was largely unaffected, the additional sodium concentration to be accounted for in the materials data was added to the general uranyl nitrate solution used for the SILENE analysis, and then renormalized to the same overall density, providing the values shown in Table 5-3 for a material definition to use in the SERPENT Monte Carlo analysis.

Table 5-3: Initial Wood River Junction Material Definitions

Isotope	ZAID	Number Density ($\frac{\text{atoms}}{\text{b-cm}}$)
Hydrogen	1001	6.254×10^{-2}
Nitrogen	7014	1.568×10^{-3}
Oxygen	8016	3.574×10^{-2}
Uranium-234	92234	1.059×10^{-6}
Uranium-235	92235	1.685×10^{-4}
Uranium-236	92236	4.347×10^{-7}
Uranium-238	92238	1.169×10^{-5}
Sodium	11023	6.504×10^{-5}

The first pulse of the excursion is reported to have a yield of approximately 1×10^{17} fissions, caused by an initial reactivity of about 1.7 dollars present in the system, which is deemed achievable by the known contents involved (Nakache et al., 1964). Because the materials involved are very similar, again the approximate value for β_d is 8×10^{-3} , which provides a value for the initial neutron multiplication factor k_{eff} of the system of about 1.014.

The geometry of the Wood River Junction vessel is a right-angle cylinder with a 22.9 centimeter radius that contains 41.0 liters of the uranyl nitrate plus sodium carbonate solution. Again, because reactivity controls the evolution of the accident, the initial multiplication vector of the system was controlled through adjustments made to the solution height, which was set at 23.5 centimeters to meet reactivity requirements. Note that this excursion was also reported to have ejected about 20% of the solution, and so the density terminating effect via material loss is highly evident in this system.

An exact profile of the evolution of this system is not available, so the time-scale of the excursion evolution cannot be compared to experimental values, which is why the SILENE S4-346 reactor experiment is a useful parameter comparison. However, knowing that the Wood River Junction accident involved 1.7 dollars of initial reactivity and the first pulse was terminated at approximately 1×10^{17} fissions provides some avenues for comparison. The results of the base calculation proceeded without the pressure gradient damping factor are presented in Figures 5-11, 5-12, and 5-13.

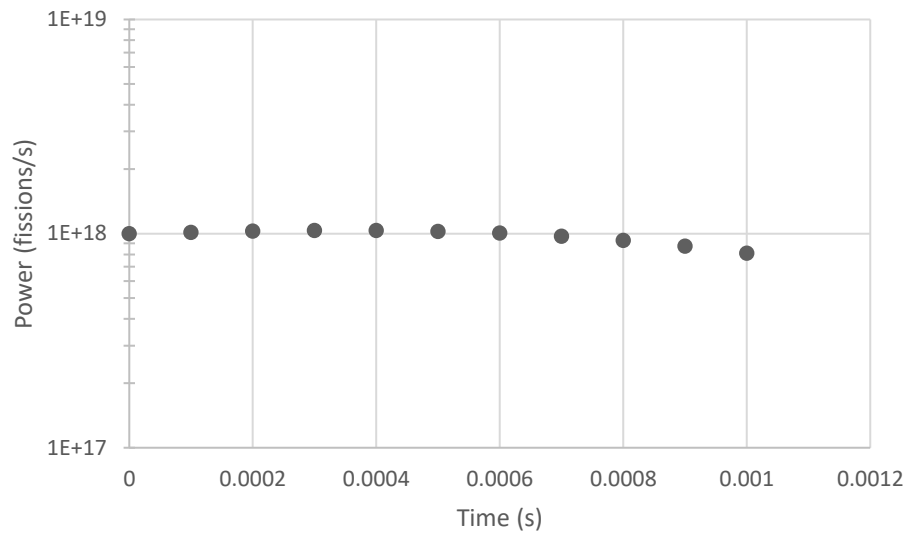


Figure 5-11: Wood River Junction Base Power Profile

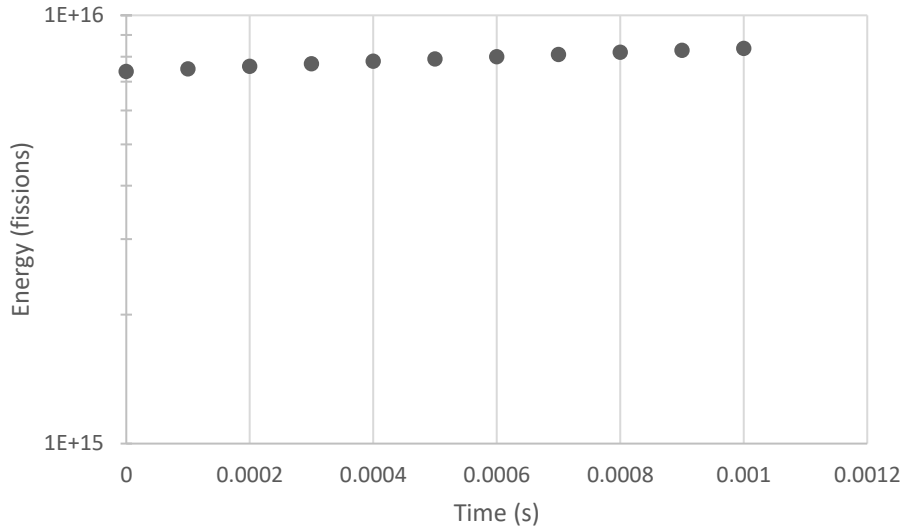


Figure 5-12: Wood River Junction Base Energy Profile

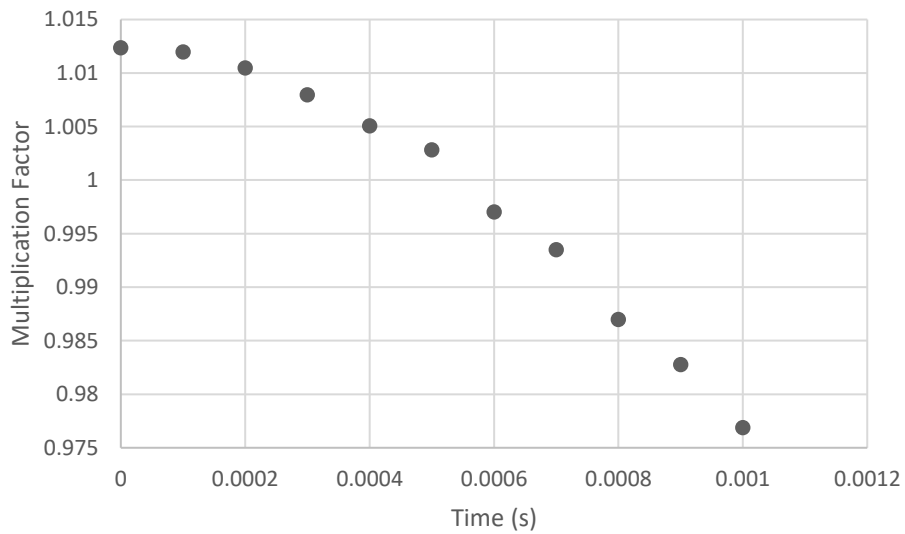


Figure 5-13: Wood River Junction Base Multiplication Factor Profile

As with the SILENE model, it can be seen that the base calculation excursion evolves extremely rapidly, and terminates with a developed integrated fission yield approximately an order of magnitude below the predicted value. The axial cross-sectional profiles generated by the SERPENT program are shown in Figures 5-14 and 5-15.

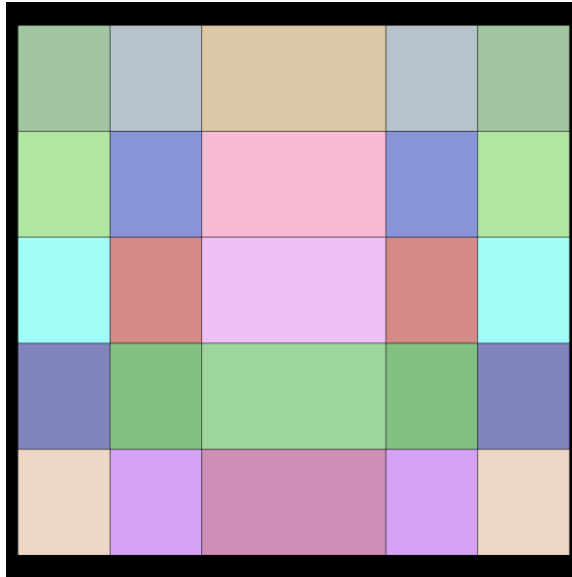


Figure 5-14: Wood River Junction Axial Profile at 0 ms, Solution Height = 23.5 cm

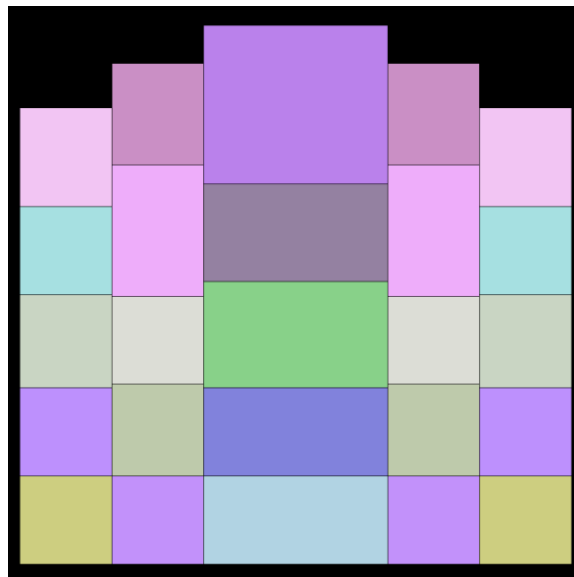


Figure 5-15: Wood River Junction Base Axial Profile at 1.0 ms, Solution Height = 28.7

cm

From these geometric profiles, it can be seen that the solution volume evolution happens at a large scale in the central regions of the container, and again the expansion is most evident towards the top of the assembly, where the atmospheric boundary condition

exists. As there are two central regions now that are not in direct expansion contact with container walls, the dissipation factor is not applied, and the difference between the central radial discretizations can be attributed to the difference in energy input through the calculated fission profile, where a higher energy is deposited in the center due to a greater neutron flux and therefore fission density at the central geometric positions.

When a pressure gradient damping factor is applied to the calculated acceleration, the evolution of the excursion slows down, as to be expected. The results of these calculations are shown in Figures 5-16, 5-17, and 5-18.

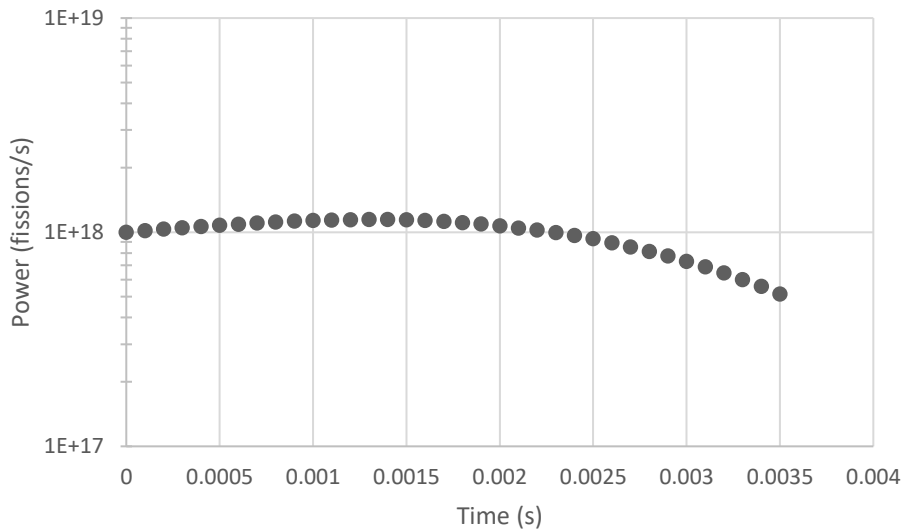


Figure 5-16: Wood River Junction Damped Power Profile

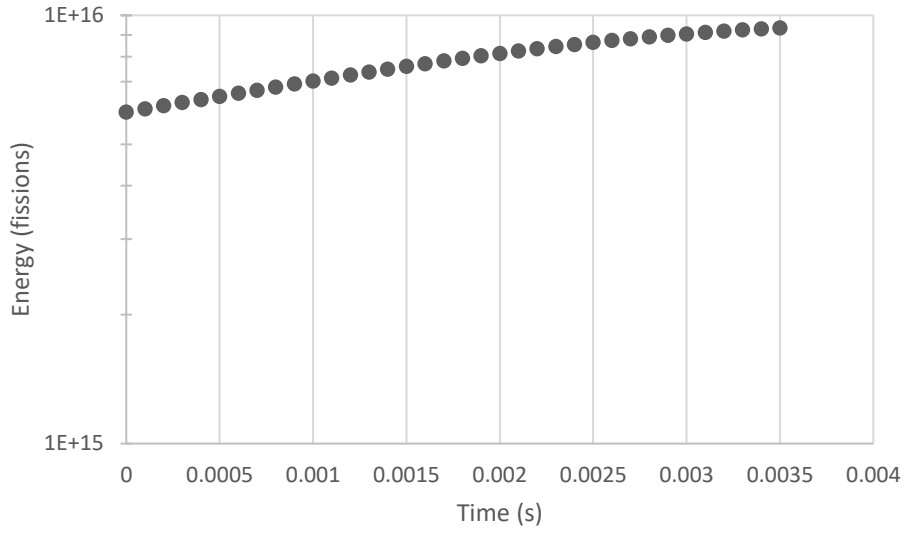


Figure 5-17: Wood River Junction Damped Energy Profile

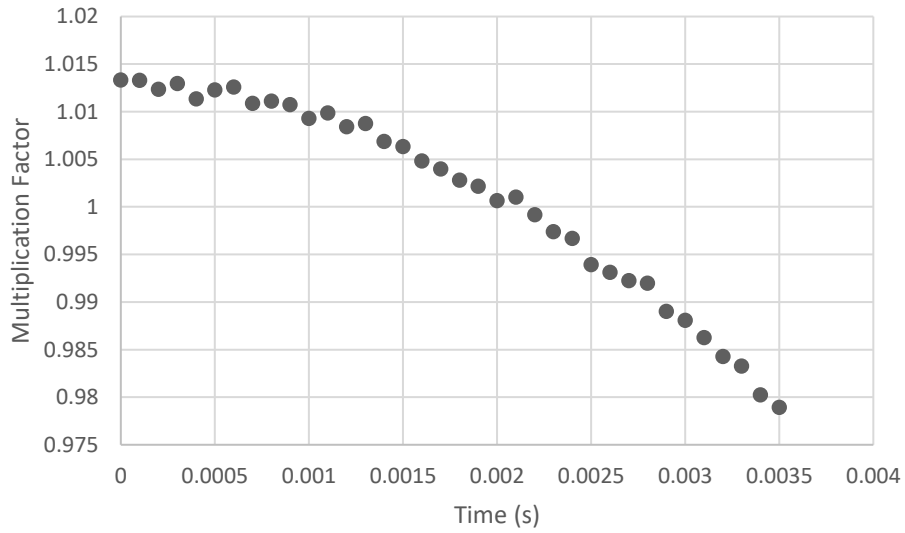


Figure 5-18: Wood River Junction Damped Multiplication Factor Profile

As can be seen, the evolution of this excursion slows down to 3.5 milliseconds prior to termination, and the integrated fission yield increases as a result. However, this fission yield still does not match the reported yield of 1×10^{17} fissions for the first spike (Nakache et al., 1964), and is once again off by approximately an order of magnitude in the damped calculation.

The geometric axial profiles of the solution system should look the same at the initial time step shown in Figure 5-14, but the profile at the point of termination is shown in Figure 5-19.

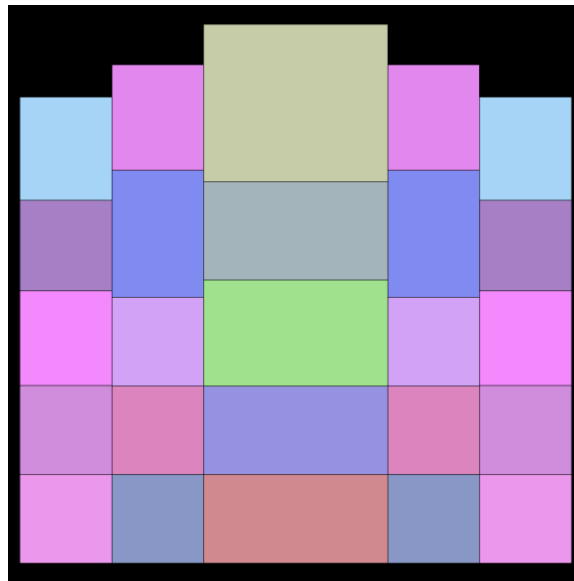


Figure 5-19: Wood River Junction Damped Axial Profile at 3.5 ms, Solution Height = 28.6 cm

As evident from the geometric material profile, the solution expands in a very similar fashion even when damped. In contrast to the SILENE models, the Wood River Junction models only have an outer wall with which to apply the dissipation effects to the acceleration term, and so again the damping factor can be seen to be providing enough

time prior to termination for the outermost radial discretizations to expand slightly before the criticality is terminated due to inertial effects.

4.5 Limiting Acceleration

Overall results indicate a clear trend of aerosolization and splashing that occurs as a result of this model, which leads to a termination of criticality. Even with a pressure gradient damping factor of effectively an order of magnitude decrease applied to the center of mass acceleration term, the approximations made to volumetric expansion are still overpredictors of the actual physical evolution of a solution excursion. It may be the case that a smaller pressure gradient damping coefficient is required to obtain a more accurate evolution profile. With these results in mind, a pressure gradient damping factor of 0.01 was applied to the calculations of both the SILENE and Wood River Junction systems, and as expected the excursion evolution slowed down even further. The excursion evolution calculations performed with a pressure gradient damping factor of 0.01 are referred to as “limited” excursions.

When a damping factor of 0.01 is applied to the SILENE S4-346 experiment, the resulting peak power is calculated to be 2.34×10^{19} fissions per second, which very closely approximates the expected value of 2.40×10^{19} fissions per second for the power of this excursion, the profile for which can be seen in Figure 5-20. The total energy deposition is calculated as being 1.44×10^{17} fissions, which again very closely approximates the expected value of this excursion, given as 1.50×10^{17} total fissions. The profile for the energy deposition of the excursion can be seen in Figure 5-21. As before, the excursion is fairly stable in terms of multiplication factor, and shows a clear trend towards termination, seen in Figure 5-22.

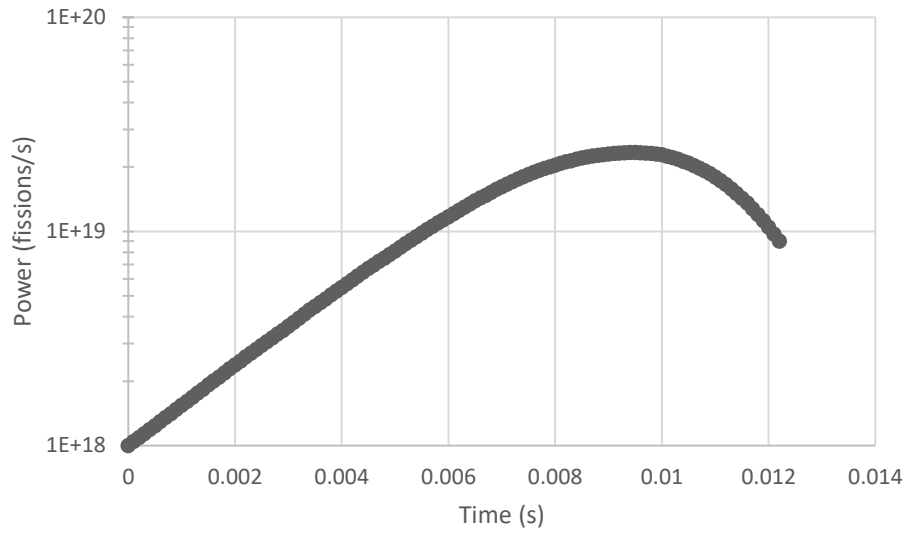


Figure 5-20: SILENE S4-346 Limited Power Profile

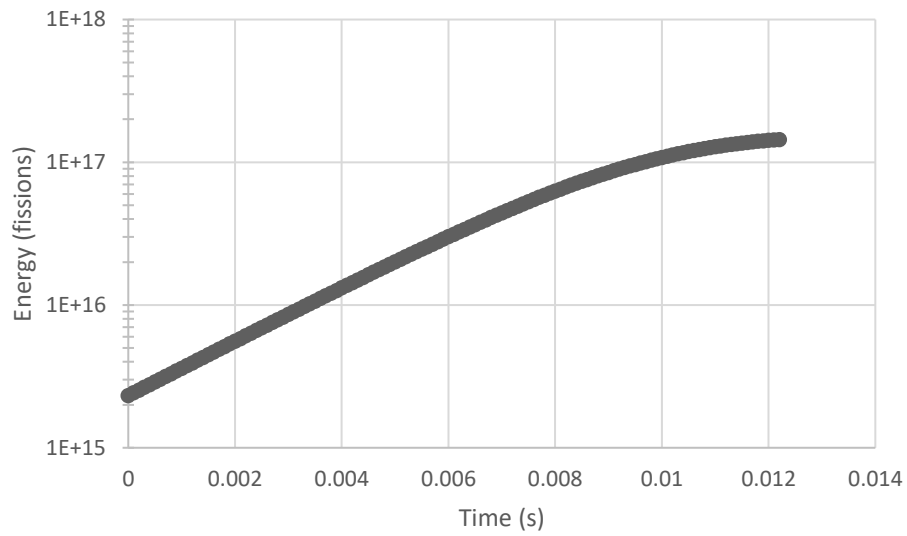


Figure 5-21: SILENE S4-346 Limited Energy Profile

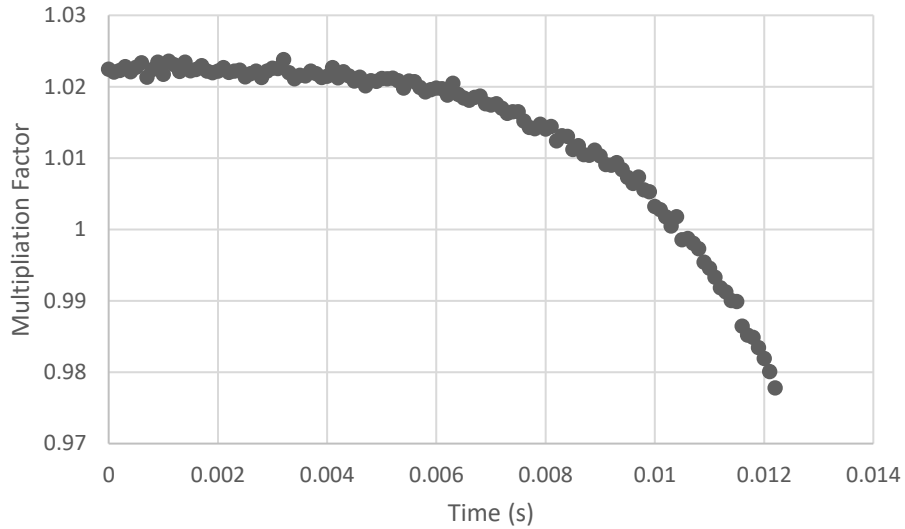


Figure 5-22: SILENE S4-346 Limited Multiplication Factor Profile

The excursion evolves from 1×10^{18} fissions per second to a point of termination at a multiplication factor of 0.98 over the course of 12.2 milliseconds, the final axial cross-sectional profile for which can be seen in Figure 5-23, which shows great promise at providing a rough estimate of the excursion evolution. The higher number of fissions known to be occurring in the central regions of the geometry show a distinct evolution of the inner radial region, promoting expansion beyond the frictional dissipation term being applied to this region.

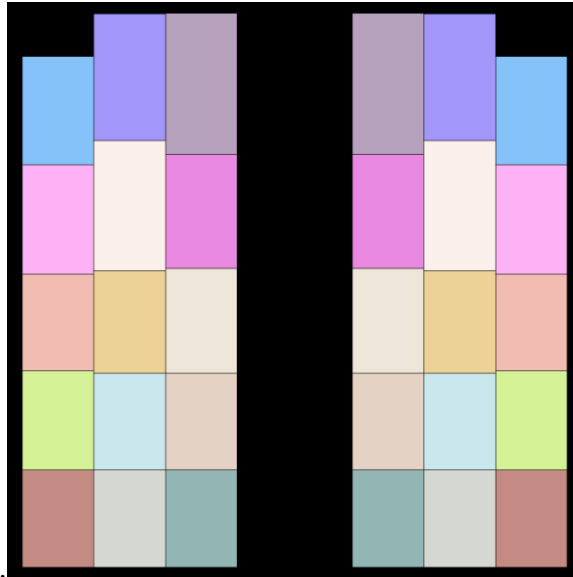


Figure 5-23: SILENE S4-346 Limited Axial Profile at 12.2 ms, Solution Height = 51.9 cm

However, when the same damping factor of 0.01 is applied to the Wood River Junction accidental excursion, the results are slightly further from the expected values. The peak power is estimated as being 1.52×10^{18} fissions per second, as shown in Figure 5-24. This provides a total energy deposition of 1.62×10^{16} fissions, the profile for which is shown in Figure 5-25. While the accident still shows a distinct termination effect as shown in Figure 5-26, the expected yield of this accident is approximately 1×10^{17} fissions of energy deposition, and so the calculated value is still an underprediction.

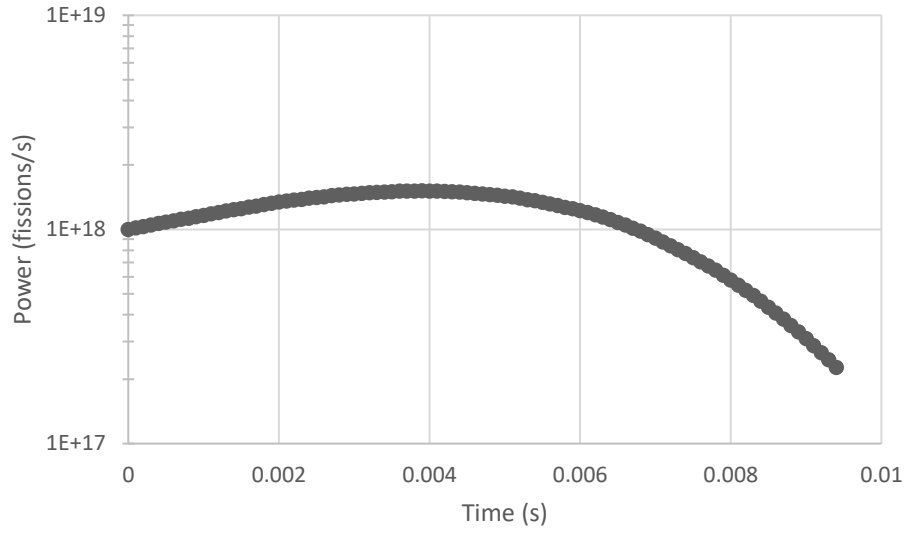


Figure 5-24: Wood River Junction Limited Power Profile

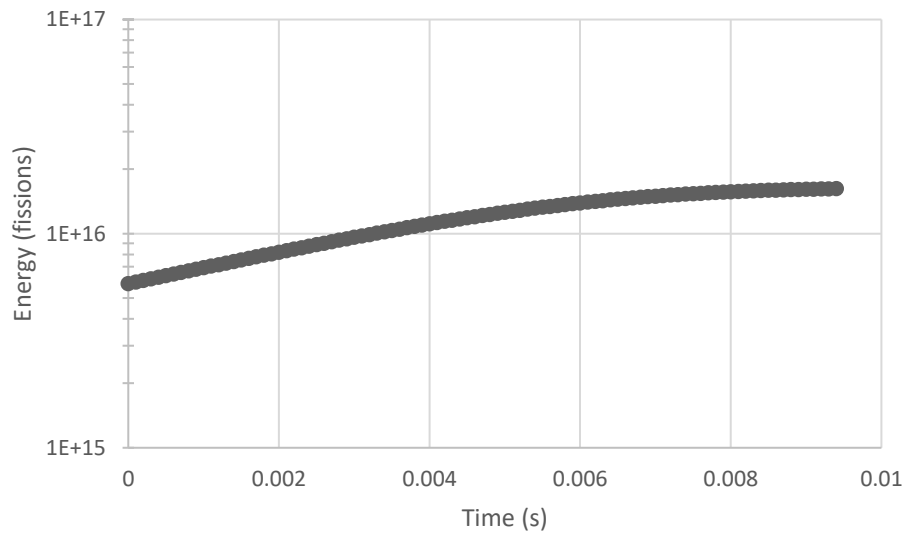


Figure 5-25: Wood River Junction Limited Energy Profile

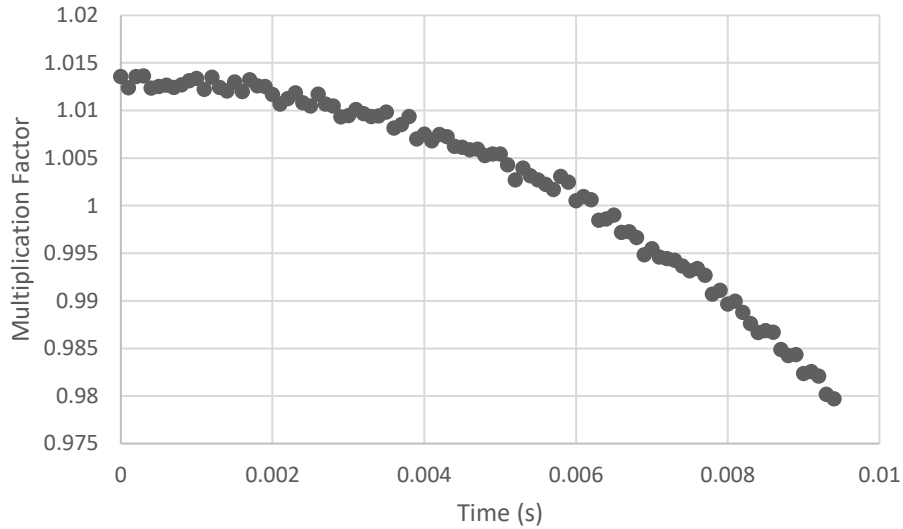


Figure 5-26: Wood River Junction Limited Multiplication Factor Profile

Possible reasons for this underpredicted value are varied, including experimental errors on the side of conservatism when approximating the fission yield in the post-accident analysis at Wood River Junction, as this was not an instrumented, fully-characterized excursion event. An overall damping effect may be present due to fluid turbulence and mixing that was effectively approximated by the two wall frictional dissipation terms seen in the SILENE S4-346 models that doesn't come into effect in the Wood River Junction models, the ending profile for which is shown in Figure 5-27, clearly displaying a large central volumetric expansion of the system. Additionally, the initial power generation of 1×10^{18} fissions per second used as a starting point for the excursion evolution may be too high, and limited the effect of the evolution at Wood River Junction. It should also be mentioned that the Wood River Junction accident was a stirred tank, which would have an additional mechanical energy input that does not get accounted for by this model.

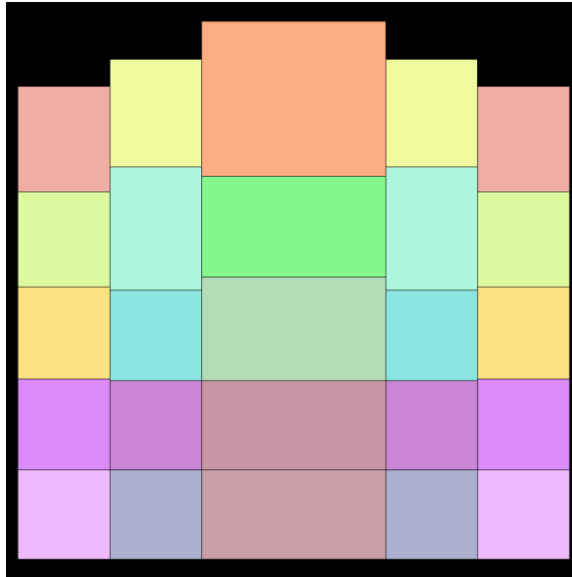


Figure 5-27: Wood River Junction Limited Axial Profile at 9.4 ms, Solution Height = 28.3 cm

While any number of reasons could be the cause of an over-prediction term at the Wood River Junction site, the very close approximation of the SILENE excursion yield is promising. The overall conclusion is that a value of 0.01 pressure gradient damping term is a close approximation of a mechanically terminated excursion, but a smaller value should be used to err on the side of conservatism when approximating the results of an excursion. A lower initial power than 1×10^{18} fissions per second for the excursion evolution calculations could also be desired to more closely approximate the evolution.

It should also be noted that the use of a value of 0.01 for the pressure gradient damping factor resulted in a large amount of pressure build-up within the system via the equations of state. Because the pressure is increased primarily through energy deposition via fissions and decreased through expansion of the material by volumetric change, limiting the volumetric change also limited the loss of pressure from the system.

Chapter 6 – Concluding Remarks

While the safety aspects of an accidental criticality involving a fissile solution system are well-accounted for by the existence of standards and regulations involving site-specific analysis, the existence of general rule-of-thumb evaluations for a solution criticality is still a worthwhile endeavor to allow for quick estimations of expected yield and accident evolution parameters.

Within the known parameters of historical accidents involving solution systems that have occurred, a bounding trend is evident between the usage of Barbry's model (Barbry, 1987) and Tuck's model (Tuck, 1974) that encompasses most of the expected yield values within a relatively high degree of accuracy in comparison to similar such evaluations that have been attempted. Barbry's model tends to over-predict the integrated fission yield of a solution system, while Tuck's model tends to under-predict. In general, both models have a high degree of over-estimation for a relatively low fission yield on the order of 1×10^{15} total fissions to 1×10^{17} total fissions, and the estimated value for an integrated fission yield begins to drop slightly below the reported value at yields larger than approximately 5×10^{17} , a trend that is common to most simple empirical models. It is suggested that should these models be used to calculate a bounding fission yield, this over-estimation to under-estimation trend be taken into account.

The existence of a simple, openly available computational model to evaluate the evolution of a solution-based criticality excursion that includes modern Monte Carlo computational methods and accounts for termination effects by means of a pressure-based acceleration term is largely still unresolved, although it is the hope that such a

model can be generated with a relatively small amount of additional analysis. The use of a multiplying factor by Hetrick and Smith (Hetrick & Smith, 1987) to affect the pressure gradient acceleration term is a concept that could be explored and refined, although using a value of 0.01 for this factor had positive results when applied to the experimental excursion. This factor could be further decreased to allow for conservatism and to more accurately predict the evolution of a less well-defined excursion, but time spent on analysis of this factor would most likely be better spent on an improvement of the solution expansion models, because decreasing the calculated acceleration term by more than two orders of magnitude most probably shows the effects of a very crude model rather than simply an inaccurate term. Additionally, the implementation of this factor produced system pressures of an unexpectedly high magnitude, meaning that further decreasing this value would likely result in a more unrealistic model.

Most minor discrepancies between the Monte Carlo calculated parameters and the empirically calculated values used for the neutronic evolution can likely be attributed both to experimental error and the statistical nature inherent in a Monte Carlo analysis technique, as well as the crude geometries utilized while modeling, such as no atmosphere, container walls, or reflective surroundings (e.g., a concrete floor). For the most part, however, the values returned from Monte Carlo analysis matched the experimental values very accurately where such values are known (Barbry, 1994).

The model used to represent the volumetric expansion mechanisms of the solution system is overall very simplified, and a very rough discretization method was imposed over it for the calculations presented herein. There are additional fluid properties that may be considered for a more refined model in terms of aerosolization, splashing models, and

turbulence effects on solution friction. Treating each volumetric element as a unit of constant properties is considered to be a crude pressure gradient calculation of just a single region, and the current numerical approximation is applied in an explicit fashion, which is subject to instabilities (Hetrick & Smith, 1987).

The model originally developed by Smith and Hetrick that used these thermodynamic profiles and Newtonian mechanics for volumetric acceleration was used with an input of a predetermined power profile (Hetrick & Smith, 1987). Dynamically evolving the power profile through the use of a neutronics code required slight alterations in the order of equation of state calculations performed to reduce the number of instabilities in the model, which is likely the cause of a rapid termination even with the damping factor. The use of a more refined model that solves the issue of extreme pressure development upon limiting the volumetric expansion should be a high priority for future work.

However, the results clearly indicate potential applications of a model of similar construction that could be used to rapidly test and determine the effects of a solution criticality. The model presented herein is meant to include very simple technologies that are easily obtained, and openly available to anyone to either continue research, improve, or utilize for other purposes.

The overall goal of this thesis was to present a collection and analysis of the current state of solution criticality modeling as is available within common avenues of research and publications. It is the sincerest hope of the author that this thesis is useful as an approximation and summary, as well as in laying the groundwork of models for use in the

construction of better-informed decisions by a safety operator, facility worker, or the layperson outside of a closed-source environment.

Appendices: Computational Model Source Code

List of Appendices:

- Appendix A: Driver Script File: `transientmodel.py`
- Appendix B: File Operations Library: `tm_fileops.py`
- Appendix C: Volume and Material Discretization: `tm_material.py`
- Appendix D: Calculational Parameters: `tm_constants.py`

The Python 3.6.3 code used for analysis purposes is included within this section. Any person should be able to utilize this code for their own purposes, as long as they have both a version of SERPENT compatible with the input files for 1.1.7 and a Python interpreter able to recognize the 3.6.3 dialect of the Python programming language.

Usage is simply a matter of running the *transientmodel.py* script file from any terminal emulator, and entering the prompted file name to use for the SERPENT input and output files. Minor modifications may need to be made to *transientmodel.py* to accommodate calling the SERPENT “sss” executable through a medium other than the Windows Subsystem for Linux framework, but this should be straightforward to implement. Calling the SERPENT executable is the only example of such an interaction, and so the modifications required are very limited.

Additional library dependencies used for the Python calculational tool at the time of writing are as follows:

- NumPy version 1.13.3
- RE version 2.2.1

- CoolProp version 6.0.0

Appendix A – Driver Script File: transientmodel.py

This is the main driver, and should be called from a terminal emulator. The purpose of this script is to import all relevant files within the same directory, then proceed with the calculations. Volume elements are created based on the values in *tm_constants.py*, an initial SERPENT input file is created, and the initial neutronics parameters are obtained from the SERPENT output file. For each volume element, the fission power profile generated by SERPENT is used to evolve the element forwards in time based on energy deposition. SERPENT is called after each evolution until a value for the neutronic multiplication parameter k_{eff} falls below 0.98, with the results of each time-step being written to a generic comma-separated-value format output file named “results.txt”.

```
#!/usr/bin/env python3
# -*- coding: utf-8 -*-
# transientmodel.py

...
A transient model for critical solution systems.

By Corey Skinner.

Dependencies:
re for regular expression pattern matching in output files
os for calling the sss and bash processes via command interface, file existence for debug
numpy for arrays and mathematical methods
CoolProp for water properties (assuming aqueous mixture is approximated by water)
... - Imported in module file "tm_material"
...

# External
from os import system, path
import re
import numpy as np

# Shared
from tm_material import Material # Requires CoolProp
import tm_constants as c
import tm_fileops as fo

def set_materials(elems, ndens, tot_height, tot_radius, **kwargs):
    '''Return a list of materials and geometries, radial columns dominant'''
    mat_counter = 1 # Materials begin with number 1
    materials = [] # Two dimensional list of materials for return
    inner_radius = 0 # cm
    # All materials should start out with the same initial density
    dens = [0.0] * len(elems) # g/cm^3
    for ind, nden in enumerate(ndens):
        dens[ind] = nden / 6.022e23 * 1e24 * c.AWEIGHT[ind] # g/cm^3
    den = sum(dens) # g/cm^3
```

```

# Initial pressures are assumed to be linear, based on rho-g-h model
# All pressures are absolute, not gauge
for ind, radius in enumerate(calc_radii(tot_radius)):
    base_height = 0.0 # cm, start at planar origin
    r_list = [] # Second dimension empty list for appending
    # From bottom to top, heights being added
    half_height = 0.0 # m, placeholder
    for height in calc_heights(tot_height):
        # The half_height value is calculated for the initial value from base
        if half_height == 0.0:
            half_height = height / 2
        av_height = (tot_height - height + half_height) / 100 # m
        av_pres = den * c.GRAV * av_height / 1000 * 100**3 / 1e6 + c.ATM # MPa
        # Equivalent to the height of the center of mass:
        com_height = tot_height - av_height * 100 # cm
        if (ind == 0 and c.INNER_RAD > 0.0) or (ind == c.NUM_RADIAL - 1):
            dissipate = 1
        else:
            dissipate = 0
        if 'temp' in kwargs:
            temperature = kwargs['temp'][mat_counter - 1] # K
            r_list.append(Material(mat_counter, elems, ndens, den, height,
                                  base_height, radius, inner_radius, com_height,
                                  dissipate, av_pres, temperature))
        else:
            r_list.append(Material(mat_counter, elems, ndens, den, height,
                                  base_height, radius, inner_radius, com_height,
                                  dissipate, av_pres))

        mat_counter += 1
        base_height = height # cm
        materials.append(r_list)
        inner_radius = radius # cm
    return materials

def propagate_power(k_eff, lifetime, beta_eff, power):
    '''Propagate the number of neutrons over delta-t'''
    reactivity = (k_eff - 1) / k_eff
    prompt_gen_time = lifetime / k_eff # s
    return power * np.exp((reactivity - beta_eff) / prompt_gen_time * c.DELTA_T) # fis/s

def energy_dep_init(k_eff, lifetime, beta_eff):
    '''Calculate the initial energy deposition at the start of the reaction'''
    reactivity = (k_eff - 1) / k_eff
    prompt_gen_time = lifetime / k_eff # s
    period = prompt_gen_time / (reactivity - beta_eff) # s
    # Assuming an initiating accident of 1 fission per second at time t=0
    # NOTE: np.log() is the natural logarithm
    time = np.log(c.INIT_POWER / 1) * period # s
    return period * (np.exp(time / period) - 1) * 1 # fissions

def calc_heights(tot_height):
    '''Returns a list of the ranges of height based on total'''
    height_diff = tot_height / c.NUM_AXIAL # cm
    heights = list(map(lambda ind: ind * height_diff, range(1, c.NUM_AXIAL + 1))) # cm
    return heights # cm

def calc_radii(tot_rad):
    '''Returns a list of the ranges of radii based on total'''
    rad_diff = (tot_rad - c.INNER_RAD) / c.NUM_RADIAL # cm
    radii = list(map(lambda ind: ind * rad_diff + c.INNER_RAD, range(1, c.NUM_RADIAL + 1))) # cm
    return radii # cm

def update_material_states(materials, fissions, tot_height, initial=False):
    '''Updates the state of all materials in profile'''
    counter = 0 # Two inner loops prevent use of enumerate()
    temperatures = [] # K
    pressures = [] # MPa
    heights = [] # cm
    top_pressure = c.ATM # MPa

```

```

for material_layer in materials:
    bot_height = 0.0 # cm
    for material in material_layer:
        material.update_temp(fissions[counter])
        counter += 1
    if not initial:
        for material in reversed(material_layer):
            material.update_pres()
            material.update_vol(top_pressure)
            top_pressure = material.bot_pressure # MPa
        for material in material_layer:
            material.update_temp(0.0, decrease=True)
            material.update_pres(decrease=True)
            temperatures.append(material.temp) # K
            pressures.append(material.av_pressure) # MPa
            material.shift_height(bot_height)
            bot_height = material.height # cm
            heights.append(material.height) # cm
    tot_height = max(heights) # cm
return tot_height, temperatures, pressures # cm, [K], [MPa]

def main():
    '''Main wrapper'''
    print("\nWelcome to the Transient Solution Modeling software.")
    print("Developed by Corey Skinner for the purposes of a revision of")
    print("DOE-HDBK-3010, Chapter 6: Accidental Criticality using the Python 3.6")
    print("programming language in 2017. Supplementary work for a Master's Thesis,")
    print("\nEvaluation of Energy Released in Nuclear Criticality Excursions in")
    print("Process Solutions\n")
    print("\nPlease enter a filename (no extension necessary):")
    filename = input(">>> ")
    if not filename.endswith(".inp"):
        filename += ".inp"
    if not filename.strip():
        print("Must include a filename...")
        raise ValueError
    tot_height = c.INIT_HEIGHT # cm
    tot_radius = c.RAD # cm
    # Set materials
    materials = set_materials(c.ELEMS, c.NDENS, tot_height, tot_radius)
    print("Running preliminary file, to determine masses, volumes, etc..")
    timer = 0 #s
    fo.write_file(filename, materials, tot_height)
    outfile = filename + "_res.m"
    detfilename = filename + "_det0.m"
    # Execute SERPENT calculation
    if not path.isfile(outfile):
        system("bash -c \"sss {}\"".format(filename))
    temperatures = [] # K
    pressures = [] # MPa
    for material_layer in materials:
        for material in material_layer:
            temperatures.append(material.temp) # K
            pressures.append(material.av_pressure) # MPa
    maxtemp = max(temperatures) # K
    maxpres = max(pressures) # MPa
    power = c.INIT_POWER # Start of the flux
    lifetime, keff, keffmax, nubar, beff = fo.get_transient(outfile) # s, _, _, n/fis, _
    timer = 0 # s
    integrated_fissions = energy_dep_init(keff, lifetime, beff) # fissions
    total_fissions = integrated_fissions # fissions
    number_fissions = power * c.DELTA_T # fissions
    # Start results file
    with open('results.txt', 'w') as resfile:
        resfile.write("Time (s), Num Fissions, Total Fissions, Max Temperature (K), " + \
            "Max Pressure (bar), Neutron Lifetime (s), nu-bar, b-eff, k-eff, " + \
            "k-eff+2sigma, Max Height (cm)\n")
    fo.record(timer, number_fissions, total_fissions, maxtemp, maxpres * 10, lifetime,
        nubar, beff, keff, keffmax, tot_height)

```

```

initial = True # Flag to calculate integrated energy deposition with initial profile
# Material addition loop
print("Beginning main calculation...")
# # Material expansion loop
print("Now expanding system by temperature...")
while keff > c.SUBCRITICAL_LIMIT:
    # Proceed in time
    timer += c.DELTA_T # s
    # Read previous output file for information and calculate new changes
    fission_profile = fo.count_fissions(detfilename)
    power = propagate_power(keff, lifetime, beff, power) # fissions/s
    # Correlation between flux profile and fission density
    number_fissions = power * c.DELTA_T # fissions
    fissions = [frac * number_fissions for frac in fission_profile] # fissions
    total_fissions += number_fissions # fissions
    # Assume that initiating fission profile does not change from the initial calculation
    if initial:
        initial = False # Only calculate one time
        integrated_dist = [frac * integrated_fissions for frac in fission_profile] # fissions
        _, _, _ = update_material_states(materials, integrated_dist, tot_height,
                                       initial) # cm, [K], [MPa]

    # Begin total expansion of material
    #if c.EXPANSION:
    #    update_pressures(materials)
    #    update_heights(materials)
    tot_height, temperatures, pressures = update_material_states(materials, fissions,
                                                                tot_height) # cm, [K], [MPa]

    maxtemp = max(temperatures) # K
    maxpres = max(pressures) # MPa
    timer_string = f"{round(timer, abs(c.TIMESTEP_MAGNITUDE)).6f}"
    filename = re.sub(r'\d', r'', filename[:filename.rfind(".inp")]).replace('.', '') \
               + timer_string + ".inp"
    outfile = filename + "_res.m"
    detfilename = filename + "_det0.m"
    # Do not need to recalculate masses (thus volumes) for materials at this stage
    fo.write_file(filename, materials, tot_height)
    # NOTE: Conditional should be "outfile", but can be "filename" for debugging purposes
    if not path.isfile(outfile):
        system("bash -c \"sss {}\"".format(filename))
    lifetime, keff, keffmax, nubar, beff = fo.get_transient(outfile)
    fo.record(timer, number_fissions, total_fissions, maxtemp, maxpres * 10, lifetime,
             nubar, beff, keff, keffmax, tot_height)
    print("Current time: {} s".format(round(timer, abs(c.TIMESTEP_MAGNITUDE) + 1)))
    print("Current k-eff: {}".format(keff))
    print("Maximum k-eff: {}".format(keffmax))
    print("Number of fissions: {0:E}".format(sum(fissions)))
    print("Maximum temperature: {}".format(maxtemp))

if __name__ == '__main__':
    try:
        main()
    finally:
        print("\nProgram terminated\n")

```

Appendix B – File Operations Library: tm_fileops.py

This is a library of functions used for file input and output. These functions include writing a SERPENT input file, reading relevant neutronics parameters from a SERPENT output file, and appending to a results file. This file is imported into the *transientmodel.py* script.

```
# -*- coding: utf-8 -*-
# tm_fileops.py
'''
Import only module. Contains operations on input and output files from SERPENT,
primarily writing input files and reading detector output files and parameter output
files.

Also contains functionality for writing overall results file.
'''

import re
import tm_constants as c

def count_fissions(filename):
    '''Read an output file to determine the fission (flux) distribution'''
    pat = re.compile(r'(\s+1)\1+\s+(\S+)')
    profile = []
    counter = 0
    with open(filename, mode='r') as detfile:
        for line in detfile:
            if re.match(pat, line):
                matches = re.findall(pat, line)
                if counter != 0:
                    profile.append(float(matches[0][1]))
                counter += 1
    return profile

def get_transient(filename):
    '''
    Read an output file to determine the transient point-reactor kinetics parameters
    Returns tuple of lifetime, k-eff, maximum k-eff, nu-bar, and beta-eff
    '''
    ltpat = re.compile(r'ANA_PROMPT_LIFETIME\s+(\idx, \s+[1:\s+2]\)\s=\s\[\s+(\S+)\s\S+\s\];')
    kepat = re.compile(r'ANA_KEFF\s+(\idx, \s+[1:\s+2]\)\s=\s\[\s+(\S+)\s(\S+)\s\];')
    nbpat = re.compile(r'NUBAR\s+(\idx, \s\S+\s+\S+)\s=\s\[\s+(\S+).+;')
    bepat = re.compile(r'BETA_EFF\s+(\idx, \s\S+\s+\S+)\s=\s\[\s+(\S+).+;')
    with open(filename, mode='r') as ofile:
        for line in ofile:
            if re.match(ltpat, line):
                matches = re.findall(ltpat, line)
                lifetime = float(matches[0]) # s
            if re.match(kepat, line):
                matches = re.findall(kepat, line)
                keff = float(matches[0][0])
                maxkeff = round(keff + 2 * float(matches[0][1]), 5)
            if re.match(nbpat, line):
                matches = re.findall(nbpat, line)
                nubar = float(matches[0]) # n/fis
            if re.match(bepat, line):
                matches = re.findall(bepat, line)
                beff = float(matches[0])
```

```

return (lifetime, keff, maxkeff, nubar, beff) # s, _, _, n/fis

def write_file(filename, materials, tot_height):
    '''Function to create the series of input files'''
    with open(filename, mode='w', newline='\n') as fhan:
        fhan.write("% Serpent Input File\n")
        fhan.write("set title \"{}\" \n\n".format(filename[:filename.rfind(".inp")]))
        # Material data
        fhan.write("\n% Materials\n")
        for material_level in materials:
            for material in material_level:
                fhan.write(str(material))
        # Surface data
        fhan.write("\n% Surfaces\n")
        # Axial distributions occur on order nx, where n is the material number
        # and x is the plane number (1 for bottom and 2 for top)
        # Radial distributions read as n, where n is increasing to NUM_RADIAL
        if c.INNER_RAD > 0.0:
            fhan.write("surf 0 cyl 0 0 {} \n".format(c.INNER_RAD))
        for rad_ind, material_level in enumerate(materials):
            fhan.write("surf {0} cyl 0 0 ".format(rad_ind + 1))
            for mat_ind, material in enumerate(material_level):
                if mat_ind == 0:
                    fhan.write("{} \n".format(material.radius))
                    fhan.write("surf {0}0 pz {1} \n".format(rad_ind + 1, material.base_height))
                fhan.write("surf {0}{1} pz {2} \n".format(rad_ind + 1, mat_ind + 1,
material.height))
            # Overall boundaries
            fhan.write("surf 1001 pz 0 \n")
            fhan.write("surf 1002 pz {} \n\n".format(tot_height))
        # Cell data
        fhan.write("\n% Cells\n")
        # Cells are numbered by n, where n is the material number
        for rad_ind, material_level in enumerate(materials):
            # Void super-radials are marked with 10n, where n is the radial number
            # Void sub-radials are marked with 11n, where n is the radial number
            fhan.write("cell 10{0} {0} void {0} \n".format(rad_ind + 1))
            if rad_ind > 0:
                fhan.write("cell 11{0} {0} void -{1} \n".format(rad_ind + 1, rad_ind))
            elif c.INNER_RAD > 0.0:
                fhan.write("cell 11{0} {0} void -0 \n".format(rad_ind + 1))
            # Void sub-axials are marked with 12n, where n is the radial number
            for mat_ind, material in enumerate(material_level):
                if mat_ind == 0:
                    fhan.write("cell 12{0} {0} void -{0}0 \n".format(rad_ind + 1))
                fhan.write("cell {0} {1} solution{0} {1}{2} -{1}{3} -{1}"
                    .format(material.matnum, rad_ind + 1, mat_ind, mat_ind + 1))
                if rad_ind > 0:
                    fhan.write(" {}".format(rad_ind))
                elif c.INNER_RAD > 0.0:
                    fhan.write(" 0")
                fhan.write("\n")
            # Void super-axials are marked with 13n, where n is the radial number
            fhan.write("cell 13{0} {0} void {0}{1} \n".format(rad_ind + 1, c.NUM_AXIAL))
            fhan.write("\n")
        # Global universe cells, marked with 100n, where n is the radial number
        if c.INNER_RAD > 0.0:
            fhan.write("cell 1000 0 void 1001 -1002 -0 \n")
        for radial_num in range(1, c.NUM_RADIAL + 1):
            fhan.write("cell 100{0} 0 fill {0} 1001 -1002 -{0} ".format(radial_num))
            if radial_num > 1:
                fhan.write(" {}".format(radial_num - 1))
            elif c.INNER_RAD > 0.0:
                fhan.write(" 0")
            fhan.write("\n")
        # Now mark global outside, still of form 100n, but with n > radial number
        fhan.write("cell 100{0} 0 outside -1001 -{1} \n".format(c.NUM_RADIAL + 1, c.NUM_RADIAL))
        fhan.write("cell 100{0} 0 outside 1002 -{1} \n".format(c.NUM_RADIAL + 2, c.NUM_RADIAL))
        fhan.write("cell 100{0} 0 outside {1} \n".format(c.NUM_RADIAL + 3, c.NUM_RADIAL))

```

```

fhan.write("\n")
# Thermal scattering S(a,b)
fhan.write("\n% Thermal scattering library\n")
for material_level in materials:
    for material in material_level:
        fhan.write("therm lwtr{0} lwe7.{1}\n".format(material.matnum, material.sab_tag))
fhan.write("\n")
# Cross-section library
fhan.write("\n% Cross-section library\n")
fhan.write("set acelib \"/xs/sss_endfb7u.xsdata"\n\n")
# Criticality parameters
fhan.write("\n% Criticality parameters\n")
# Leave a guess of 1.0 for k-eff
fhan.write("set pop {0} {1} {2} 1.0\n\n"
          .format(c.NUM_PARTICLES, c.NUM_CYCLES, c.NUM_DROPS))
# Include unresolved resonance probability tables
fhan.write("\n% Unresolved resonance probability calculations\n")
fhan.write("set ures 0\n\n")
# Geometry plot
fhan.write("\n% Geometry plot\n")
fhan.write("plot 1 1000 1000 0 -{0} {0} -1 {1}\n\n".format(c.RAD + 1, tot_height + 1))
# Flux detectors
fhan.write("\n% Flux detectors\n")
# Total detector of fissions
fhan.write("det 100 du 0 dr -6 void\n")
for material_level in materials:
    for material in material_level:
        fhan.write("det {0} dc {0} dr -6 void dt 3 100\n".format(material.matnum))

def record(time, numfissions, totfissions, maxt, maxp, lifetime, nubar, beff, keff,
          keffmax, maxheight):
    '''Record current step to a results file'''
    with open("results.txt", 'a') as appfile:
        appfile.write("{0}, {1:E}, {2:E}, {3}, {4}, {5}, {6}, {7}, {8}, {9}, {10}\n"
                    .format(round(time, abs(c.TIMESTEP_MAGNITUDE) + 1), numfissions,
                            totfissions, maxt, maxp, lifetime, nubar, beff, keff,
                            keffmax, maxheight))

```

Appendix C – Volume and Material Discretization: `tm_material.py`

This is a class definition used for each volume-discretized element in the analysis. This file is used as an import to `transientmodel.py` as the framework for discretization objects that are created, and allows for those objects to maintain their own states, such as temperature, pressure, density, geometric position, and so on. This file also allows each object to propagate itself forward in one time-step based on energy deposition, including expansion in space and production of radiolytic gas. Such propagation calculations are explicitly called by `transientmodel.py`, where the height shift and pressure balances with respect to atmosphere can be accounted for on an overall scale not achievable by these discretized elements. These volume objects also have their string representations overloaded to be compatible with SERPENT input files for material definitions, allowing for number densities of each volume object to be dynamically stored as specified by this class definition.

```
# -*- coding: utf-8 -*-
# tm_material.py
...
Import only module. Material definition for transient model, defined as a discretized
segment of overall solution volume.

Dependencies:
CoolProp for material properties
numpy for mathematical constants (should be included as part of main file import already)
...

# External
from CoolProp.CoolProp import PropsSI # Assuming that the solution is approximated by water
import numpy as np # Bring pi into namespace for cylindrical volume calculations

# Shared
import tm_constants as c # Required for the included tag dictionaries

class Material():
    '''Generic class for the material in question, and associated geometry'''
    def __init__(self, matnum, elems, ndens, dens, height, base_height, radius,
                 inner_radius, com_height, dissipate, pres=c.ATM, temp=300):
        self.dissipate = dissipate # Governs if the material is decelerated due to friction
        self.matnum = matnum
        self.elems = elems
        self.ndens = ndens # a/b-cm
        self.temp = temp # K
        self.height = height # cm, note that this is the ABSOLUTE HEIGHT of the material from 0
```

```

self.base_height = base_height # cm
self.radius = radius # cm
self.inner_radius = inner_radius # cm
self.dens = dens # g/cm^3
self.init_dens = dens # g/cm^3
self.mass = 0.0 # g, placeholder until calculated
self.volume = 0.0 # cm^3, placeholder until calculated
self.base = 0.0 # cm^2, placeholder until calculated
self.kappa = 0.0 # 1/Pa, isothermal compressibility, placeholder until needed
self.beta = 0.0 # 1/K, isobaric compressibility, placeholder until needed
self.delta_temp = 0.0 # K, initially zero upon definition
self.delta_pres = 0.0 # Pa, initially zero upon definition
self.atoms = [0.0] * len(ndens) # _, placeholder until calculated
self.volfrac_gas = 0.0 # _, initially no radiolytic gas in solution
self.mass_h2 = 0.0 # g, initially no radiolytic gas in solution
# Pressure: Assume atmospheric conditions (allow for expansion of fluid)
self.av_pressure = pres # MPa, gauge value
self.calc_bottom_pressure() # MPa, calculate from average pressure input
self.com_height = com_height # cm
self.com_accel = 0.0 # cm/s^2, initially not in motion
self.com_vel = 0.0 # cm/s, initially not in motion
self.delta_com = 0.0 # cm, placeholder, no initial delta
self.delta_vol = 0.0 # cm^3, placeholder, no initial delta
self.xs_tag = "03c"
self.sab_tag = "00t"
self.gas_production_flag = False # Once radiolytic gas is produced, keep producing it
if temp != 300: # K
    self.__update_xs_tag()
    self.__update_sab_tag()
self.__calc_init()

def shift_height(self, baseheight):
    '''Shift each segment upwards by a set distance'''
    shift = baseheight - self.base_height # cm
    self.base_height = baseheight # cm
    self.height += shift # cm
    self.com_height += shift # cm

def update_temp(self, fissions, decrease=False):
    '''Update temperature of the solution based on energy input'''
    # Assume that the system properties do not diverge greatly from those for water
    spec_heat = PropsSI('O', 'T', self.temp, 'Q', 0.0, 'WATER') # J/kg-K
    # Assume that 180 MeV is deposited in the solution per fission event
    if not decrease:
        self.delta_temp = (fissions * 180 * 1.6022e-13) / spec_heat / (self.mass / 1000) # K
    else:
        beta_0 = PropsSI('ISOBARIC_EXPANSION_COEFFICIENT', 'T', self.temp,
            'Q', 0.0, 'WATER') # 1/K
        kappa_0 = PropsSI('ISOTHERMAL_COMPRESSIBILITY', 'T', self.temp,
            'Q', 0.0, 'WATER') * 1e6 # 1/MPa
        surf_tens = PropsSI('I', 'T', self.temp, 'Q', 0.0, 'WATER') * 1e-6 # MN/m
        self.beta = beta_0 * (1 - self.volfrac_gas) + self.volfrac_gas / self.temp \
            * (self.av_pressure + 2 * surf_tens / c.RAD_GAS_BUBBLE) \
            / (self.av_pressure + 4 * surf_tens / 3 / c.RAD_GAS_BUBBLE) # 1/K
        self.kappa = kappa_0 * (1 - self.volfrac_gas) + self.volfrac_gas \
            / (self.av_pressure + 4 * surf_tens / 3 / c.RAD_GAS_BUBBLE) # 1/MPa
        self.delta_temp = -(self.beta * self.temp / (self.kappa * 1e-6) \
            * (self.delta_vol / 100**3)) / spec_heat / (self.mass / 1000) # K
    self.temp += self.delta_temp # K

def update_vol(self, top_pres):
    '''Update center of mass acceleration, and volume'''
    self.calc_bottom_pressure(top_pres)
    self.com_accel = (self.base / 100**2) / (self.mass / 1000) \
        * (self.bot_pressure - top_pres) * 1e6 * 100 - c.GRAV * 100 # cm/s^2
    dissipation = self.dissipate * c.DISSIPATION * self.com_vel # cm/s^2
    if np.abs(self.com_accel) < dissipation:
        self.com_accel = 0 # cm/s^2
    else:

```

```

        self.com_accel -= np.abs(dissipation) * np.sign(self.com_accel) # cm/s^2
# Pressure gradient dampening factor
self.com_accel *= c.DAMPING_FACTOR # cm/s^2
com_vel_i = self.com_vel # cm/s
com_vel_f = com_vel_i + self.com_accel * c.DELTA_T # cm/s
self.com_vel = com_vel_f # cm/s, update information for next snapshot
self.delta_com = com_vel_i * c.DELTA_T + 1 / 2 * self.com_accel * c.DELTA_T**2 # cm
self.com_height += self.delta_com # cm
half_height = self.com_height - self.base_height # cm
self.height = self.base_height + 2 * half_height # cm
old_vol = self.volume # cm^3
self.volume = self.base * (self.height - self.base_height) # cm^3
self.dens = self.mass / self.volume # g/cm^3
# Restrict material by density to disallow compression, allow expansion
if self.dens > self.init_dens:
    self.dens = self.init_dens # g/cm^3
    self.volume = self.init_vol # cm^3
    self.height = self.volume / self.base + self.base_height # cm
    self.com_vel = 0.0 # cm/s
    self.com_accel = 0.0 # cm/s^2
    self.com_height = (self.base_height + self.height) / 2 # cm
self.delta_vol = self.volume - old_vol # cm^3
self.ndens = [atom * 1e-24 / self.volume for atom in self.atoms] # a/b-cm

def update_pres(self, decrease=False):
    '''Update pressure of the solution system based on intensive properties'''
    beta_0 = PropsSI('ISOBARIC_EXPANSION_COEFFICIENT', 'T', self.temp,
                    'Q', 0.0, 'WATER') # 1/K
    kappa_0 = PropsSI('ISOTHERMAL_COMPRESSIBILITY', 'T', self.temp,
                     'Q', 0.0, 'WATER') * 1e6 # 1/MPa
    surf_tens = PropsSI('I', 'T', self.temp, 'Q', 0.0, 'WATER') * 1e-6 # MN/m
    self.beta = beta_0 * (1 - self.volfrac_gas) + self.volfrac_gas / self.temp \
                * (self.av_pressure + 2 * surf_tens / c.RAD_GAS_BUBBLE) \
                / (self.av_pressure + 4 * surf_tens / 3 / c.RAD_GAS_BUBBLE) # 1/K
    self.kappa = kappa_0 * (1 - self.volfrac_gas) + self.volfrac_gas \
                / (self.av_pressure + 4 * surf_tens / 3 / c.RAD_GAS_BUBBLE) # 1/MPa
    if not decrease:
        self.delta_pres = self.beta / self.kappa * self.delta_temp # MPa
    else:
        self.delta_pres = -(self.delta_vol / 100**3) / self.kappa * (self.volume / 100**3) #
MPa
    self.av_pressure += self.delta_pres # MPa

def calc_bottom_pressure(self, top_pres=None):
    '''Called to calculate bottom pressure, overloaded with top pressure if known'''
    if top_pres is None:
        self.bot_pressure = self.av_pressure + self.dens * c.GRAV \
                            * (self.height - self.base_height) / 2 * 100**2 / 1000 / 1e6 #
MPa
    else:
        self.bot_pressure = 2 * self.av_pressure - top_pres # MPa

def __update_xs_tag(self):
    '''Update the materials cross-section tag; called when new temperature calculated'''
    round_value = 300 # technically K
    rounded_temp = int(round_value * round(self.temp / round_value))
    self.xs_tag = c.XS_TEMP.get(rounded_temp, "18c")

def __update_sab_tag(self):
    '''Update the thermal scattering correction tag; called when new temperature calculated'''
    round_value = 50 # technically K
    rounded_temp = int(round_value * round(self.temp / round_value))
    self.sab_tag = c.SAB_TEMP.get(rounded_temp, "18t")

def __produce_gas(self, fissions):
    '''Produce a mass of radiolytic gas in the solution; called from self.update_pressure()'''
    # 180 MeV deposited in solution per fission event
    energydep = fissions * 180 * 1.6022e-19 # MJ
    self.mass_h2 += c.RADIOLYTIC_G * energydep * 1000 # g

```

```

self.__update_volfrac_gas()

def __update_volfrac_gas(self):
    '''Update the volume fraction of gas, f_e; called from self.produce_gas()'''
    # Surface tension is re-called for program clarity (prevents multiple function passes)
    self.volfrac_gas = self.mass_h2 / 1000 * c.RH2 * self.temp \
        / (self.volume / 100**3
           * (self.av_pressure * 1e6 + 2 \
              * PropsSI('I', 'T', self.temp, 'Q', 0.0, 'WATER')
              / c.RAD_GAS_BUBBLE))

def __calc_init(self):
    '''Self-called method to calculate some constants after initial file run'''
    # Ideally only called ONE time after each material definition
    self.base = np.pi * (self.radius**2 - self.inner_radius**2) # cm^2
    self.volume = self.base * (self.height - self.base_height) # cm^3
    self.init_vol = self.volume # cm^3
    self.atoms = [nden * 1e24 * self.volume for nden in self.ndens] # a
    self.mass = self.dens * self.volume # g

def __str__(self):
    # Material representation, overload built-in string definition
    #round_value = 300 # K
    #rounded_temp = int(round_value * round(self.temp / round_value)) # K
    ret = "mat solution{0} sum moder lwtr{0} 1001 tmp {1}\n".format(self.matnum, self.temp)
    template = "{0}.{1} {2}\n"
    for ind, elem in enumerate(self.elems):
        ret += template.format(elem, self.xs_tag, self.ndens[ind])
    return ret + "\n" # str

```

Appendix D – Calculational Parameters: tm_constants.py

This can simply be thought of as a listing of settings and constants for the calculations. Most unit conversions are hard-coded into the relevant equations, and so changing the constants to different units is not recommended without requiring a refactoring of the overall code, but routines are in place to allow for changes such as the number of discretizations in either the axial or radial direction, the geometry of the system, material definitions, and time-step magnitude. Any change made to this file is contributed to the overall calculational tool, with the intention of having an easily modifiable tool for use with any given cylindrical system of fissionable material.

```
# -*- coding: utf-8 -*-
# tm_constants.py

...
Import only module. Contains constants for the Python calculations of solution
criticality excursions.
...

# SILENE annular geometry
#RAD = 18.0 # cm
#INNER_RAD = 3.8 # cm
#INIT_HEIGHT = 45.5 # cm

# Wood River geometry
RAD = 22.9 # cm
INNER_RAD = 0.0 # cm
INIT_HEIGHT = 23.5 # cm

# Calculation parameters
EXPANSION = True # Allow for material to be expanded
TEMPERATURE = True # Allow for temperature to be increased
DAMPING_FACTOR = 0.01 # Multiplier on the center of mass acceleration
TIMESTEP_MAGNITUDE = -4
DELTA_T = 10**TIMESTEP_MAGNITUDE # s
NUM_AXIAL = 5 # Currently limited to < 10 by Serpent definitions
NUM_RADIAL = 3 # Currently limited to < 10 by Serpent definitions
NUM_MATERIALS = NUM_AXIAL * NUM_RADIAL # Equivalent to the number of regions in the model
# Calculated as a threshold value, 1e15 fissions per liter before radiolytic nucleation
THRESHOLD = 1.5e17 # fissions/liter
SUBCRITICAL_LIMIT = 0.98 # Limit for k_eff at which the excursion is considered terminated

# Equation of state
# Wood River uses 1e16, Silene uses 1e18
INIT_POWER = 1e18 # fis/s, small initiating fission accident source -> Flux build-up
GRAV = 9.80665 # m/s^2
#GRAV = 0.0 # m/s^2
ATM_ABS = 0.101325 # MPa, atmospheric value
ATM = 0.0 # MPa, calculated with gauge pressures instead of absolute
# Radius of radiolytic gas bubbles, from Forehand dissertation, 1981
# -> Independent of pressure, temperature, surface tension, gas and fissile concentration
RAD_GAS_BUBBLE = 5e-6 / 100 # m
```

```

# Specific ideal gas constant for diatomic H-1
RH2 = 8.3145 / (1.0078250321 * 2) * 100**3 # m^3-Pa/kg-K
# Radiolytic gas constant from Forehand dissertation
# -> (rough average of KEWB Core 5, CRAC 05, and CRAC 08)
RADIOLYTIC_G = 2.30e-4 # kg/MJ
DISSIPATION = 4400 # 1/s

# SILENE uranyl nitrate
#ELEMS = ["1001", "7014", "8016", "92234", "92235", "92236", "92238"]
#NDENS = [6.258e-2, 1.569e-3, 3.576e-2, 1.060e-6, 1.686e-4, 4.350e-7, 1.170e-5] # a/b-cm
#AWEIGHT = [1.0078250321, 14.003074005, 15.9949146196, 234.040952, 235.043930,
#           236.045568, 238.050788] # g/mol

# Wood River uranyl nitrate
ELEMS = ["1001", "7014", "8016", "92234", "92235", "92236", "92238", "11023"]
NDENS = [6.254e-2, 1.568e-3, 3.574e-2, 1.059e-6, 1.685e-4, 4.347e-7, 1.169e-5, 6.504e-5] # a/b-cm
AWEIGHT = [1.0078250321, 14.003074005, 15.9949146196, 234.040952, 235.043930,
           236.045568, 238.050788, 22.989769] # g/mol

# Convergence and entropy constants
NUM_PARTICLES = 10000 # Neutrons per cycle
NUM_CYCLES = 500 # Calculation cycles
NUM_DROPS = 50 # Initial cycles to drop from k-convergence

# Thermal scattering cross section for light water
SAB_TEMP = {
  300: "00t",
  350: "02t",
  400: "04t",
  450: "06t",
  500: "08t",
  550: "10t",
  600: "12t",
  650: "14t",
  800: "18t"
}

# Cross section temperatures
XS_TEMP = {
  300: "03c",
  600: "06c",
  900: "09c",
  1200: "12c",
  1500: "15c",
  1800: "18c"
}

```

Nomenclature and Acronyms

Nomenclature

A_i	Circular cross-sectional area of volume element i – cm ²
B_i	Height of the base of volume element i measured from the system base – cm
ΔC	Change in the z-coordinate position of the center of mass – cm
C_i	Position of the center of mass of volume element i from the system base – cm
c_v	Constant volume mass-specific heat capacity – MJ/°C-kg
d	Solution density – g/cm ³
ΔE	Energy deposition in a given timestep – MJ
f_e	Volume fraction of radiolytic gas present in system
f_i	Fraction of total fissions that occur in volume element i
g	Gravitational constant of acceleration – m/s ²
H_i	Height of the top of volume element i measured from the system base – cm
h_i	Height of solution above the base of volume element i – cm
k_{eff}	Neutron multiplication factor
l	Prompt neutron lifetime – s
m	Mass of solution system – kg
m_{gas}	Mass of radiolytic gas present in system - kg
N_B	Total number of fissions in initial burst
N_e	Number of fissions that occurred prior to start of excursion evolution
N_f	Total number of fissions
N_i	Number of fissions in volume element i
N_P	Total number of fissions in plateau region
P	System pressure – MPa
\bar{P}_i	Average pressure of volume element i – MPa
P_i	Pressure at the top of volume element i – MPa
R_{gas}	Specific ideal gas constant – m ³ -Pa/kg-°C
r_b	Radius of bubble of radiolytic gas – m
T	System temperature – °C
ΔT	Change in temperature – °C
T_e	Time elapsed prior to start of excursion evolution – s
t	Excursion duration – s
Δt	Timestep length – s
V	Solution volume – l
ΔV	Change in volume due to expansion – cm ³
v_{COM_i}	Velocity of the center of mass of volume element i – cm/s
W	Total number of fissions per second occurring in the system
W_0	Initial number of fissions per second that occurred in the system
β	Effective isobaric expansion coefficient – °C ⁻¹
β_0	Isobaric expansion coefficient of liquid – °C ⁻¹

β_d	Delayed neutron fraction of total neutrons produced
κ	Effective isothermal compressibility coefficient – MPa ⁻¹
κ_0	Isothermal compressibility coefficient of liquid – MPa ⁻¹
Λ	Dissipation constant of acceleration – s ⁻¹
Λ_p	Prompt neutron generation time – s
$\bar{\nu}$	Average number of neutrons emitted per fission
ρ	Neutronic reactivity of the system
$\rho_\$$	Neutronic reactivity of the system expressed in terms of prompt criticality – \$
σ	Surface tension of liquid
τ	Neutronic period – s

Acronyms

ANS	American Nuclear Society
CEA	Commissariat à l'énergie atomique et aux énergies alternatives
CRAC	Consequences Radiologiques d'un Accident de Criticite
DOE	Department of Energy
ISO	International Organization for Standardization
JCO	Japan Nuclear Fuel Conversion Company
KEWB	Kinetic Experiments on Water Boilers
SERPENT	Three-dimensional continuous-energy Monte Carlo particle transport code
SILENE	Critical experiment facility at Valduc Laboratory in France
ZAID	Nuclide identification number consisting of Z (number of protons) and A (total number of nucleons) used in Monte Carlo particle transport codes

References

- ANS. (2007). *Nuclear Criticality Accident Emergency Planning and Response* (No. ANSI/ANS-8.23-2007 (R2012)). American Nuclear Society.
- Barbry, F. (1987). Model to Estimate the Maximum Fission Yield in Accidental Solution Excursions. *Transactions of the American Nuclear Society*, 55, 412.
- Barbry, F. (1993). *A Review of the SILENE Criticality Excursions Experiments* (No. Rapport SRSC 93). Commissariat à l’Energie Atomique: IPSN.
- Barbry, F. (1994). *SILENE Reactor Results of Selected Typical Experiment* (No. SRSC-223).
- Barbry, F., Fouillaud, P., Grivot, P., & Reverdy, L. (2009). Review of the CRAC and SILENE Criticality Accident Studies. *Nuclear Science and Engineering*, (161), 160–187.
- Bell, I., Wronski, J., Quoilin, S., & Lemort, V. (2014). Pure and Pseudo-pure Fluid Thermophysical Property Evaluation and the Open-Source Thermophysical Property Library CoolProp. *Industrial & Engineering Chemistry Research*, 53(6), 2498–2508.
- Bickley, A., Mather, D. J., & Shaw, P. M. (1987). The Code CRITEX to Simulate Transient Criticality in Fissile Solutions. *Transactions of the American Nuclear Society*, 55, 406–407.
- DOE. (1994). *Airborne Release Fractions/Rates and Respirable Fractions for Nonreactor Nuclear Facilities* (DOE Handbook No. DOE-HDBK-3010-94). Washington, D.C. 20585: U.S. Department of Energy.

- Dunenfeld, M. S., & Stitt, R. K. (1963). *Summary Review of the Kinetics Experiments on Water Boilers* (No. NAA-SR-7087). Canoga Park, California: Atomic International.
- Forehand, H. (1981, March 18). *Effect of Radiolytic Gas on Nuclear Excursions in Aqueous Solutions* (Dissertation). The University of Arizona.
- Hetrick, D. L., & McLaughlin, T. P. (1993). Estimating Maximum Pulse Yields for Solution Criticality Accidents. *Transactions of the American Nuclear Society*, 69, 249–250.
- Hetrick, D. L., & Smith, A. B. (1987). Nuclear Excursions in Aqueous Solutions of Fissile Materials. *Transactions of the American Nuclear Society*, 55, 407–408.
- Hurt, C. J., Pevey, R. E., & Angelo, P. L. (2012). Simulation of Criticality Accident Transients in Uranyl Nitrate Solution with COMSOL Multiphysics. *Transactions of the American Nuclear Society*, 107.
- ISO. (2011). *Nuclear Criticality Safety - Estimation of the Number of Fissions of a Postulated Criticality Accident* (No. ISO/DIS 16117). International Organization for Standardization.
- Kimpland, R. (1993, August 9). *A Multi-Region Computer Model for Predicting Nuclear Excursions in Aqueous Homogeneous Solution Assemblies* (Dissertation). The University of Arizona.
- Korn, G. A. (1989). *Interactive Dynamic System Simulation*. McGraw-Hill Book Company.

- Leppänen, J., Pusa, M., Viitanen, T., Valtavirta, V., & Kaltiasenaho, T. (2015). The Serpent Monte Carlo Code: Status, Development, and Applications in 2013. *Annals of Nuclear Energy*, 82, 142–150.
- McLaughlin, T., Monahan, S., Pruvost, N., Frolov, V., Ryazanov, B., & Sviridov, V. (2000). *A Review of Criticality Accidents* (No. LA-13638). Los Alamos, New Mexico 87545: Los Alamos National Laboratory.
- McLaughlin, T. P. (1991). *Process Criticality Accident Likelihoods, Consequences, and Emergency Planning* (No. LA-UR-91-2325). Los Alamos, New Mexico 87545: Los Alamos National Laboratory.
- McLaughlin, T. P. (2003). Process Criticality Accident Likelihoods, Magnitudes and Emergency Planning - A Focus on Solution Accidents (Vol. 19, pp. 831–836). Presented at the Japan Atomic Energy Research Institute Conference.
- Nakache, F. R., Shapiro, M. M., Soodak, H., Marotta, C., & Schamberger, R. (1964). *The Nuclear Aspects of the Accidental Criticality at Wood River Junction, Rhode Island*. United Nuclear Corporation.
- Nakajima, K. (2003). Applicability of Simplified Methods to Evaluate Consequences of Criticality Accident Using Past Accident Data. In *Proceedings of the 7th International Conference on Criticality Safety* (Vol. 19, pp. 746–751). Tokai, Japan.
- Nomura, Y., & Okuno, H. (1995). Simplified Evaluation Models for Total Fission Number in a Criticality Accident. *Nuclear Technology*, 109, 142–152.
- Olsen, A. R., Hooper, R. L., Uotinen, V. O., & Brown, C. L. (1974). *Empirical Method for Estimating the Total Number of Fissions from Accidental Criticality in*

- Uranium and Plutonium Systems* (No. BNWL-1840). Richland, Washington: Pacific Northwest Laboratory.
- Smith, A. (1989, October 20). *Nuclear Excursions in Aqueous Solutions of Fissile Materials* (Master's Thesis). The University of Arizona.
- Smith, D., & Stratton, W. (1989). *A Review of Criticality Accidents* (Nuclear Criticality Technology No. DOE/NCT-04). Nuclear Criticality Information System, U.S. Department of Energy Office of Safety Appraisals.
- Spiegler, P., Bumpus, C. F. J., & Norman, A. (1962). *Production of Void and Pressure by Fission Track Nucleation of Radiolytic Gas Bubbles During Power Bursts in a Solution Reactor* (No. NAA-SR-7086). Canoga Park, CA: Atomics International. Div. of North American Avation, Inc.
- Stratton, W. (1967). *A Review of Criticality Accidents* (No. LA-3611). Los Alamos Scientific Laboratory of the University of California.
- Tuck, G. (1974). Simplified Methods of Estimating the Results of Accidental Solution Excursions. *Nuclear Technology*, 23, 177–188.
- USNRC. (1977). *Assumptions Used for Evaluating the Potential Radiological Consequences of Accidental Nuclear Criticality in a Fuel Reprocessing Plant* (No. US NRC Regulatory Guide 3.33). Nuclear Regulatory Commission.
- USNRC. (1979a). *Assumptions Used for Evaluating the Potential Radiological Consequences of Accidental Nuclear Criticality in a Plutonium Processing and Fuel Fabrication Plant* (No. US NRC Regulatory Guide 3.35). Nuclear Regulatory Commission.

USNRC. (1979b). *Assumptions Used for Evaluating the Potential Radiological Consequences of Accidental Nuclear Criticality in a Uranium Fuel Fabrication Plant* (No. US NRC Regulatory Guide 3.34). Nuclear Regulatory Commission.

van Rossum, G., Warsaw, B., & Coghlan, N. (2001). *Style Guide for Python Code* (No. PEP 8).